NUCLEAR WASTE MANAGEMENT ORGANIZATION
SOCIÉTÉ DE GESTION DES DÉCHETS NUCLÉAIRES

# Phase 2 Geoscientific Preliminary Assessment

# Lineament Interpretation

## TOWN OF BLIND RIVER, CITY OF ELLIOT LAKE AND AREA, ONTARIO

**APM-REP-01332-0218**

**NOVEMBER 2017**

*This report has been prepared under contract to the NWMO. The report has been reviewed by the NWMO, but the views and conclusions are those of the authors and do not necessarily represent those of the NWMO.*

*All copyright and intellectual property rights belong to the NWMO.*

*For more information, please contact:*
**Nuclear Waste Management Organization**
22 St. Clair Avenue East, Sixth Floor
Toronto, Ontario M4T 2S3 Canada
Tel 416.934.9814
Toll Free 1.866.249.6966
Email contactus@nwmo.ca
www.nwmo.ca

# Phase 2 Geoscientific Preliminary Assessment
# Lineament Interpretation, Blind River, Elliot Lake and Area, Ontario

**Report Prepared for**

## Nuclear Waste Management Organization

nwmo
NUCLEAR WASTE MANAGEMENT ORGANIZATION
SOCIÉTÉ DE GESTION DES DÉCHETS NUCLÉAIRES

.

**Report Prepared by**

srk consulting

SRK Consulting (Canada) Inc.
SRK Project Number: 3CN020.006
NWMO Report Number: APM-REP-01332-0218
November 24, 2017

# Phase 2 Geoscientific Preliminary Assessment, Lineament Interpretation, Blind River, Elliot Lake and Area, Ontario

## Nuclear Waste Management Organization

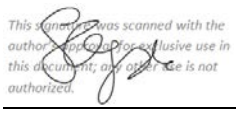
22 St. Clair Avenue East, Sixth Floor
Toronto, Ontario, Canada
M4T 2S3
E-mail: contactus@nwmo.ca
Website: www.nwmo.ca
Tel: +1 416 934 9814
Fax: +1 416 934 9526

**SRK Consulting (Canada) Inc.**
1300, 151 Yonge Street
Toronto, Ontario, Canada
M5C 2W7
E-mail: toronto@srk.com
Website: www.srk.com
Tel: +1 416 601 1445
Fax: +1 416 601 9046

**SRK Project Number: 3CN020.006**
**NWMO Report Number: APM-REP-01332-0218**

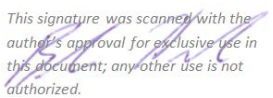
**November 27, 2017**

**Authored by:**




Simon Craggs, MSc
Senior Consultant (Structural Geology)

**Reviewed by:**




Blair Hrabi, PGeo
Principal Consultant (Structural Geology)

# Executive Summary

This technical report documents the results of an updated surficial and geophysical lineament interpretation study conducted as part of the Phase 2 Geoscientific Preliminary Assessment to further assess the suitability of the North of Huron area to safely host a deep geological repository. This study follows the successful completion of the Phase 1 Geoscientific Desktop Preliminary Assessment (Golder, 2014).

The purpose of the Phase 2 lineament interpretation was to provide an updated interpretation of the geological and structural characteristics of the bedrock units within the area identified in the Phase 1 desktop assessment. The assessment area considered for the lineament study includes the area covered by the newly acquired Phase 2 airborne surveys (SGL, 2017). The interpretation of lineaments was conducted using the new high-resolution airborne magnetic and digital elevation data (DEM), as well as high-resolution digital aerial imagery (OMNR, 2009).

The lineament interpretation followed a systematic workflow involving three steps. The first step included an independent lineament interpretation by two individual interpreters for each data set and the assignment of a certainty level (low, medium, or high) of the interpreted lineaments. The second step involved the integration of the interpreted lineaments for each individual data set and a determination of reproducibility. The third and final step involved the integration of the lineament interpretations for the surficial data sets (DEM and digital aerial imagery) followed by the integration of the combined surficial data set with the aeromagnetic data set, with the determination of lineament coincidence in each integration step. Over the course of these three steps, a comprehensive list of attributes for each lineament was compiled. The four key lineament attributes and characteristics used in the assessment include certainty, length, density, and orientation.

Geophysical lineaments were interpreted using the newly acquired high-resolution aeromagnetic data (SGL, 2017), which provides a significant improvement to the overall resolution and quality of aeromagnetic data compared with the available data interpreted during the Phase 1 preliminary assessment. Dyke lineaments were interpreted as linear magnetic highs, while brittle lineaments were interpreted as linear or curvilinear magnetic lows. Lineaments interpreted using the aeromagnetic data are typically less affected by the presence of overburden than surficial data sets, and more likely reflect potential structures at depth that may or may not have surficial expressions. The geophysical lineament interpretation identified 844 lineaments, including 149 brittle and 695 dyke lineaments throughout the assessment area. The reproducibility assessment identified coincidence for 56% and a lack of coincidence for 44% of all geophysical lineaments, with 74% assigned the highest level of certainty (three), while 20% were assigned a moderate certainty value of two, and 6% were assigned a low certainty value of one. Brittle lineaments occur throughout the area, except within the southwestern part of the area. Brittle lineaments display a broad southeast, to north-south orientation, as well as a north-northeast-trending orientation, and an east-west-trending orientation. Dyke lineaments occur throughout the area with a single dominant southeast orientation with a range in orientation from 124° to 158° that corresponds to the southeast-trending Sudbury dyke swarm, and the southeast- to south-southeast-trending Matachewan dyke swarm. The density of the brittle and dyke lineaments is relatively uniform, with few discrete zones of elevated and lower lineament density throughout. Zones of elevated lineament density occur throughout the area and are typically the result of clusters of southeast-trending dyke lineaments and where these clusters intersect with tight-spaced brittle lineaments and south-southeast-trending dyke lineaments.

Surficial lineaments were interpreted using the high-resolution digital elevation data (DEM) from the airborne surveys, and high-resolution digital aerial imagery with a ground resolution cell of 0.4 m. Surficial lineaments were interpreted as linear traces along topographic features such as valleys, escarpments, and drainage patterns such as rivers, streams, and linear lake shorelines. These linear traces may represent the expression of bedrock fractures on the land surface. However, it is uncertain what proportion of surficial lineaments represent actual geological structures and, if they do, whether the structures extend to significant depth. The observed distribution and density of surficial lineaments is in part influenced by the presence of overburden cover and water bodies, which can mask the surface expressions of potential fractures. The combination of interpreted DEM and digital aerial imagery lineaments yielded 1427 integrated surficial lineaments throughout the assessment area. The reproducibility assessment identified coincidence for 19% of the surficial lineaments and

a lack of coincidence for 81% of all surficial lineaments, with 23% assigned the highest level of certainty (three), while 49% were assigned a moderate certainty value of two, and 28% were assigned a low certainty value of one. Surficial lineaments display a broad southeast- to south-southeast orientation, and additional, subordinate north-northeast and northeast orientations. The dominant glacial flow direction was from northeast to southwest, therefore care must be taken when evaluating northeast-trending surficial lineaments to ensure they are related to bedrock features. Surficial lineament density is relatively uniform throughout the area, with few discrete zones of elevated and lower lineament density throughout. Zones of elevated lineament intersection density typically occur along or at the intersection of tight-spaced southeast- and northeast-trending surficial lineaments. However, the areas of highest surficial lineament density are correlated with areas of higher topographic elevation. While overburden is not abundant in the assessment area, zones of glaciofluvial deposits are located around and south of Mozhabong Lake, and west of Armstrong Lake, but these are thought to have a limited impact on the abundance of interpreted surficial lineaments in these areas.

The integration of the geophysical and surficial lineament data sets resulted in the final integrated lineament data set. This data set identified 1887 lineaments, including 1248 brittle and 639 dyke lineaments through the assessment area. The reproducibility assessment between geophysical and surficial features revealed that 28% of the interpreted geophysical lineaments were also interpreted in at least one of the two surficial data sets. In general, reproducibility values for the final integrated data reveal a low coincidence between surficial and geophysical lineaments. Throughout the assessment area, only 6% of the final integrated lineaments were identified in all three data sets, and 16% of the final integrated lineaments were identified in two of the three data sets. Low coincidence between surficial and geophysical lineaments does not necessarily imply a low degree of confidence that the lineaments represent a true bedrock structure. The lineaments derived from different datasets should be considered to be complementary, because individual lineaments may have a better expression in different datasets. Lineaments that were reproduced in all three data sets (RA_2=3), and lineaments with the highest certainty value (3) typically represent the longest lineaments (i.e., greater than 5 km). The orientation and distribution of brittle and dyke lineaments show a dominant, broad southeast to south-southeast orientation, and subordinate north-northeast and northeast trends. As with the geophysical and surficial data sets, the density of the final integrated brittle and dyke lineaments is relatively uniform with rare discrete zones of elevated and lower lineament density throughout the assessment area. Areas of higher brittle and dyke density correspond to areas with clusters of southeast- and south-southeast-trending dyke lineaments and where these clusters intersect with tight-spaced brittle lineaments. Brittle lineaments in each orientation set are observed to offset and truncate, and be offset and truncated by brittle and dyke lineaments in all the other orientation sets. The complexity and inconsistency of the structural relationships observed between all brittle lineaments suggest a protracted deformation history that likely includes multiple generations of brittle reactivation.

# Table of Contents

**Executive Summary** ..... ii

**Table of Contents** ..... iv

**List of Tables** ..... vi

**List of Figures (in order following text)** ..... vii

**1 Introduction** ..... 8
1.1 Scope of Work and Work Program ..... 8
1.2 Assessment Area ..... 9
1.3 Qualifications of SRK and SRK Team ..... 9

**2 Summary of Geology** ..... 11
2.1 Geological Setting ..... 11
2.2 Bedrock Geology ..... 11
2.2.1 Ramsey-Algoma Granitoid Complex ..... 12
2.2.2 Benny Lake Greenstone Belt ..... 13
2.2.3 Mafic Dykes ..... 14
2.3 Structural History ..... 14
2.3.1 Mapped Structures ..... 18
2.4 Metamorphism ..... 18
2.5 Quaternary Geology ..... 19

**3 Methodology** ..... 20
3.1 Source Data Description ..... 20
3.1.1 High-resolution Aeromagnetic Data ..... 20
3.1.2 Digital Elevation Model ..... 21
3.1.3 High-resolution Digital Aerial Imagery ..... 21
3.2 Lineament Interpretation Workflow ..... 21
3.2.1 Step 1: Lineament Interpretation and Certainty Level ..... 24
3.2.2 Step 2: Lineament Reproducibility Assessment 1 (RA_1) ..... 25
3.2.3 Step 3: Coincidence Assessment (RA_2) ..... 26
3.2.4 Lineament Trends ..... 28
3.2.5 Lineament Length ..... 28
3.2.6 Lineament Density ..... 29

**4 Lineament Interpretation Results** ..... 30
4.1 Geophysical Lineaments (RA_1) ..... 30
4.2 Surficial Lineaments ..... 31
4.2.1 DEM Lineaments (RA_1) ..... 31
4.2.2 FRI Digital Aerial Imagery Lineaments (RA_1) ..... 32
4.3 Integrated Surficial Lineaments (RA_2) ..... 33
4.4 Integrated Final Lineaments (RA_2) ..... 34

**5 Discussion** ..... 36
5.1 Lineament Reproducibility (RA_1) and Coincidence (RA_2) ..... 36
5.2 Lineament Trends ..... 38
5.2.1 Relationship between Lineament Sets and Regional Stress Field ..... 39
5.3 Lineament Length ..... 39
5.4 Density ..... 41
5.4.1 Lineament Density ..... 41
5.4.2 Lineament Intersection Density ..... 42

5.5 Lineament Truncation and Relative Age Relationships ..... 43
5.5.1 Mapped Structure and Lineament Relationships ..... 44
**6 Summary of Results ..... 46**
**7 References ..... 49**
**APPENDIX A: Additional Supporting Figures ..... 58**
**APPENDIX B: Summary of Lineament Statistics ..... 64**
**Figures ..... 68**

# List of Tables

Table 1: Bounding Coordinates of the Phase 2 Lineament Assessment Area ..... 9
Table 2: Geological and Structural History of the Area (adapted from JDMA, 2014a)..... 16
Table 3: FRI Digital Aerial Imagery Band Ranges and Resolution..... 21
Table 4: Attribute Table Fields Populated for the Lineament Interpretation..... 23
Table 5: Summary of Geophysical Lineament Orientations for the Area..... 31
Table 6: Summary of DEM Lineament Orientations for the Area..... 32
Table 7: Summary of FRI Lineament Orientations for the Area..... 33
Table 8: Summary of Integrated Surficial Lineament (RA_2) Orientations for the Area..... 34
Table 9: Summary of Integrated Final Lineament (RA_2) Orientations for the Area..... 35

# List of Figures (in order following text)

Figure 1: Location and Overview of the Area North of Elliot Lake and Blind River

Figure 2: Bedrock Geology of the Area North of Elliot Lake and Blind River

Figure 3: Terrain Features of the Area North of Elliot Lake and Blind River

Figure 4: Pole Reduced Magnetic Data (First Vertical Derivative) of the Area North of Elliot Lake and Blind River

Figure 5: Digital Elevation Data of the Area North of Elliot Lake and Blind River

Figure 6: Forest Resource Inventory Digital Aerial Imagery of the Area North of Elliot Lake and Blind River

Figure 7: Form Lines from Pole Reduced Magnetic Data of the Area North of Elliot Lake and Blind River

Figure 8: Interpreted Lineaments from Pole Reduced Magnetic Data of the Area North of Elliot Lake and Blind River

Figure 9: Interpreted Lineaments from Digital Elevation Data of the Area North of Elliot Lake and Blind River

Figure 10: Interpreted Lineaments from Forest Resource Inventory (FRI) Imagery of the Area North of Elliot Lake and Blind River

Figure 11: Interpreted Lineaments from Surficial Data of the Area North of Elliot Lake and Blind River

Figure 12: Interpreted Lineaments from Pole Reduced Magnetic Data of the Area North of Elliot Lake and Blind River

Figure 13: Select Final Integrated Lineaments of the Area North of Elliot Lake and Blind River

Figure 14: Interpreted Lineaments from Pole Reduced Magnetic Data (by Length) of the Area North of Elliot Lake and Blind River

Figure 15: Interpreted Lineaments (by Length) from Surficial Data of the Area North of Elliot Lake and Blind River

Figure 16: Final Integrated Lineaments (by Length) of the Area North of Elliot Lake and Blind River

Figure 17: Lineament Density for All Interpreted Lineaments from Pole Reduced Magnetic Data of the Area North of Elliot Lake and Blind River

Figure 18: Lineament Density for Interpreted Lineaments from Surficial Data of the Area North of Elliot Lake and Blind River

Figure 19: Lineament Density for All Final Integrated Lineaments of the Area North of Elliot Lake and Blind River

Figure 20: Lineament Intersection Density for All Interpreted Lineaments from Pole Reduced Magnetic Data of the Area North of Elliot Lake and Blind River

Figure 21: Lineament Intersection Density for Interpreted Surficial Lineaments of the Area North of Elliot Lake and Blind River

Figure 22: Lineament Intersection Density for All Final Integrated Lineaments of the Area North of Elliot Lake and Blind River

Figure 23: Lineament Relative Age Relationships of the Area North of Elliot Lake and Blind River

# 1 Introduction

This technical report documents the results of an updated geophysical and surficial lineament interpretation study conducted as part of the Phase 2 Extension – Structural Lineament Interpretation to further assess the suitability of an area located north of the Blind River and Elliot Lake communities to safely host a deep geological repository. This study follows the successful completion of a Phase 1 Geoscientific Desktop Preliminary Assessment (NWMO, 2014a,b; JDMA, 2014a; Golder, 2014), which identified several potentially suitable areas warranting further studies, such as high-resolution geophysical surveys and geological mapping.

The purpose of the Phase 2 lineament interpretation was to provide an updated interpretation of the geological and structural characteristics of the bedrock units within the potentially suitable areas identified in the Phase 1 desktop assessment. The assessment area considered for the lineament study includes the area covered by newly acquired Phase 2 airborne geophysical surveys (SGL, 2017).

The interpretation of geophysical lineaments was conducted using newly acquired high-resolution airborne magnetic data (SGL, 2017). The interpretation of surficial lineaments was conducted using newly acquired digital elevation data (SGL, 2017) and high-resolution digital aerial imagery of the area (Forest Resource Inventory digital aerial imagery: OMNR, 2009).

## 1.1 Scope of Work and Work Program

The scope of work for this study included the completion of a structural lineament interpretation of remote sensing data for the area in north central Ontario (Figure 1). The lineament study involved the interpretation of remotely-sensed data sets, including surficial (digital elevation and digital aerial imagery) and geophysical (magnetic) data sets (SGL, 2017) for the area. The investigation interpreted lineament locations and orientations in terms of their potential impact as bedrock structural features (e.g., individual fractures or fracture zones) and evaluated their relative timing relationships within the context of the local and regional geological setting. For the purpose of this report, a lineament was defined as “a linear or curvi-linear geophysical, DEM or surficial feature.” The approach undertaken in this lineament investigation was based on the following:

- Lineaments were interpreted using newly acquired high-resolution aeromagnetic and digital elevation data (SGL, 2017), and purchased high-resolution digital aerial imagery (Forest Resource Inventory digital aerial imagery; OMNR, 2009).
- Lineament interpretations for each data set were made by two specialist interpreters using a standardized workflow.
- Lineaments were interpreted as having a brittle or dyke character by each interpreter.
- Lineaments were analyzed based on an evaluation of the quality and limitations of the available data sets.
- Lineaments were evaluated using: age relationships; reproducibility tests, particularly the coincidence of lineaments identified by different interpreters; coincidence of lineaments interpreted from different data sets; and comparison to literature and mapped geology.
- Classification was applied to indicate the significance of lineaments based on certainty, length, and reproducibility.

These elements help to address the issues of uncertainty, subjectivity and reproducibility normally associated with lineament investigations. Their incorporation into the methodology increases the confidence in the resulting lineament interpretation.

## 1.2 Assessment Area

The area used for the lineament assessment and interpretation is located approximately 65 kilometres (km) northeast of Elliot Lake and 97 km northeast of Blind River, and covers an area of approximately 757 square kilometres ($km^2$) in one block (Figure 1). The approximate coordinates defining the boundaries of the Phase 2 assessment area are listed in Table 1 (UTM NAD83, Zone 17N).

**Table 1: Bounding Coordinates of the Phase 2 Lineament Assessment Area**

| X UTM | Y UTM |
|---|---|
| 389,573 | 5,206,151 |
| 422,517 | 5,206,249 |
| 422,714 | 5,176,067 |
| 405,749 | 5,175,968 |
| 398,773 | 5,192,101 |
| 392,993 | 5,194,736 |

## 1.3 Qualifications of SRK and SRK Team

The SRK Group comprises more than 1,400 professionals, offering expertise in a wide range of resource engineering disciplines. The independence of the SRK Group is ensured as it holds no equity in any project it investigates and its ownership rests solely with its staff. Consequently, SRK can provide its clients with conflict-free and objective recommendations on crucial issues. SRK has a proven track record in undertaking independent assessments of mineral resources and mineral reserves, project evaluations and audits, technical reports and independent feasibility evaluations to bankable standards on behalf of exploration and mining companies, and financial institutions worldwide. Through its work with a large number of major international mining companies, the SRK Group has established a reputation for providing valuable consultancy services to the global mining industry.

The lineament interpretation and the compilation of this report were completed by Mr. Simon Craggs and Dr. Jean-François Ravenelle, PGeo. Dr. James P. Siddorn, PGeo and Mr. Blair Hrabi, PGeo served as technical advisors and reviewed lineament interpretations and drafts of this report prior to their delivery to the NWMO as per SRK internal quality management procedures.

Following is a brief description of the qualifications and roles of the project team members.

**Mr. Simon Craggs, MSc** is a Senior Consultant (Structural Geology) who specializes in regional mapping, detailed analysis of fracture/fluid flow mechanics, and the structural controls on epithermal ore deposit formation. Mr. Craggs has conducted several structural interpretations for vein-type precious metal deposits in poly-deformed terranes across Canada. He recently completed structural lineament interpretations for the Phase 1 Schreiber (SRK, 2013a), Manitouwadge (SRK, 2014a), and White River (SRK, 2014b) areas for the NWMO. In this study, Mr. Craggs was the lead interpreter and the report author.

**Dr. Jean-François Ravenelle, PGeo** (Principal Consultant – Structural Geology) is an expert in the structural geology analysis of Archean terranes. Jean-Francois also specializes in understanding the structural geology of highly deformed and metamorphosed precious metal deposits through diligent surface analysis, lineament interpretations, and 3D modelling. Over the past 15 years, Jean-Francois conducted several aeromagnetic lineament interpretations, geotechnical studies, and structural analyses in various geological settings. He completed the Phase 1 structural lineament interpretation of the Ear Falls (SRK, 2013b) study area for the NWMO in 2013. In this study, Dr. Ravenelle was the second interpreter.

**Dr. James Siddorn, PGeo** is a Practice Leader (Structural Geology) and specialist in applied structural interpretation of remotely sensed data combined with the structural analysis of ore deposits. Dr. Siddorn has conducted numerous detailed interpretations of magnetic and electromagnetic data sets for gold and diamond exploration, and rock mechanics/hydrogeological engineering studies. He oversaw the Phase 1 structural lineament interpretations for the Schreiber (SRK, 2013a), Ear Falls (SRK, 2013b), White River (SRK, 2014b), and Manitouwadge (SRK, 2014a) areas, as well as the Phase 2 structural lineament interpretations for the Creighton (SRK, 2015a), Schreiber (SRK, 2015b), and Ignace (SRK, 2015c) areas. In this study, Dr. Siddorn was a senior reviewer.

**Mr. Blair Hrabi**, MSc, PGeo is a Principal Consultant (Structural Geology) with SRK, based in the Toronto office. He is a structural geologist with 22 years of experience gained in the exploration industry, government geological surveys, and academic settings. He has extensive experience in field mapping and structural analysis of Archean and Proterozoic terranes from regional to detailed scales. Mr. Hrabi was the project lead for the Phase 1 observation of general geological features (OGGF) in Creighton, Saskatchewan and Ignace, Ontario areas, the project leader of the Phase 2 geological mapping of the Manitouwadge area, Ontario and a second interpreter in the Phase 2 lineament interpretation of the Manitouwadge area. In this study, Mr. Hrabi was a senior reviewer.

**Mr. Jason Adam** is an Associate Consultant (GIS) who has a broad experience in GIS (geographical information systems). Mr. Adam provided GIS support for the study, mainly in the preparation of figures, under the direction of Mr. Craggs.

# 2 Summary of Geology

Details of the geology of the area were described in the Phase 1 Geoscientific Desktop Preliminary Assessment (Golder, 2014). The following sections provide brief descriptions of the geologic setting, bedrock geology, structural history and mapped structures, metamorphism, and Quaternary geology of the area. The focus of the following sections are the bedrock units identified during Phase 1 as being potentially suitable to host a deep geological repository and the important structural features in the area.

## 2.1 Geological Setting

The area is located within the Archean Superior Province of the Canadian Shield. The Superior Province is a stable craton created from a collage of ancient plates and accreted juvenile arc terranes that were progressively amalgamated over a period of more than 2 billion years (e.g., Percival et al., 2006). The Superior Province covers an area of approximately 1,500,000 km$^2$ and is divided into subprovinces, including the Abitibi Subprovince within which the area is located.

The Abitibi Subprovince is bounded to the west by the Kapuskasing structural zone and Wawa Subprovince and to the north by the Opatica Subprovince. Its southern boundary is overlain by metasedimentary and metavolcanics rocks of the Huronian Supergroup of the Southern Province. The Abitibi Subprovince developed between 2.8 and 2.6 billion years ago (Ga) (Thurston, 1991) and comprises multiple units of volcanic and associated metasedimentary rocks (greenstone belts) separated by extensive granitic plutons and batholiths. These greenstone belts typically occur in elongate geometries and represent a significant percentage of the rocks in the northern portion of the subprovince, while occurring less so in the southern portion of the subprovince. The surrounding granitoid bodies are composed primarily of tonalite to granodiorite, and represent the vast majority of the rocks present throughout the area.

Six generations of Proterozoic diabase dyke swarms, ranging in age from ca. 2.473 Ga to 590 million years ago (Ma) intrude the bedrock units in the area (Krogh et al., 1987; Kamo et al., 1995; Buchan et al., 1996; Hamilton et al., 2002; Buchan and Ernst, 2004).

## 2.2 Bedrock Geology

The Abitibi Subprovince is composed of low metamorphic grade volcanic rocks and granitoid plutonic and gneiss-dominated rocks, the latter of which occupy most of the area and are represented by the Ramsey-Algoma granitoid complex (e.g., Jackson and Fyon, 1991).

The Ramsey-Algoma granitoid complex is a large heterogeneous group of granitoid bodies that intruded the older metavolcanic and subordinate metasedimentary rocks of the Whiskey Lake and Benny Lake greenstone belts. The vast majority of the area is underlain by the Ramsey-Algoma granitoid complex (shown in pink on Figure 2), which extends beyond the study area in all directions. The area also includes a thin sliver of the westernmost portion of the Benny Lake greenstone belt (Figure 2).

Several generations of Proterozoic diabase dyke swarms, ranging in age from 2.473 Ga to 590 Ma, cut all Archean bedrock units in the area. The most prominent of these dyke swarms include the northwest-trending Sudbury swarm, ca. 1.238 Ga (Krogh et al., 1987); the north-northwest-trending

Matachewan swarm, ca. 2.473 Ga (Buchan and Ernst, 2004); and the north-trending Marathon dyke swarm, ca. 2.121 Ga (Buchan et al., 1996; Hamilton et al., 2002). Less numerous dykes belonging to the northeast-trending Biscotasing, ca. 2.167 Ga (Hamilton et al., 2002), west-northwest-trending North Channel, ca. 1.6 to 2.5 Ga (OGS, 2011), and east-northeast-trending Grenville, ca. 590 Ma (Kamo et al., 1995) dyke swarms also crosscut the area.

The main geological units of interest occurring in the area are further described below.

### 2.2.1 Ramsey-Algoma Granitoid Complex

The Ramsey-Algoma granitoid complex is a large complex of granitoid and gneissic rocks divided in three large domains: the Chapleau gneiss, Ramsey gneiss and Algoma plutonic domains (Jackson and Fyon, 1991). In the area, the granitoid complex is dominated by the Algoma plutonic domain. Although some portions of the Algoma plutonic domain have been mapped in detail (e.g., Robertson, 1965a,b,c; Robertson and Johnson, 1965; Giblin, 1976; Giblin et al.,1977), the Algoma plutonic domain remains poorly studied. The Ramsey-Algoma granitoid complex is generally described in the literature as consisting largely of a massive to foliated granite-granodiorite suite intruding a tonalite-granodiorite suite. In addition, several narrow slivers of metavolcanic rock are commonly mapped within the gneissic tonalite portion of the Ramsey-Algoma granitoid complex. In the study area, however, these metavolcanic rocks are observed within the massive to foliated granite-granodiorite suite.

The Algoma plutonic domain consists of granitic and granodioritic rocks and granitic gneisses with numerous greenstone enclaves and massive to foliated granite, granodiorite, and syenite intrusions (Card, 1979); although, a variety of facies have been observed throughout the granitoid complex in the vicinity of the area. In the area of Rawhide Lake, approximately 15 km north of Elliot Lake, the Algoma plutonic domain consists generally of uniform, massive, medium to coarse-grained, equigranular granite (Ford, 1993). Approximately 45 km northwest of Elliot Lake, in the area of Kirkpatrick Lake, the plutonic complex is reported to be predominantly composed of massive to foliated biotite-bearing to hornblende-bearing granitic rock with up to 30% amphibole. Minor, more leucocratic phases are typically quartz monzonite to granodiorite and trondhjemite. In the Wakomata Lake area, approximately 30 km northwest of Blind River, outcrops of pink to grey, equigranular, fine- to coarse-grained trondhjemite, quartz monzonite and granodiorite have been reported, of which grey, medium- to coarse-grained, leucocratic trondhjemite predominates (Siemiatkowska, 1977). Sage (1988) described granitic rock in the Seabrook Lake area (65 km northwest of Blind River) as massive, medium- to coarse-grained, red to red-brown, leucocratic, granodiorite to quartz monzonite. In the area of East Bull Lake (25 km east-northeast of Blind River), Easton et al. (2004) reported mixtures of strongly foliated granitic gneiss and migmatitic facies enclosing mafic gneiss, whereas McCrank et al. (1989) described that area as comprising weakly to moderately foliated granodiorite and porphyroblastic granite. Lastly, Gordon (2012) noted massive, homogeneous syenogranite as the main plutonic phase in Otter Township, west of the study area.

Geochronology for the Algoma plutonic domain includes an age of 2.716 billion years old in the Batchawana area, approximately 60 km west of Blind River and Elliot Lake (Corfu and Grunsky, 1987), and 2.662 billion years for the area south of Ramsey, about 50 km north of the area (van Breemen et al., 2006). Heather et al. (1995) reported a preliminary age of ca. 2.727 billion years for biotite tonalite from immediately south of the Swayze greenstone belt approximately 60 km northeast of the area. More recently, Easton (2010) obtained preliminary dates of 2.675 and 2.651 billion years for two samples of granite and granodiorite near Elliot Lake. The wide range of dates suggests that the Ramsey-Algoma granitoid complex contains distinct plutonic and gneissic lithologies emplaced over a period of 75 million years and possibly longer. This interpretation is

supported by van Breemen et al. (2006) who subdivided granitic rocks in the Swayze area, approximately 120 km north of Elliot Lake, into the following five broad categories:

- Synvolcanic diorite and hornblende tonalite intrusions ranging in age from ca. 2.740 to 2.696 billion years old.
- A transitional suite of tonalite and quartz monzonite intrusions ranging from ca. 2.695 to 2.686 billion years old.
- Syntectonic hornblende granodiorite intrusions ranging from ca. 2.685 to 2.686 billion years old.
- A younger transitional suite of tonalite and quartz monzonite intrusions ranging from ca. 2.680 to 2.665 billion years old.
- Non-foliated ca. 2.665-billion-year-old post-tectonic granite intrusions occurring within areas of synvolcanic and syntectonic intrusions.

Although the Swayze area is located further north, it shares a similar tectonic setting to the northern part of the area. Van Breeman et al. (2006) may therefore offer an interpretative framework for the largely unmapped Ramsey-Algoma granitoid complex within the area. Heather et al. (1995) also described a large body of massive Algoma biotite granite in the area southwest of Ramsey, approximately 50 km north of the assessment area.

### 2.2.2 Benny Lake Greenstone Belt

The Benny Lake greenstone belt consists of Archean metavolcanic and metasedimentary rocks that form a 40 km long by 5 km wide east-striking greenstone belt extending from the Geneva Lake area to the Mink Lake area, some 70 km northeast of Elliot Lake. The greenstone belt extends only 4 km into the area (shown in green on Figure 2) to its mapped termination south of Mink Lake. Card and Innes (1981) described the central part of the greenstone belt as consisting of intercalated mafic flows and pyroclastic rocks with intermediate tuffs and tuff-breccia with some volcanogenic metasedimentary rocks including tuffaceous greywacke and siltstone, chert, and iron formation. The stratigraphic sequence in this part of the belt comprises cyclic repetitions of mafic, intermediate, and felsic metavolcanics, plus sulphide-bearing tuffs and tuffaceous metasedimentary rocks that commonly lie along contact zones between the metavolcanic units.

Felsic plutonic rocks are noted to surround and intrude the greenstone rocks. Card and Innes (1981) subdivided these rocks into an older gneissic, granodioritic complex that occurs mainly to the north of the greenstone belt and a younger, relatively massive, homogeneous quartz monzonite that forms most of the terrain to the south. Quartz monzonite may overlap with a number of fields in the currently used International Union of Geological Sciences (IUGS) classification. Although there is no published information on the age of the Benny Lake greenstone belt, Easton (2010) noted that the ages obtained for the Whiskey Lake greenstone belt, located approximately 50 km to the southwest, were consistent with 2.690- to 2.685-billion-year old volcanism in the southern part of the Abitibi Subprovince.

The greenstone sequence dips steeply to the south with a schistosity subparallel to the primary stratification. Movements on major northwest and north-northwest trending faults such as those along the Spanish River have resulted in progressive northward displacement of the Benny Lake greenstone belt from east to west (JDMA, 2014a).

### 2.2.3 Mafic Dykes

Six generations of Proterozoic diabase dyke swarms crosscut the area (Buchan and Ernst, 2004), a subset of which are shown on Figure 2. The generations of dyke swarm include:

- North-northwest-trending Matachewan Suite dykes (ca. 2.473 Ga; Buchan and Ernst, 2004). This dyke swarm is one of the largest in the Canadian Shield and is predominant in the area. Individual dykes are generally up to 10 metres wide, and have vertical to subvertical dips. The Matachewan dykes comprise mainly quartz diabase dominated by plagioclase, augite and quartz (Osmani, 1991).
- Northeast-trending Biscotasing Suite dykes (ca. 2.167 Ga; Hamilton et al., 2002). The dykes form prominent northeast trending regional features, with individual dykes typically 50 to 100 metres in width. The Biscotasing dykes are quartz tholeiitic features with fine-grained chilled margins and medium- to coarse-grained interiors (Buchan et al., 1993; Halls et al., 2008), dominated by plagioclase, pyroxene and quartz with minor magnetite-ilmenite intergrowths These dykes are fairly minor in the area.
- North-trending Marathon Suite dykes (ca. 2.121 Ga; Buchan et al., 1996; Hamilton et al., 2002). These form a fan-shaped distribution pattern around the northern, eastern, and western flanks of Lake Superior, and are relatively uncommon in the area. The dykes vary in orientation from northwest to northeast, and occur as steep to subvertical sheets, typically a few metres to tens of metres thick, but occasionally up to 75 metres thick (Hamilton et al., 2002). The Marathon dykes comprise quartz diabase (Osmani, 1991) dominated by equigranular to subophitic clinopyroxene and plagioclase.
- West-northwest-trending North Channel Suite dykes (ca. 1.6 to 2.5 Ga; OGS, 2011). This dyke swarm may be temporally associated with the ca. 1.884 Ga Molson dyke swarm in Manitoba, and the Wabigoon dyke swarm in northwestern Ontario (OGS, 1997; Buchan and Ernst, 2004). These dykes are not considered to be numerous in the area.
- Northwest–trending Sudbury Suite dykes (ca. 1.238 Ga; Krogh et al., 1987). Individual dykes are generally less than 10 metres wide, and appear to have filled the space of older northwest-trending faults (Easton, 2009). Sudbury dykes typically range in composition from olivine diabase, amphibole diabase, diabase, magnetite-bearing diabase to lamprophyre diabase.
- East-northeast-trending Grenville Suite dykes (ca. 590 Ma; Kamo et al., 1995). Within the Superior Province these dykes are parallel to the Ottawa graben, and individual dykes are generally less than 15 metres in width. These dykes are not considered to be numerous in the area.

Within an aeromagnetic data set, the dyke swarms in the area are generally distinguishable by their unique strike directions, cross-cutting relationships and, to a lesser extent, by the amplitude of the associated, magnetic anomalies.

## 2.3 Structural History

The structural history of the area is complex. Investigations within the study area and its vicinity conclude that the region has undergone complicated polyphase deformation (e.g., Card et al., 1972; Young, 1983; Riller et al., 1999; Jackson, 2001; Easton, 2005). The most comprehensive studies on the structural geology of the area and its vicinity have been carried out by Zolnai et al. (1984), Riller et al. (1999) and Jackson (2001). These and other investigations documenting the structural geology of particular portions of the area (e.g. Easton, 2005) support the presence of up to three main deformation orogenic phases which have overprinted all bedrock lithologies, and have been assigned

to the Blezardian, Penokean, and Grenville orogenies. It should be noted, however, that the occurrence of the Penokean Orogeny in the area remains controversial (e.g. Davidson et al., 1992; Piercey et al. 2003), and evidence for the Grenville Orogeny is scarce. As the aforementioned studies were performed at various scales and from various perspectives, the following summary of the structural history of the area should be considered as a best-fit model that incorporates relevant findings from all studies. The structural history of the area is described below and summarized in Table 2.

It is understood that there are potential problems in applying a regional deformation numbering (Dx) system into a local geological history. Nonetheless, the following summary offers an initial interpretation for the area, which may be modified in the future if site-specific information is collected.

The earliest deformation phase ($D_1$) is associated with ca. 2.72- to 2.7-billion-year old penetrative deformation of rocks of the Whiskey Lake and Benny Lake greenstone belts. According to Jensen (1994), this penetrative deformation is represented by foliation closely paralleling the strike and dip of the metavolcanic and metasedimentary strata composing the greenstone belts. The foliation was likely developed concurrent with folding which is expressed by a west-northwest-trending, isoclinal syncline. Easton (2010) reported the existence of an east-trending shear zone apparently overprinting only the greenstone rocks. Later truncation of the foliation by plutonic material indicates that much of this deformation occurred prior to at least the youngest phase of emplacement of the ca. 2.716 to 2.651-billion-year old Ramsey-Algoma granitoid complex (Jensen, 1994).

Subsequent to emplacement of the Ramsey-Algoma granitoid complex, $D_2$ deformation comprised a series of northeast-striking sinistral strike-slip faults and shear zones, and later subvertical east-northeast-striking sinistral-oblique faults and shear zones that were formed along the margins of the greenstone belts. At least two regionally extensive east- to northeast-trending faults (the Murray and Flack Lake faults) may have initiated during $D_2$. The Flack Lake Fault transects the southern portion of the assessment area, while the Murray Fault occurs approximately 60 km south of the assessment area along the north shore of Lake Huron and continues northeast to transect the Sudbury Igneous complex. The age of $D_2$ fault initiation is poorly constrained to between ca. 2.651 and 2.5 billion years ago (JDMA, 2014a). The Flack Lake Fault has been variously interpreted as a Neoarchean thrust fault or listric-normal fault that was inverted during the Neoarchean and reactivated during the Blezardian ($D_4$) and Penokean ($D_5$) orogenies (Jensen, 1994 and Jackson, 2001); or as a listric normal fault that initiated in relation to rifting of the Archean continental margin during the early Proterozoic (Zolnai et al. 1984; Spray et al., 2004). Jensen (1994) suggests that south of the study area in the Whiskey Lake greenstone belt, two episodes of Archean faulting produced northeast-trending, arcuate sinistral faults and subsequent east-northeast-trending, subvertical sinistral faults.

**Table 2: Geological and Structural History of the Area (adapted from JDMA, 2014a)**

| Approximate Time Period (years before present) | Geological Event |
|---|---|
| 2.72 to 2.651 Ga | Kenoran Orogeny<br>• Deposition, emplacement and deformation of the ca. 2.72- to 2.68-billion-year old Whiskey Lake and Benny Lake greenstone belts and ca. 2.716- to 2.651-billion-year old Ramsey-Algoma granitoid complex.<br>• Development of folds and east-trending foliation in the greenstone belts (ca. 2.72 to 2.70 billion years ago). [$D_1$] |
| <2.651 to 2.50 Ga | • Early (re)activation of NE-, ENE-, E-W-, WNW- and NW-striking faults (e.g., Murray and Flack Lake faults) [$D_2$] |
| 2.497 to 2.47 Ga | Onset of continental break-up [$D_3$]; rifting across Lake Superior.<br>• Deposition of volcanic rocks and basal sedimentary rocks of the Huronian Supergroup.<br>• Reactivation, or continued activity, of WNW- to NW- and E-striking faults.<br>Widespread mafic magmatism, and emplacement of:<br>• Agnew Lake intrusion and East Bull Lake intrusion (2.49 to 2.47 billion years);<br>• Matachewan dyke swarm (ca. 2.473 billion years). |
| 2.47 to > 2.30 Ga | Blezardian Orogeny [$D_4$]<br>• Thick-skinned folding of Archean basement and basal rocks of the Huronian Supergroup. Initiation of Quirke Lake syncline and Chiblow anticline. |
| <2.3 and > 2.10 Ga | Transition to passive margin setting<br>• Continued deposition of sedimentary rocks of Huronian Supergroup.<br>Emplacement of:<br>• Biscotasing dyke swarm (ca. 2.167 billion years);<br>• Marathon dyke swarm (ca. 2.121 billion years). |
| 2.10 to 1.89 Ga | Denudation of bedrock and formation of peneplain. |
| 1.89 to 1.84 Ga | Penokean Orogeny [$D_5$]<br>• Crustal shortening and development of thrust-and-fold belt in rocks of the Huronian Supergroup, buckling and faulting of Archean basement.<br>• Subgreenschist and amphibolite grade metamorphic overprint to north and south of Murray fault, respectively.<br>Emplacement of:<br>• Sudbury Igneous Complex (ca. 1.85 billion years);<br>• North Channel dyke swarm (ca. 1.6 to 2.5 billion years, and associated with 1.884 billion year old Molson dyke swarm and Wabigoon dyke swarm). |
| 1.75 to 1.70 Ga | Emplacement of ca. 1.70-billion-year old Cutler pluton, associated metasomatism of the Huronian Supergroup, and metamorphic overprint of rocks south of Murray fault, ca. 1.75 to 1.70 billion years ago (Fedo et al., 1997). |
| 1.238 to 1.235 Ga | Emplacement of Sudbury dyke swarm and related intrusions of unclassified olivine diabase dykes. |
| 1.25 to 0.98 Ga | Grenville Orogeny<br>• Develop of Midcontinental Rift (ca. 1.1 billion years ago) [$D_6$] |
| <1.1 to present | Denudation of bedrock, formation of peneplain, ca. 1.1 to 0.54 billion years ago (continuation of $D_{6)}$.<br>Sedimentation, erosion, ingression and regression of sea water, shallow sea, glaciations.<br>Exhumation of peneplain ca. 0.54 billion years ago to present. |
| Ca. 0.59 Ga | Emplacement of Grenville dyke swarm |

Jolly (1978) and Zolnai et al. (1984) suggest that subsequent to $D_2$, Archean faulting was followed by a large-scale rifting event ($D_3$) that overprinted the area in association with the ca. 2.497- to 2.47-billion-year old break-up of the Superior Craton (Williams et al., 1991). This was associated with the development of east-trending rifts and overlapped in time with the earliest Proterozoic deposition of the basal volcano-sedimentary rocks of the Huronian Supergroup (Jensen, 1994); the widespread emplacement of mafic intrusions such as the Agnew Lake and East Bull Lake intrusions (Vogel et al., 1998; Easton, 2009) southeast of the study area; and emplacement of the pervasive Matachewan dyke swarm. $D_3$ was associated with reactivation of regional $D_2$ faults, including the Murray and Flack Lake faults, as down-to-the-south synsedimentary growth faults during the formation of the Huronian Supergroup (Zolnai et al., 1984). This event was accompanied by the initiation, or dextral reactivation, of east-southeast- to southeast-striking faults that cross-cut earlier formed structures throughout the Huronian Supergroup (Jackson, 2001). These younger faults also cut the Archean basement and the Murray fault (Jackson, 2001). Jensen (1994) indicates that the southeast-trending faults are intruded by undeformed feldspar porphyry dykes, presumably associated with the Matachewan and Sudbury dyke swarms. While typically assumed to be the youngest generation of faulting, Jensen (1994) and Jackson (2001) concede that some of the southeast-trending faults may have initiated as Late Archean ($D_2$) structures that subsequently experienced a long history of reactivation during and post-dating the $D_5$ Penokean Orogeny.

The Blezardian Orogeny is assigned as the fourth deformation event, $D_4$, in the area. The Blezardian Orogeny produced steeply south-dipping reverse faults and upright, kilometre-scale folds (Zolnai et al., 1984). The timing of the Blezardian Orogeny is poorly constrained. It is thought to have occurred between ca. 2.4 (possibly as early as 2.47 billion years ago), and 2.3 billion years ago (Riller et al., 1999; Raharimahefa et al., 2011).

The ca. 1.89- to 1.84-billion-year old Penokean Orogeny ($D_5$) involved dextral shearing and horizontal shortening (Riller et al., 1999) in the area. Crustal shortening and fault reactivation enhanced the previously buckled (Blezardian) structure of the Archean basement and further compressed, folded and faulted rocks of the Huronian Supergroup, so that overlapping thrusted blocks stacked up to possibly 15 km in burial thickness (Zolnai et al., 1984). South of the assessment area, and south of the Murray Fault, medium to high grade metamorphic assemblages developed within Huronian Supergroup rocks, and penetrative, ductile deformation features developed that included cleavage, stretching lineation, and rotation of the tectonic fabric to a near-vertical orientation (Zolnai et al., 1984). Ductile deformation features associated with $D_5$ are not observed in the assessment area. Northwest-trending strike-slip faults such as the Spanish American, Pecors Lake and Horne Lake faults that cut the Huronian Supergroup sequence and the parallel Nook Lake fault within the Archean basement directly north of the Quirke Lake syncline (Robertson, 1968), may have been formed during the Penokean Orogeny, or they may be reactivated Archean faults as suggested by Jackson (2001). The effect that the syn-Penokean meteorite impact, which produced the Sudbury Igneous Complex, had on the geological and structural evolution of the area is unclear.

Deformation associated with the Grenville Orogeny ($D_6$), ca. 1.250 to 0.98 billion years ago, is considered the final major deformation episode. In spite of the scarcity of evidence and problems of deformation overprinting and fault reactivation, it seems that the Murray fault remained active or was reactivated during this orogeny (Robertson, 1970; Card, 1978; McCrank et al., 1989; Piercey, 2006). The Midcontinent Rift (ca. 1.1 to 1.0 billion years ago) was developed contemporaneously with the long-lived Grenville Orogeny and is also included as part of $D_6$, although its effect on the area is not known. There are poor constraints on any subsequent fault reactivation in the area, therefore all possible post-Grenville fault reactivation is included as part of a protracted $D_6$ event.

### 2.3.1 Mapped Structures

In the area, the regional scale arcuate east-trending Flack Lake fault extends for approximately 150 km and transects the Ramsey-Algoma granitoid complex in the southern portion of the study area. The Flack Lake fault is interpreted as a north-directed listric thrust that reactivated an earlier normal fault. Its movement history may be related to the Penokean event (Bennett et al., 1991).

## 2.4 Metamorphism

Studies on metamorphism in Precambrian rocks across the Canadian Shield have been summarized in a few publications since the 1970s (e.g., Fraser and Heywood,1978; Kraus and Menard, 1997; Menard and Gordon, 1997; Berman et al., 2000; Easton, 2000a; 2000b; Holm et al., 2001, and Berman et al., 2005) and the thermochronological record for large parts of the Canadian Shield is documented in a number of studies (Berman et al., 2005; Bleeker and Hall, 2007; Corrigan et al., 2007; and Pease et al., 2008).

The Superior Province of the Canadian Shield largely preserves low-pressure–high-temperature Neoarchean (ca. 2.710-2.640 Ga) metamorphic rocks. The relative timing and grade of regional metamorphism in the Superior Province corresponds to the lithological composition of the subprovinces (Easton, 2000a; Percival et al., 2006). Subprovinces comprising volcano-sedimentary assemblages and synvolcanic to syntectonic plutons (i.e., granite-greenstone terranes) are affected by relatively early lower greenschist to amphibolite facies metamorphism. Subprovinces comprising both metasedimentary- and migmatite-dominated lithologies, such as English River and Quetico, and dominantly plutonic and orthogneissic domains, such as Winnipeg River, are affected by relatively late middle amphibolite to granulite facies metamorphism (Breaks and Bond, 1993; Corfu et al., 1995). Subgreenschist facies metamorphism in the Superior Province is restricted to limited areas, notably within the central Abitibi greenstone belt (e.g., Jolly, 1978; Powell et al., 1993).

In general, most of the Canadian Shield preserves a complex episodic history of Neoarchean metamorphism overprinted by Paleoproterozoic tectonothermal events culminating at the end of the Grenville orogeny ca. 950 Ma. The distribution of contrasting metamorphic domains in the Canadian Shield is a consequence of relative uplift, block rotation, and erosion resulting from Neoarchean orogenesis, subsequent local Proterozoic orogenic events and broader epeirogeny during later Proterozoic and Phanerozoic eons.

Metamorphic grade in the area is largely of subgreenschist facies north of the Murray Fault, east and north of Blind River. South of the Murray Fault (Piercey, 2006), metamorphism increases to localized lower amphibolite facies extending eastward between Blind River, Sudbury and the Grenville Front (Riller et al., 1999). Most authors (e.g., Zolnai et al., 1984) have considered the medium grade metamorphism reached south of the Murray fault to be a product of tectonothermal burial. However, Jackson (2001) pointed out that the high temperature-low pressure metamorphism reached could not be solely the result of burial, and he advanced the alternative of a second period of crustal extension in the area. This hypothesis would not only account for the required heat for medium grade metamorphism but would also explain the emplacement of Nipissing intrusions south of the area. Holm et al. (2001) suggested that peak Penokean Orogeny metamorphism occurred ca. 1.835 billion years ago, based on monazite ages. More recently, Piercey (2006) showed that the Penokean Orogeny was only the first of several accretionary events that impinged on the southern Laurentide margin and presented evidence of a younger and more significant metamorphic event, possibly related to the Yavapai tectonothermal pulse at ca. 1.7 billion years ago. This event may have affected the metamorphic conditions in the area and possibly increased the metamorphic overprint to greenschist facies, at least in the area proximal to the Cutler pluton on the north side of the Murray

fault. Fedo et al. (1997) indicated that a ca. 1.7 to 1.75 billion years ago metasomatic event is evident in potassic and sodic alterations of the Huronian Supergroup north of the Murray Fault. This event likely replaces most metamorphic minerals in the Huronian Supergroup with white mica and is presumably related to fluid-flow driven by post-orogenic uplift of the Penokean Orogeny. Minor contact metamorphism exists in the metavolcanic rocks of the greenstone belt near some of the large Proterozoic mafic intrusions (Rogers, 1992).

## 2.5 Quaternary Geology

Quaternary geology of the area is described in detail in the terrain evaluation completed as part of the Phase 1 Desktop Preliminary Assessment (JDMA, 2014b). An overview of the relevant Quaternary features are presented in Figure 3, and summarized below.

The Quaternary geology of the area is dominated at surface by different types of glacial deposits that accumulated with the progressive retreat of the ice sheet during the end of the Wisconsinan glaciation. This period of glaciation began approximately 115,000 years ago and peaked approximately 21,000 years ago, at which time the glacial ice front extended south of Ontario into what is now Ohio and Indiana (Barnett, 1992).

The area is dominated by exposed bedrock or bedrock having only a thin cover of unconsolidated sediments. Quaternary deposits are predominantly located in bedrock controlled valleys. Overburden deposits within this area were mapped as part of the Northern Ontario Engineering Terrain Study (NOEGTS), a program undertaken between 1977 and 1981 (Gartner, 1978a,b,c; 1980 a,b; Roed and Hallet, 1979a,b,c,d; 1980a,b; VanDine, 1979a,b,c,d; 1980a,b,c,d; Gartner et al., 1981). These studies divided the landscape into a set of distinct terrain units within which the engineering characteristics are broadly predictable. Major landforms mapped by the NOEGTS program are shown on Figure 3.

Data on ice flow direction compiled from the literature (Karrow, 1987) reveal that glacial ice flowed in a generally southwesterly direction across the area from the Hudson Bay basin. Ford (1993) recognized two dominant orientations in glacial striations, lunate fractures, drumlinoid features, and till flutings in the Rawhide Lake area to the north of the City of Elliot Lake. These are recorded as 175° (165° to 180°) and 195° (190° to 210°). At three sites, older 100° to 120° striations were found intersecting either the 175° or 195° sets.

The most widely occurring and oldest known stratigraphic unit in the area is a silty sand to sandy silt till found overlying bedrock in low relief areas and along the flanks of topographic lows. It is typically thin and discontinuous and is coarse-textured, unsorted, and boulder-rich, although there are some areas of compact, massive to fissile and gravelly to silty and sandy till (Barnett et al., 1991). Glaciolacustrine sediments have more limited distribution and are limited to only very small mappable surficial units (Ford, 1993) largely along river valleys. These units are typically composed of laminated silt and fine sand and silt-clay rhythmites, and may be related to the series of postglacial lakes of the Lake Huron basin.

Deposits of glaciofluvial outwash are commonly encountered along valleys in the area. Glaciofluvial outwash is common in low-lying areas and occasionally in esker ridges with the local formation of terraces related to changing lake levels in the Lake Huron basin. Thick deposits of alluvial sand and gravel are found along many of the rivers in the region. Recent swamp, lake, and stream deposits are also common throughout the area (JDMA, 2014b). A more detailed accounting of glacial deposits in the area is provided by JDMA (2014b).

# 3 Methodology

The structural lineament interpretation of the area was based on high-resolution remote sensing data sets, including a high-resolution airborne magnetic survey contracted by the NWMO to Sander Geophysics Limited (SGL, 2017), digital elevation data (DEM) collected during the airborne magnetic survey (SGL, 2017), and high-resolution Ontario Ministry of Natural Resources Forest Resources Inventory (FRI) digital aerial imagery procured from Land Information Ontario (OMNR, 2009).

## 3.1 Source Data Description

All data were assessed for quality, enhanced, and reviewed before use in the lineament interpretation. The geophysical data were used to evaluate potential deeper bedrock structures, and were instrumental in identifying potential bedrock structures beneath areas of surficial cover. Furthermore, the geophysical data were instrumental in establishing the age relationships among the different lineament sets. Topographic (DEM) and FRI digital aerial imagery data sets were used to identify surficial lineaments expressed in the topography, drainage, and vegetation. For this study, the best resolution data available was used for the lineament interpretation.

### 3.1.1 High-resolution Aeromagnetic Data

Sander Geophysics Limited (SGL) completed a fixed-wing high-resolution airborne magnetic survey in the area (SGL, 2017; Figure 4).

The airborne survey in the area included a total of 10,057 km of flight lines. Flight operations were conducted out of the Municipal Airport (CYEL), in Elliot Lake, Ontario, using two Britten Norman Islanders. Data were acquired along traverse lines flown in a north-south direction spaced at 100 m, and control lines flown east-west spaced at 500 m. The survey was flown at a target altitude of 70 m above ground level, with an average ground speed of 95 knots (approximately 176 km/h or 49 m/s). The survey acquisition parameters are listed below:

- Traverse line spacing of 100 m
- Traverse line azimuth of 000 - 180°
- Control line spacing of 500 m
- Control line azimuth of 090 - 270°
- Grid cell size of 25 m
- Targeted sensor height of 70 m
- Acquisition date of April 2016 to May 2016 and from February 2017 to March 2017

Acquired data were processed by SGL (SGL, 2017) and provided to SRK as GRD files. The following products of the high resolution airborne magnetic survey were available for this structural lineament interpretation:

- Total magnetic intensity.
- First vertical derivative of the reduced to pole total magnetic intensity.
- Second vertical derivative of the reduced to pole total magnetic intensity.
- Tilt derivative of the reduced to pole total magnetic intensity.

The reduced to pole total magnetic intensity, first and second vertical derivatives, and tilt derivative grids were converted to ERS images in ERMapper, then shaded by intensity, and the data ranges and colour were enhanced to highlight potential structures. Ultimately, a series of compressed raster images was created in ERMapper for use in ArcGIS.

### 3.1.2 Digital Elevation Model

Digital elevation data (DEM) were collected during the magnetic survey conducted by SGL (SGL, 2017). The survey acquisition parameters are identical to those described for the high-resolution magnetic data in Section 3.1.1.

DEM data were processed by SGL and provided to SRK as GRD files. The data grid was then converted to an ERS image in ERMapper, and the data ranges, hill shading (using sun angles of 000°, 045°, and 315°), and colour ranges of the DEM were enhanced to highlight potential structures (Figure 5). Compressed raster images were created in ERMapper for use in ArcGIS.

### 3.1.3 High-resolution Digital Aerial Imagery

High resolution digital aerial imagery was obtained from the Ontario Ministry of Natural Resources Forest Resources Inventory (FRI) (OMNR, 2009).

Digital aerial imagery was collected using a Leica ADS40 Airborne Digital Sensor. The ADS40 sensor captures multispectral bands simultaneously at the same true resolution, and therefore produces a four-band, truly co-registered and equal resolution imagery (not pan sharpened) from the data acquisition. The spectral ranges and spatial resolution of each band are listed in Table 3.

Prior to release to the public, the imagery tiles were run through a bidirectional reflectance distribution function (BRDF) process to remove atmospheric distortions associated with sun angles. Subsequently, blocks of orthorectified tile imagery were compiled and processed to be normalized using the brightest and darkest values within the multi-date acquisition. Each image consists of a mosaic of 5-by-5-kilometre orthorectified tiles of four-band data.

A natural colour composite of the FRI digital aerial imagery was created in ArcGIS and used for the lineament interpretations (Figure 6).

**Table 3: FRI Digital Aerial Imagery Band Ranges and Resolution**

| Band | Range (nm) | Resolution (m) |
|---|---|---|
| Panchromatic | 465 - 680 | 0.2 |
| Blue | 428 - 492 | 0.4 |
| Green | 533 - 587 | 0.4 |
| Red | 608 - 662 | 0.4 |

## 3.2 Lineament Interpretation Workflow

The structural lineament assessment of the area was conducted to identify the location and orientation of potential individual fractures or fracture zones, and dykes, and to evaluate their relative timing relationships within the context of the local and regional geological setting.

Lineaments were interpreted using a workflow designed to address issues of subjectivity and reproducibility that are inherent to any lineament interpretation. The workflow followed a set of detailed guidelines using the high-resolution airborne geophysical (magnetic) and high-resolution surficial (DEM and FRI digital aerial imagery) data sets described above. Throughout the report the term geophysical lineaments refers to structures interpreted from the high-resolution magnetic data. The interpretation guidelines involved three steps:

- Step 1: Independent lineament interpretation by two individual interpreters for each data set and assignment of certainty level (1, 2, or 3 representing low, medium and high certainty);
- Step 2: Integration of lineament interpretations for each individual data set and first determination of reproducibility;
- Step 3: Integration of lineament interpretations for the surficial data sets (DEM and digital aerial imagery) followed by integration of the combined surficial data set with the geophysical data set, with determination of coincidence in each integration step.

Each identified lineament feature was classified in an attribute table in ArcGIS. The description of the attribute fields used is included in Table 4. Fields 1 to 9, and Fields 19 and 20 were populated during Step 1. Fields 10 and 11 were populated during Step 2. Fields 12 to 18 were populated during Step 3.

The interpreted geophysical and final integrated lineaments were classified into three general categories based on a working knowledge of the structural history and bedrock geology of the area. These categories include form lines, brittle and dyke lineaments, described as follows:

- **Form lines:** Features interpreted to represent the internal fabric of the rock units (including sedimentary or volcanic layering, tectonic foliation or gneissosity, and magmatic foliation). Form lines are typically characterized by semi-continuous linear to curvi-linear magnetic highs that appear to define the grain of the rock units. See Appendix Figure A1 for example.
- **Brittle lineaments:** Features interpreted as fractures (joints or joint sets, faults or fault zones, and veins or vein sets). This category also includes brittle partings interpreted to represent discontinuous reactivation parallel to the ductile fabric (e.g., form lines). Brittle lineaments are commonly characterized by continuous magnetic lows, offsets of magnetic highs, offset of form lines, and breaks in topography and vegetation. At the desktop stage of the investigation, this category also includes features of unknown affinity. See Appendix Figure A2 for example.
- **Dyke lineaments**: Features interpreted as dykes, on the basis of their distinct character (e.g., scale orientation, geophysical signature and topographic expression). Dykes were dominantly interpreted from the magnetic data set, and are typically characterized by continuous linear magnetic highs. The interpretation of dykes is also combined with pre-existing knowledge of the bedrock geology of the study area. See Appendix Figure A3 for example.

It should be noted that in previous Phase 2 lineament interpretations (e.g. SRK, 2015a, b, and c), an additional category of lineament was interpreted (termed “unclassified lineaments”). The unclassified lineaments were defined as linear to curvi-linear features that did not exhibit characteristics to easily form an interpretation. The possible interpretations of the unclassified lineaments included ductile or brittle-ductile shear zones, or the internal fabric of the rock. Lineaments with these characteristics were not identified in this assessment area, and as such unclassified lineaments have been omitted from this interpretation.

**Table 4: Attribute Table Fields Populated for the Lineament Interpretation**

| ID | Attribute | Brief Description |
|---|---|---|
| 1 | Rev_ID | Reviewer initials |
| 2 | Feat_ID | Feature identifier |
| 3 | Data_typ | Data set used (MAG, DEM, FRI) |
| 4 | Feat_typ | Type of feature used to identify each lineament<br><br>Digital Aerial Imagery:<br>1. Lineaments drawn along straight or curved lake shorelines<br>2. Lineaments drawn along straight or curved changes in intensity or texture (i.e., vegetation)<br>3. Lineaments drawn down centre of thin rivers or streams<br>4. Lineaments drawn along a linear chain of lakes<br>5. Other (if other, define in comments)<br><br>Digital Elevation Model:<br>1. Lineaments drawn along straight or curved topographic valleys<br>2. Lineaments drawn along straight or curved slope walls<br>3. Other (if other, define in comments)<br><br>Airborne Geophysics (magnetic and electromagnetic data):<br>1. Lineaments drawn along straight or curved magnetic high<br>2. Lineaments drawn along straight or curved magnetic low<br>3. Lineaments drawn along straight or curved steep gradient<br>4. Other (if other, define in comments) |
| 5 | Name | Name of feature (if known) |
| 6 | Certain | Value describing the interpreters confidence in the feature being related to bedrock structure (1-low, 2-medium or 3-high) |
| 7 | Length* | Length of feature is the sum of individual lengths of mapped polylines and is expressed in kilometres. Lineament lengths only reflect the length of the portion of the lineament that is contained within the individual lineament assessment block |
| 8 | Width** | Width of feature; this assessment is categorized into 5 bin classes:<br>A. < 100 metres<br>B. 100 – 250 metres<br>C. 250 – 500 metres<br>D. 500 – 1,000 metres<br>E. > 1,000 metres |
| 9 | Azimuth | Lineament orientation expressed as degree rotation between 0 and 180 degrees |
| 10 | Buffer_RA_1 | Buffer zone width for first reproducibility assessment (in metres) |
| 11 | RA_1 | Feature value (1 or 2) based on reproducibility assessment |
| 12 | Buffer_RA_2 | Buffer zone width for coincidence assessment (in metres) |
| 13 | RA_2 | Feature value (1, 2 or 3) based on coincidence assessment |
| 14 | MAG | Feature identified in geophysical data set (Y or Blank) |
| 15 | DEM | Feature identified in DEM data set (Y or Blank) |
| 16 | SAT | Feature identified in satellite imagery data set (Y or Blank) |
| 17 | F_Width | Final interpretation of the width of feature |
| 18 | Rel_age | Interpretation of relative age of feature, in accord with regional structural history |
| 19 | Comment | Comment field for additional relevant information on a feature |
| 20 | Object | Geological element identified, e.g., form lines, brittle lineament, dyke lineament. |

* The length of each interpreted feature is calculated based on the sum of all segment lengths that make up that lineament.

** The width of each interpreted feature is determined by expert judgment and utilization of a GIS-based measurement tool. Width determination takes into account the nature of the feature as assigned in the Feature type (Feat_typ) attribute.

A detailed description of the three workflow steps and the methodology for determining the associated attribute fields for each interpreted lineament is provided below.

### 3.2.1 Step 1: Lineament Interpretation and Certainty Level

To accommodate the generation of the best possible unbiased lineament interpretation, two individual interpreters followed an identical process for structural lineament analysis during Step 1. The first step of the lineament interpretation was to have each individual interpreter independently produce GIS lineament maps, and detailed attribute tables, for each of the three data sets. Step 1 of the structural lineament analysis was conducted up to a scale of 1:25,000 and followed a designated workflow.

The interpretation of magnetic data followed a two-step process. The first step involved the drawing of form lines (Figure 7). Form lines were drawn along linear to curvi-linear magnetic highs as seen in the high-resolution first vertical derivative magnetic data. Locally, where the magnetic contrast was low, the tilt angle derivative data were used to enhance magnetic features. The form lines were interpreted to trace the geometry of stratigraphy, or tectonic foliation within metavolcanic and metasedimentary rocks, and the internal fabric (foliation or magmatic layering) within granitoid batholiths and gneissic rocks. Magnetic highs associated with dykes (i.e., linear cross-cutting magnetic highs in orientations identified in the literature as dyke orientations) were not included in this process.

Form line construction highlighted discontinuities between form lines (e.g., form lines intersecting or truncating) that may represent structures (faults, folds), unconformities, or intrusive contacts. The process of drawing form lines was instrumental in highlighting other lineaments in the magnetic data.

The second step involved drawing a structural base layer that represented all interpreted lineaments regardless of interpreted age, type (e.g., brittle or dyke), or kinematics. Evidence for lineaments was derived from several sources in the magnetic data, including discontinuities between form lines, offset of magnetic units, or the presence of linear magnetic lows or highs. The first vertical derivative magnetic data was used mainly with the tilt angle derivative data to further enhance this interpretation.

The lineament interpretation of DEM data involved tracing linear or curvi-linear features along topographic valleys, slope walls, and any other relevant features that were visible in a colour shaded DEM derived from the airborne geophysical survey data. Similarly, the lineament interpretation of digital aerial imagery involved tracing linear or curvi-linear features along visible shore lines, changes in colour intensity or texture (e.g., vegetation), linear rivers and streams, and along linear chains of features associated with lakes that were visible in the FRI imagery. Particular care was taken for lineaments that were coincident with eskers in the FRI data. Unless there was clear evidence for a surficial lineament to be associated with a bedrock feature, lineaments that were coincident with eskers were not drawn.

Lineaments from each of the data sets were assigned attributes by each interpreter to characterize what type of feature the lineament corresponded to, the interpreter's certainty that the lineament represented a bedrock structure, and the approximate width of the topographic feature.

Lineaments identified in the DEM and or the digital aerial imagery that were interpreted to be related to glacial events were excluded from the lineament interpretation data set. The following criteria were used to decide whether a DEM or digital aerial imagery lineament should be excluded:

- The lineament coincided with a mapped ice-flow feature, moraine, or esker.
- The lineament was parallel to known eskers or moraines and was marked by narrow, curving ridges.
- The lineament was parallel to the local ice flow direction and was accompanied by drumlin-shaped hills in the DEM data set.

The Step 1 lineament analysis resulted in the generation of one interpretation for each data set (e.g., magnetic, DEM, digital aerial imagery) for each interpreter, resulting in a total of six individual GIS layer-based interpretations. Where evident, lineament segments were merged, and lineament lengths calculated, resulting in final lineament lengths that corresponded to the sum of all merged segments.

During Step 1, identified lineaments were attributed with Fields 1 to 9, and Fields 19 and 20 (Comment and Object attribute) as listed in Table 4.

### 3.2.2 Step 2: Lineament Reproducibility Assessment 1 (RA_1)

During Step 2, individual lineament interpretations produced by each interpreter were compared for each data set (e.g., two individual DEM lineament interpretations). This included a reproducibility assessment based on the coincidence, or lack thereof, of the interpreted lineaments within a data set specific buffer zone. The two individual lineament interpretations for each data set were then integrated and a single interpretation was generated for each data set (Figure 8 to Figure 10). A discussion of the parameters used during this step follows.

#### Buffer Size Selection

Buffer sizes for lineaments in each data set were based on the magnetic grid resolution. The buffer size was determined using trial-and-error over a selected portion of the lineament interpretation. A buffer size of five times the grid cell resolution (25 m) was selected as it provided a balanced result for assessing reproducibility. A buffer of 125 m (either side of the lineament) was generated for the magnetic data. Given that the DEM data were extracted from the same survey, the same buffer size was applied to the DEM data. A 125-metre buffer was also applied to the digital aerial imagery data in order to be consistent with the magnetic and DEM buffer size.

The buffer size widths were included in the attribute fields of each interpretation file (Table 4). The buffers were used as an initial guide to determine coincidence between lineaments, with the expert judgement of the interpreter ultimately determining which lineaments were coincident.

#### Reproducibility Assessment

The generation of an integrated lineament interpretation for each data set, including the reproducibility assessment, followed a three-step process:

- Lineament buffers were generated for both individual Step 1 interpretations. The lead interpreter's Step 1 lineaments were then overlain on top of these buffers, and all lineaments that occurred within overlapping buffers were carried forward and copied into a new file for Step 2. These lineaments were attributed with a reproducibility value (RA_1;Table 4) of two in the Step 2 attribute table. In addition, if two lineaments were deemed coincident, the highest certainty value from either lineament was carried forward. During this process, based

upon insight gained from analyzing the separate interpretations together, the geometry of the lineament that was carried forward was occasionally adapted to better reflect the underlying data.

- The remaining lineaments in the lead Step 1 interpretation were then manually analyzed by both interpreters on the basis of the available imagery for each data set. In some instances, this included adapting the shape and extent of individual lineaments to increase the accuracy of spatial location or length of the lineament, and carrying the adapted lineament forward into the Step 2 interpretation file. These lineaments were attributed a RA_1 value of one in the Step 2 attribute table. Where it was determined by the two interpreters that these features were not representative of potential bedrock structure, they were removed from the data set.
- Finally, the second Step 1 lineament interpretation was overlain on top of the Step 2 integrated file, and all remaining lineaments in the second interpreter's Step 1 interpretation were then manually analyzed by both interpreters on the basis of the available imagery for each data set. In some instances, this included adapting the shape and extent of individual lineaments to increase the accuracy of spatial location or length of the lineament, and carrying the adapted lineament forward into the Step 2 interpretation file. These lineaments were attributed a RA_1 value of one in the Step 2 attribute table. All remaining lineaments that were attributed a certainty value of one were analyzed by both interpreters, and removed if it was determined that these features were not representative of potential bedrock structures.

As specified above, the decision on whether or not to adapt the shape and extent of an individual lineament, or whether the lineament was carried forward to the next step was based on analysis of the specified lineament with the available dataset and a discussion between the two interpreters. If a lineament was drawn continuously by one interpreter but as individual, spaced, or disconnected segments by the other interpreter, the longer lineament, or the lineament that most accurately represented the underlying feature was carried forward to the Step 2 interpretation with a RA_1 value of two.

The resulting Step 2 interpretations for each data set (e.g., magnetics, DEM, and FRI digital aerial imagery) were then slightly refined to avoid any structurally inconsistent or geologically improbable relationships. Any modifications of lineaments were minor, took place within the limits of the assigned buffer zone, and respected the underlying data.

### 3.2.3 Step 3: Coincidence Assessment (RA_2)

During Step 3, the integrated lineament interpretations for each data set were amalgamated into one final interpretation. First, lineaments derived from the DEM and digital aerial imagery were merged to produce an integrated surficial lineament data set (Figure 11). Subsequently, the geophysical lineaments (Figure 12) were integrated with the integrated surficial lineaments to produce a final integrated interpretation (Figure 13). A discussion of the parameters used during this step follows below.

#### Surficial Lineament Integration

The FRI digital aerial imagery data have a resolution of 40 cm while the DEM data have a resolution of approximately 25 m. Furthermore, the orientation of minor and intermediate topographic features as identified in the DEM can be ambiguous due to the resolution of the data, while these features could be drawn with greater precision from the FRI digital aerial imagery. Therefore, lineaments derived from the FRI data were used as the lead data set, and lineaments drawn from DEM data were used as the secondary data set.

A buffer of 125 m (five times the resolution of the DEM data) was generated around the DEM lineaments and the FRI lineaments were overlain on top of this buffer. Similar to the procedure in RA_1, all lineaments that occurred within overlapping buffers were carried forward and copied into a new file. These lineaments were attributed with a RA_2 reproducibility value of two (RA_2; Table 4). In addition, if two lineaments were deemed coincident, the highest certainty value from either lineament was carried forward. During this process, based upon insight gained from analyzing the separate interpretations together, the geometry of the lineament that was carried forward was occasionally adapted within the boundaries of the buffer to better reflect the underlying data.

All remaining lineaments were then manually analyzed by both interpreters on the basis of the available imagery for each data set. In some instances, this included minor adaptations to the shape and extent of individual lineaments, within the limitations of the buffer, to increase the accuracy of spatial location, length of the lineament, and (or) preserve structural relationships. All these lineaments were then carried over and attributed with an RA_2 value of one in the attribute table (RA_2; Table 4). No lineaments were removed or significantly modified at this stage of the integration.

## Final Lineament Integration

The geophysical data supplied important information regarding structures in the subsurface. Therefore, for this step of the interpretation, the lineaments derived from geophysical data were given precedence over lineaments derived from surficial data, since the latter primarily provided information regarding the surface expression of potential structures.

On this premise, all lineaments derived from the magnetic data were included in the final interpretation. A buffer of 125 m (five times the resolution of the geophysical and DEM data) was generated around the integrated surficial lineaments, and the geophysical lineaments were overlain on top of this buffer. This buffer size was included as an attribute field for all interpreted lineaments (Buffer RA_2; Table 4). Similar to the procedure in RA_1, all lineaments that occurred within overlapping buffers were carried forward and copied into a new file. These lineaments were attributed with a RA_2 reproducibility value of two or three, depending on how many surficial data sets they were observed in (RA_2; Table 4). During this process, based upon insight gained from analyzing the separate interpretations together, the geometry of the lineament that was carried forward was occasionally adapted within the boundaries of the buffer to better reflect the underlying data.

The following rules were applied for determining coincidence between the data set specific lineament maps:

- If any coincidence of lineaments occurred between the two lineament data sets, the longest lineament was carried forward and attributed as derived from two (or more) data sets, regardless of the length of overlap between the lineaments. This meant that if any part of a lineament derived from one data set was identified in another data set, it was considered that this lineament was reproduced. In addition, if two lineaments were deemed coincident, the highest certainty value from either lineament was carried forward.
- A lineament derived from DEM and (or) FRI digital aerial imagery data that occurred within the buffer of a lineament derived from geophysical data was attributed as reproduced in the relevant data sets, if the orientation of the lineaments did not deviate significantly.
- Short (less than 500 m) discontinuous DEM and FRI digital aerial imagery data lineaments that were at low angles to geophysical data lineaments but extended outside the geophysical lineament buffer were considered to be coincident.
- Short (less than 500 m) DEM and FRI digital aerial imagery data lineaments that were at high angles to geophysical data lineaments, largely overlapped with the buffer zone from the

geophysical data lineament, and had no further continuity (i.e., singular elements), were carried forward to the final interpretation. This was done on the basis that these short segments may represent a bedrock structure, and as such, should be contained within the final integrated data set.

All remaining lineaments were then manually analyzed by both interpreters on the basis of the available imagery for each data set. In some instances, this included minor adaptations to the shape and extent of individual lineaments, within the limitations of the buffer, to increase the accuracy of spatial location, length of the lineament, and or preserve structural relationships. All these lineaments were then carried over and attributed with an RA_2 value of one (or two if observed in both surficial data sets) in the attribute table (RA_2; Table 4). No lineaments were removed or significantly modified at this stage of the integration. This resulted in a combined interpretation with lineaments derived from the magnetic and surficial data sets.

During this process, each lineament was attributed with a text field highlighting in which data sets it was identified. The final reproducibility value (RA_2; Table 4) was then calculated as the sum of the number of data sets in which each lineament was identified, i.e., a value of 1 to 3.

Subsequently, the relative age of each lineament was interpreted and populated in the attribute table (Rel_Age; Table 4). This incorporated a working knowledge of the structural history of the area, combined with an understanding of the characteristics in each lineament population (e.g., brittle, dyke). The structural history of the area is described in Section 2.3 based on the existing literature.

### 3.2.4 Lineament Trends

An analysis of lineament trends revealed different sets of structures, which can then be related to the known structural history of the area. Lineament orientations were assessed for each data set as a whole, within individual subareas, and within distinct geological units, to determine the dominant lineament trends, and potential conjugate sets.

Lineament orientations (azimuth) were calculated using ET EasyCalculate 10, an add-in extension to ArcGIS. This add-in provides a function (polyline_GetAzimuth.cal) that calculates the azimuth of each polyline at a user-specified point and populates an assigned attribute field. SRK used the mid-point of each interpreted lineament to calculate the azimuth. A limitation is acknowledged, however, for calculating a single orientation for curvi-linear structures.

Rose diagrams are circular or semi-circular histograms that depict orientation (azimuthal) data and frequency for each data bin. The histogram peaks show the frequency of occurrence of lineament orientations within each bin. Rose diagrams were produced in Spheristat, with frequencies divided into 10-degree bins, and weighted by length. The length weighting uses a linear function directly related to the lineament length, whereby a lineament with a length of 2 kilometres will have twice the weighting of a lineament with a length of 1 kilometre.

### 3.2.5 Lineament Length

Lineament lengths were calculated using a simple geometrical calculation of the total length of the polyline in ArcGIS. The length distribution of the various integrated data sets was analyzed through a comparison of summary statistics, histograms, and cumulative frequency plots. Histograms and summary statistics were computed using the Stanford Geostatistical Modelling Software (SGeMS). Histogram bins were computed using arbitrary 500-metre bins. Lineament lengths displayed and reported in the figures, statistics tables, and histogram plots only reflect the length of the portion of the lineament that is contained within the individual lineament assessment block.

There is no information available on the depth extent into the bedrock of the lineaments interpreted for the area. In the absence of available information, the interpreted length can be used as a proxy for the depth extent of the identified structures (Nur, 1982). A preliminary assumption may be that the longer interpreted lineaments in the area may extend to greater depths than the shorter interpreted lineaments. However, this is highly dependent on the style and structural history of a given lineament.

### 3.2.6 Lineament Density

Lineament density analyses were conducted using the ArcGIS Analysis and Spatial Analyst toolsets, and included creating lineament line density plots and lineament intersection point density plots for the magnetic, surficial, and final integrated lineament data sets.

Lineament line density of all interpreted lineaments in the area was determined by examining the statistical density of individual lineaments using ArcGIS Spatial Analyst. A grid cell size of 50 m and a search radius of 1.25 km (equivalent to half the size of the longest boundary of the minimum area size of a potential repository siting area) were used. The spatial analysis used a circular search radius examining the lengths of polylines intersected within the circular search radius around each grid cell.

The lineament intersection point density of all intersecting lineaments in the area was determined by extracting all points where two or more lineaments intersected, and then calculating the statistical density of these intersection points. Lineament intersections were extracted using the ArcGIS Analysis Tools Intersect function. The density distribution of these points was then calculated in ArcGIS Spatial Analyst by defining a neighbourhood around each raster cell centre, calculating the number of points that fall within the neighbourhood, and dividing by the area of the neighbourhood. A grid cell size of 50 m and a search radius of 1.25 km (equivalent to half the size of the longest boundary of the minimum area size of a potential siting area) were used.

# 4 Lineament Interpretation Results

The following section describes the results of the lineament interpretation for the area based on analysis of the geophysical and surficial (DEM, FRI digital aerial imagery) data sets. Lineaments interpreted and integrated from the various data sets are presented below and in Figure 7 to Figure 13. A summary of lineament statistics is presented in Appendix B.

## 4.1 Geophysical Lineaments (RA_1)

The interpretation of magnetic data allows for the identification of form lines, brittle, and dyke lineaments. Form lines traced from the magnetic data set are shown in Appendix A: Figure A1 and Figure 7, and are interpreted to represent the internal fabric of the rock units, including the internal fabric (foliation and magmatic layering) within plutonic and gneissic rocks. Discontinuities between form lines highlight potential brittle-ductile, and brittle structures (potential shear zones and/or fractures), unconformities, or intrusive contacts. Therefore, they constitute an essential data component that should be used along with the first vertical derivative of the magnetic data for interpreting brittle lineaments. A brief discussion of form lines is included in this report to provide context to the lineament interpretation, but were not included in the statistical analyses of the lineament data sets.

Within the lineament assessment area, a total of 844 geophysical lineaments were interpreted and classified as brittle and dyke lineaments. Each of these lineaments were identified and merged by the two interpreters based on interpretation from the geophysical data (Figure 8). Of the total number of geophysical lineaments 149 were interpreted as brittle lineaments, and 695 were interpreted as dyke lineaments. The length of all geophysical lineaments ranges from 0.10 to 28.36 km, with a median of 0.88 km and a mean of 1.77 km. Of the total geophysical lineaments, the reproducibility assessment between two interpreters identified coincidence for 470 lineaments (56%; RA_1 = 2) and a lack of coincidence for 374 lineaments (44%; RA_1 = 1). For the brittle lineaments, the reproducibility assessment between two interpreters identified coincidence for 55 lineaments (37%; RA_1 = 2) and a lack of coincidence for 94 lineaments (63%; RA_1 = 1). For the dyke lineaments, the reproducibility assessment between two interpreters identified coincidence for 415 lineaments (60%; RA_1 = 2) and a lack of coincidence for 280 lineaments (40%; RA_1 = 1).

Of the 844 lineaments interpreted, 620 (74%) were assigned the highest level of certainty (three), while 172 (20%) were assigned a moderate certainty value of two, and 52 (6%) were assigned a low certainty value of one. The certainty value reflects the certainty that the interpreted lineament represents a bedrock feature. For the 149 brittle lineaments, 73 (49%) were assigned the highest level of certainty (three), while 51 (34%) were assigned a certainty value of two, and 25 (17%) were assigned a lower certainty value of one. For the 695 dyke lineaments the certainty increased, with 547 (79%) assigned the highest level of certainty (three), 121 (17%) assigned a certainty value of two, and 27 (4%) were assigned a lower certainty value of one. Appendix B presents a summary of geophysical lineaments statistics. All brittle and dyke lineaments were included in the statistical analyses, and are shown in Appendix A: Figures A2 and A3, and Figure 8.

Azimuth data weighted by length for the interpreted brittle lineaments display a broad southeast, to north-south orientation (one high confidence peak at 147°, one medium to high confidence peak at 128°, and one medium confidence peak at 169°), as well as a north-northeast-trending orientation (one medium to high confidence peak at 018°), and an east-west-trending orientation (one medium confidence peak at 087°) (see rose diagram inset in Figure 8 and Table 5). Southeast-, to north-south-

trending brittle lineaments are typically long and continuous. The north-northeast-trending-trending brittle lineaments tend to comprise both long and continuous lineaments, as well as short and segmented lineaments, while east-west-trending lineaments are typically short and segmented. In general, the style of the different orientations of brittle lineaments (i.e., length, continuity, etc.) closely resembles the style of the dyke lineaments in the equivalent orientations.

Azimuth data weighted by length for the interpreted dyke lineaments display a single dominant southeast orientation (one high confidence peak at 140°), (see rose diagram inset in Figure 8 and Table 5). The southeast dyke lineament trend has a range in orientation from 124° to 158° corresponds to a combination of the southeast-trending Sudbury dyke set, and the southeast- to south-southeast-trending Matachewan dyke set, both of which tend to be continuous and can occur in swarms or clusters that manifest as multiple tight-spaced dyke lineaments. Minor north-, northeast-, east-northeast-, and east-southeast-trending dyke lineaments are also observed in the interpretation and correspond to the Marathon, Biscotasing, Grenville, and North Channel dyke sets, respectively. The abundance of dyke lineaments associated with the Sudbury and Matachewan dyke sets means that the significantly less abundant Marathon, Biscotasing, Grenville, and North Channel are not well-represented in the orientation data. The north-trending Marathon, and northeast-trending Biscotasing dyke lineaments are typically segmented to continuous and long, and occur as single isolated dykes. The east-northeast-trending Grenville dyke lineaments are segmented, short to long, sporadically curvilinear, and occur as single isolated dykes. The east-southeast-trending North Channel dyke lineaments are segmented to continuous and long, and can occur as single isolated dykes, or sporadically as swarms or clusters that manifest as multiple tight-spaced dyke lineaments, particularly toward the south of the area.

**Table 5: Summary of Geophysical Lineament Orientations for the Area**

| Lineament Type | Orientation Set | Peak (deg) | Range (deg) | Frequency (%) | Confidence |
|---|---|---|---|---|---|
| Brittle | SSE - NNW | 147 | 137 - 155 | 12.4 | High |
| | N - S | 169 | 155 - 178 | 10.1 | Medium - High |
| | NNE - SSW | 018 | 010 - 029 | 10.0 | Medium - High |
| | E - W | 087 | 082 - 094 | 8.7 | Medium |
| | SE - NW | 128 | 124 - 135 | 7.8 | Medium |
| Dyke | SE - NW | 140 | 124 - 158 | 23.1 | High |

## 4.2 Surficial Lineaments

Surficial lineaments include lineaments interpreted from the DEM and FRI digital aerial imagery data sets, and are shown on Figure 9 and Figure 10, respectively. Unlike the lineaments identified from the magnetic data, surficial lineaments cannot be easily differentiated into brittle or dyke lineaments based solely upon their expression in surficial data. Therefore, all surficial lineaments are classified only by the data set from which they were identified (i.e., DEM lineament and FRI lineament). An overview of the results of the surficial lineament interpretation is provided below.

### 4.2.1 DEM Lineaments (RA_1)

A total of 641 DEM lineaments were interpreted within the lineament assessment area. These comprise lineaments that were identified and merged by the two interpreters based on interpretation from the DEM data (Figure 9). Of the 641 lineaments interpreted, 137 (21 %) were assigned the highest level of certainty (three), while 317 (50%) were assigned a moderate certainty values of two, and 187 (29%) were assigned a low certainty value of one. The certainty value reflects the certainty that the interpreted lineament represents a bedrock feature. The length of all DEM lineaments ranges

from 0.35 to 31.12 km, with a median of 1.56 km and a mean of 2.35 km. Of the total DEM lineaments, 268 lineaments were coincident between the two interpreters (42%; RA_1 = 2) and there was a lack of coincidence for 373 lineaments (58%; RA_1 = 1). Appendix B presents a summary of statistical analyses for the interpreted DEM lineaments.

Azimuth data weighted by length for the interpreted DEM lineaments display a broad southeast to south-southeast orientation (one high confidence peak at 133°, and one medium to high confidence peak at 153°), and subordinate north-south (one medium to low confidence peak at 170°) north-northeast orientations (one medium to low confidence peak at 028°) (see rose diagram inset in Figure 9 and Table 6). The range in orientations are well represented throughout the area. Throughout the area, broad southeast to south-southeast-trending DEM lineaments are typically abundant and continuous (Figure 9). North-northeast-trending DEM lineaments are moderately abundant, variable in length, and continuous to segmented. North-south trending DEM lineaments are typically short and discontinuous.

The abundance of DEM lineaments is directly influenced by the degree of topography in a given area, i.e., areas with subdued topography and a lack of elevation contrast impede the interpretation of topographic lineaments. This can be observed where low relief regions (coloured blue in Figure 9) have a relatively low number of interpreted DEM lineaments, such as in the northeast portion of the assessment area, around Moose Narrows, and Mink Lake (Figure 9).

**Table 6: Summary of DEM Lineament Orientations for the Area**

| Lineament Type | Orientation Set | Peak (deg) | Range (deg) | Frequency (%) | Confidence |
|---|---|---|---|---|---|
| DEM | SE - NW | 133 | 120 - 147 | 13.1 | High |
| | SSE - NNW | 153 | 150 - 157 | 7.7 | Medium - High |
| | N - S | 170 | 165 - 173 | 5.8 | Medium - Low |
| | NNE - SSW | 028 | 025 - 035 | 5.7 | Medium - Low |

### 4.2.2 FRI Digital Aerial Imagery Lineaments (RA_1)

A total of 1351 FRI lineaments were interpreted within the lineament assessment area. These comprise lineaments that were identified and merged by the two interpreters based on interpretation from the FRI digital aerial imagery data (Figure 10). Of the 1351 lineaments interpreted, 318 (24 %) were assigned the highest level of certainty (three), while 639 (47%) were assigned a moderate certainty value of two, and 394 (29%) were assigned a low certainty value of one. The certainty value reflects the certainty that the interpreted lineament represents a bedrock feature. The length of all FRI lineaments ranges from 0.07 to 10.77 km, with a median of 0.49 km and a mean of 0.82 km. Of the total FRI lineaments, the reproducibility assessment identified coincidence for 620 lineaments (46%; RA_1 = 2) and a lack of coincidence for 731 lineaments (54%; RA_1 = 1). Appendix B presents a summary of statistical analyses for the interpreted FRI lineaments.

Azimuth data weighted by length for the interpreted FRI lineaments display a broad southeast to south orientation (three high confidence peaks at 138°, 155°, and 171°), and a broad north-northeast orientation (one high confidence peak at 015°, and one medium confidence peak at 030°) (see rose diagram inset in Figure 10 and Table 7). All lineament orientations are well represented throughout the area.

Throughout the area, each of the lineament orientation sets are dominated by fairly short lineaments traces with sporadic isolated longer lineaments. Overburden is not abundant in the assessment area, however, the abundance of lineaments tends to be directly influenced by the quality of surficial

features in a given area. Areas characterized by well-defined lake boundaries, breaks in vegetation, linear rivers, etc., often yield numerous FRI lineaments, versus areas with fewer lakes and rivers, and subdued surficial features, which yield fewer FRI lineaments. This can be observed where regions with numerous lakes and rivers (such as around Moose Narrows seen in Figure 10) typically have a relatively high number of interpreted FRI lineaments. Unlike the DEM or geophysical lineaments, the lineaments observed in the FRI imagery are often short and discontinuous due to the way in which bedrock features are expressed in digital aerial imagery, however sporadic southeast- to north-south-trending FRI lineaments are long and continuous and are associated with linear rivers or linear chains of lakes.

**Table 7: Summary of FRI Lineament Orientations for the Area**

| Lineament Type | Orientation Set | Peak (deg) | Range (deg) | Frequency (%) | Confidence |
|---|---|---|---|---|---|
| FRI | SE - NW | 138 | 122 - 145 | 11.1 | High |
| | SSE - NNW | 155 | 147 - 165 | 10.9 | High |
| | N - S | 171 | 168 - 175 | 9.1 | High |
| | NNE - SSW | 015 | 009 - 022 | 7.7 | High |
| | NNE - SSW | 030 | 025 - 037 | 6.3 | Medium |

## 4.3 Integrated Surficial Lineaments (RA_2)

The lineaments interpreted based on DEM and FRI digital aerial imagery data were integrated into a single set of surficial lineaments following the methodology outlined in Section 3. Similar to the interpretation of DEM and FRI lineaments, surficial lineaments cannot be differentiated into brittle and dyke lineaments based solely upon their expression in surficial data, and are, therefore, all classified as surficial lineaments. The integrated surficial lineaments are shown in Figure 11 on the mapped bedrock geology based on the Ontario Geological Survey (OGS 2011). The figure also shows mapped faults and mapped dykes, based on either field mapping evidence or an interpretation from historic aeromagnetic data. An overview of the results of the integrated surficial lineaments is provided below and summarized in Appendix B.

The integration of DEM and FRI lineaments yielded a total of 1427 surficial lineaments (Figure 11). The merging of DEM and FRI lineaments commonly resulted in lineaments of new lengths, and in some cases an individual lineament may appear either shorter or longer than its original interpreted length. The length of all surficial lineaments ranges from 0.07 to 19.38 km, with a median of 0.79 km and a mean of 1.38 km. Of the 1427 integrated surficial lineaments, 323 (23 %) were assigned the highest level of certainty (three), while 698 (49%) were assigned a moderate certainty value of two, and 406 (28%) were assigned a low certainty value of one. The certainty value reflects the certainty that the interpreted lineament represents a bedrock feature. A total of 270 lineaments (19%; RA_2 = 2) were coincident in both the DEM and FRI data sets whereas 1157 lineaments only occurred in one of the two data sets (81%; RA_2 = 1).

Azimuth data weighted by length for the integrated surficial lineaments display a broad southeast- to south-southeast orientation (two high confidence peaks at 130° and 152°), and additional, subordinate north-northeast (one medium confidence peak at 023°) and northeast (one medium to low confidence peak at 045°) orientations (see rose diagram inset in Figure 11 and Table 8). In general, these orientations match those observed in the individual interpretations (DEM and FRI; Figure 9 and Figure 10). All lineament orientations are well represented throughout the area. The longer surficial lineaments tend to be largely inherited from the integrated DEM lineaments, whereas many of the shorter and discontinuous surficial lineaments are inherited from the FRI imagery

lineaments. Variation in lineament lengths from the DEM and FRI lineament data sets is due to the way in which bedrock features manifest in these respective data sets.

In general, the southeast- to south-southeast-trending surficial lineaments are most abundant and show a wide variability in their lengths. This orientation is oblique to orthogonal to the dominant trend of glaciation (Figure 3), and as such the lineaments are not considered to be associated with glaciation. Overall, the abundance of surficial lineaments tends to be directly influenced by the intensity of surficial features in a given area, i.e., presence of topographic relief, vegetation changes, linear lakeshores, etc. In areas of subdued surficial features, fewer and shorter lineaments were interpreted and integrated into the surficial lineament data set. These areas include: west of Jeanne, Jackson, and Armstrong lakes, around and south of Mozhabong Lake, and west of Armstrong Lake. While overburden is not abundant in the assessment area, a zone of glaciofluvial deposits is located around and south of Mozhabong Lake, and west of Armstrong Lake, and as such may contribute to the lack of interpreted surficial lineaments in these areas. A narrow zone of glaciofluvial deposits is also present proximal to a north-northwest-trending river valley, west of Jeanne, Jackson, and Armstrong lakes, however, the width of the zone of glaciofluvial deposit in this area is narrow and is thought to have a limited impact on the ability to identify surficial lineaments (Figure 11).

**Table 8: Summary of Integrated Surficial Lineament (RA_2) Orientations for the Area**

| Lineament Type | Orientation Set | Peak (deg) | Range (deg) | Frequency (%) | Confidence |
|---|---|---|---|---|---|
| Integrated Surficial Lineaments | SE - NW | 130 | 123 - 145 | 11.4 | High |
| | SSE - NNW | 152 | 147 - 159 | 9.2 | High |
| | NNE - SSW | 023 | 016 - 034 | 6.2 | Medium |
| | NE - SW | 045 | 038 - 052 | 5.7 | Medium - Low |

## 4.4 Integrated Final Lineaments (RA_2)

The final integrated lineament data set produced by merging all lineaments interpreted from the geophysical (Figure 12) and surficial (DEM and aerial imagery, Figure 11) data is presented in Figure 13. Based upon the geophysical interpretation, and the geological understanding of the area, the final integrated lineaments were differentiated into brittle and dyke lineaments. An overview of the results of the final integrated lineaments is provided below, summarized in Appendix B, and presented in Figure 13.

The integration of geophysical and surficial lineament sets produced a total of 1,887 final integrated lineaments (Figure 13), of which 1,248 are classified as brittle lineaments and 639 as dyke lineaments. The length of all final integrated lineaments ranges from 0.07 to 29.13 kilometres, with a median of 0.87 kilometres and a mean of 1.63 kilometres. Of the 1,887 final integrated lineaments, 847 (45 %) were assigned the highest level of certainty (three), while 689 (36%) were assigned a certainty value of two, and 351 (19%) were assigned a certainty value of one. The certainty value reflects the certainty that the interpreted lineament represents a bedrock feature. The reproducibility assessment identified coincidence in all three data sets for 124 lineaments (6%; RA_2 = 3), and coincidence in two out of three data sets for 296 lineaments (16%; RA_2 = 2) and 13% of the interpreted geophysical lineaments were also interpreted in at least one of the two surficial data sets. A total of 1467 (78%) lineaments were not coincident with any other data set (RA_2 = 1).

Azimuth data weighted by length for the interpreted integrated brittle lineaments displays dominant, broad southeast to south-southeast (two high confidence peaks at 150° and 167°, and one medium to high confidence peak at 130°), and subordinate north-northeast (one medium to high confidence peak at 023°) and northeast (one medium to low confidence peak at 046°) trends (see rose diagram

inset in Figure 13 and Table 9). All brittle lineament orientations are well represented throughout the area. The southeast- to south-southeast-trending brittle lineaments are abundant and tend to be long and continuous relative to lineaments in other orientations. North-northeast- to northeast-trending brittle lineaments are abundant, and display a more variable length. Less abundant east-west-trending brittle lineaments tend to display are typically short and discontinuous.

Azimuth data weighted by length for the interpreted dyke lineaments display a single dominant southeast orientation (one high confidence peak at 135°) (see rose diagram inset in Figure 13 and Table 9). The southeast dyke lineament trend has a range in orientation from 124° to 158° corresponds to the southeast-trending Sudbury dyke set, and the southeast- to south-southeast-trending Matachewan dyke set, both of which tend to be continuous and can occur in swarms or clusters that manifest as multiple tight-spaced dyke lineaments. Minor north-, northeast-, east-northeast-, and east-southeast-trending dyke lineaments are also observed in the interpretation and correspond to the Marathon, Biscotasing, Grenville, and North Channel dyke sets, respectively. The abundance of dyke lineaments associated with the Sudbury and Matachewan dyke sets means that the significantly less abundant Marathon, Biscotasing, Grenville, and North Channel are not well-represented in the orientation data. The north-trending Marathon, and northeast-trending Biscotasing dyke lineaments and are typically segmented to continuous and long, and occur as single isolated dykes. The east-northeast-trending Grenville dyke lineaments are segmented, short to long, sporadically curvilinear, and occur as single isolated dykes. The east-southeast-trending North Channel dyke lineaments are segmented to continuous and long, and can occur as single isolated dykes, or sporadically as swarms or clusters that manifest as multiple tight-spaced dyke lineaments, particularly toward the south of the area.

In terms of their spatial distribution, brittle lineaments are abundant throughout the study area, while dykes are more significantly abundant than brittle lineaments in the western to southwestern half of the study area (Figure 13).

**Table 9: Summary of Integrated Final Lineament (RA_2) Orientations for the Area**

| Lineament Type | Orientation Set | Peak (deg) | Range (deg) | Frequency (%) | Confidence |
|---|---|---|---|---|---|
| Brittle | SSE - NNW | 150 | 143 - 157 | 10.7 | High |
| | SSE - NNW | 167 | 160 - 179 | 7.9 | High |
| | SE - NW | 130 | 125 - 133 | 7.4 | Medium - High |
| | NNE - SSW | 023 | 010 - 032 | 7.1 | Medium - High |
| | NE - SW | 046 | 039 - 051 | 5.6 | Medium - Low |
| Dyke | SE - NW | 135 | 124 - 159 | 25.2 | High |

# 5 Discussion

This lineament interpretation provides an understanding of potential structures within the bedrock units of the lineament assessment area. The results of the lineament interpretation, including lineament reproducibility, orientation, length, and density are discussed below. The relationship of the integrated lineament data sets relative to the regional structural history and their relative ages are also discussed.

## 5.1 Lineament Reproducibility (RA_1) and Coincidence (RA_2)

Lineament reproducibility and coincidence are assessed in several steps during the analysis (as outlined in Section 3). First, the two individual interpretations for each data set were integrated to produce single data set specific (RA_1) interpretations. During this step, the reproducibility (RA_1 value) of each lineament was assessed (Section 3.2.2). Secondly, the individual data set interpretations were integrated to produce the final integrated (RA_2) data set. During this step, the coincidence (RA_2 value) between lineaments identified in the various data sets was evaluated (Section 3.2.3). A breakdown of all reproducibility and coincidence values is presented in Section 4 and Appendix B.

The evaluation of RA_1 data for all lineament types (geophysical, DEM, and FRI) reveals a moderate reproducibility between interpreters for the geophysical lineaments (56% of lineaments RA_1=2), the DEM lineaments (42% of lineaments RA_1=2), and the FRI lineaments (46% of lineaments RA_1=2). The slightly higher reproducibility between interpreters for the geophysical lineaments relative to the other data sets is largely attributed to the abundance of well-defined dyke lineaments in the assessment area that were identified by both interpreters.

Reproducibility values (RA_1) vary between geophysical lineaments types, with dyke lineaments having the highest reproducibility (60% of dyke lineaments RA_1=2), and brittle lineaments having a lower reproducibility (37% of brittle lineaments RA_1=2). The lower reproducibility of brittle geophysical lineaments can be attributed to the subtle magnetic signature of the lineaments that can inhibit their identification. The high reproducibility for dyke lineaments is expected, as their geophysical signatures are typically well-defined (long, continuous magnetic highs), and are therefore easily interpreted. Low lineament reproducibility values are the result of differences in the individual lineament interpretations from each interpreter for the same data set, and can be attributed to the judgement and subjectivity of the expert carrying out the interpretation.

Coincidence between lineaments identified from the DEM and FRI data sets was evaluated for the second reproducibility assessment (RA_2). Overall, a total of 19% of the surficial lineaments were interpreted in both the DEM and FRI data sets. The coincidence between lineaments of these data sets is in part explained by the fact that lineaments interpreted from the FRI imagery and the DEM data represent surficial expressions of the same bedrock feature. For example, a lineament drawn along a stream channel shown on the FRI imagery is expected to be coincident with a lineament that captures the trend of the associated topographic valley expressed in the DEM data. The lack of coincidence between the two surficial data sets may be the result of several factors, including, the difference in resolution, and the different styles in which structures manifest in the DEM and FRI data sets. The DEM data were collected during the magnetic survey (25-metre grid cell size), with a much lower resolution than the FRI imagery (0.4 m resolution). Therefore, a structure that is apparent in the FRI imagery may not be apparent in the DEM data. Alternatively, a structure present in the DEM data may be represented as multiple structures within the higher resolution FRI data. In

addition, certain structures observed in the DEM data may be obscured by vegetation in the FRI data, and conversely, structures defined by a change in vegetation in the FRI data may not have a topographic expression in the DEM data.

The coincidence assessment (RA_2) between geophysical and surficial features revealed that 28% of the interpreted geophysical lineaments were also interpreted in at least one of the two surficial data sets. When considering the entire final integrated lineament data set, only 6% of the final integrated lineaments were identified in all three data sets, and 16% of the final integrated lineaments were identified in two of the three data sets. The remaining 78% of the lineaments lack any coincidence (RA_2=1) and were only identified in a single data set.

The final integrated lineament data set can be further assessed to identify coincidence between data sets for each of the specific types of lineaments (i.e., brittle and dyke). For the 1248 brittle lineaments interpreted in the final integrated lineament data set, 5% of the lineaments were identified in all three data sets, and 18% of the lineaments were identified in two of the three data sets. The remaining 77% of the lineaments lack any coincidence and were only identified in a single data set. In particular, over half (63%) of the brittle lineaments that are lacking coincidence with any other data set are derived from the FRI data.

In addition, it is apparent that interpreted dyke lineaments from the geophysical data set also had some sort of surficial lineament expression. Considering the 639 dyke lineaments interpreted, 20% of these lineaments were coincident with at least one of the two surficial data sets, and 9% were interpreted in both surficial data sets.

The lack of coincidence between different sets of lineaments may be attributed to multiple factors, including:

- Deeper structures identified in the geophysical data may not have a surficial expression
- Certain structures identified in the geophysical data may have a subdued or no surficial expression
- Surface expression of geophysical lineaments may be masked by the presence of overburden (e.g., large river valleys covered by Quaternary sediments)
- Structures identified in the surficial data may not extend to significant depths and therefore may not be recognizable in the magnetic data
- Structures identified in the surficial data may not possess sufficient magnetic susceptibility contrast to be recognized in the magnetic data

Considering the above factors, it is necessary to objectively analyze the results of the RA_2 assessment with the understanding that RA_2 = 1 does not necessarily imply a low degree of confidence that the specified lineament represents a true bedrock structure. The lineaments derived from different datasets should be considered to be complementary because individual lineaments may have a better expression in different datasets.

Lineaments that were coincident in two or three data sets were commonly long and continuous. Within the geophysical data, these lineaments were defined by continuous magnetic lows or highs, whereas in the surficial data sets, these lineaments were defined by continuous topographic valleys, long linear lakes, and vegetation changes.

## 5.2 Lineament Trends

Lineament orientations within the assessment area can be observed visually (Figure 8 to Figure 13), and via length weighted azimuth plots (see rose diagram insets in Figure 8 to Figure 13). A summary of lineament orientation data for the assessment area is presented in Appendix A and Figure A4.

Lineaments identified from both the geophysical and surficial data sets within the area tend to reveal two general lineament orientation sets: southeast to south-southeast, and northeast to north-northeast, with an additional east-west trend (Figure A4 and Figure 8 to Figure 13 Of these lineament orientations, the southeast to south-southeast-trending lineaments tend to be broadly distributed but are well-defined in all lineament data sets.

Length weighted orientation data for the geophysical lineaments tend to exhibit a dominant but broad southeast, to north-south lineament orientation, with subordinate north-northeast and east-west orientations (Figure 12). These geophysical lineaments can also be subdivided into orientation sets based on the lineament type (i.e. brittle and dyke lineaments). The dyke lineament orientations exhibit a single dominant southeast orientation (one high confidence peak at 140°), which can be attributed to a combination of the southeast-trending Sudbury dyke set, and the southeast- to south-southeast-trending Matachewan dyke, both of which are common and most abundant in the west and southwest parts of the study area, but are not easily distinguished on the rose diagram plots. Minor north-, northeast-, east-northeast-, and east-southeast-trending dyke lineaments are also interpreted and are not well represented in the rose diagram plots. These correspond to the Marathon, Biscotasing, Grenville, and North Channel dyke swarms, respectively. The southeast- to south-southeast-trending dyke lineaments often occur as clusters of tightly spaced dyke lineaments, separated by kilometre-scale zones with rare interpreted dyke lineaments. In contrast, interpreted dyke lineament orientations attributed to the Marathon, Biscotasing, Grenville, and North Channel dyke swarms are typically widely spaced and distributed throughout the assessment area. The orientation of brittle lineaments interpreted in the geophysical display a broad southeast, to north-south orientation (one high confidence peak at 147°, one medium to high confidence peak at 128°, and one medium confidence peak at 169°), as well as a north-northeast-trending orientation (one medium to high confidence peak at 018°), and an east-west-trending orientation (one medium confidence peak at 087°)

For the most part, the interpreted surficial lineaments tend to exhibit broad orientation trends similar to those of the geophysical lineaments (Figure 11 and Figure A4) with a broad southeast- to south-southeast orientation (two high confidence peaks at 130° and 152°), and additional, subordinate north-northeast (one medium confidence peak at 023°) and northeast (one medium to low confidence peak at 045°) orientations. As with the interpreted geophysical brittle lineaments, some of the surficial lineament trends are coincident with orientations of the Matachewan, and Sudbury dyke swarms, however surficial lineaments are rarely coincident with the Marathon, Biscotasing, Grenville, and North Channel dyke swarms. The dominant southeast- to south-southeast orientation is oblique to orthogonal to the dominant trend of glaciation, and as such the lineaments are not considered to be associated with glaciation. While prominent glacial landforms are not common in the study area, the north-northeast and northeast lineament orientations are oriented parallel to the regional glacial trend, and may in fact represent glacial features. Although an effort was made to avoid interpreting glacially derived linear features (e.g., eskers, etc.) as tectonic lineaments, the coincidence in orientation suggests using caution when interpreting the nature of north-northeast and northeast-trending surficial lineaments. Despite this uncertainty, the north-northeast- surficial lineaments are also coincident with the distribution of sporadic north-northeast- -trending brittle and dyke geophysical lineaments.

As expected, the final integrated brittle lineaments (Figure 13) generally show similar trends as seen in the geophysical and surficial data sets, with dominant, broad southeast to south-southeast (two high confidence peaks at 150° and 167°, and one medium to high confidence peak at 130°), and subordinate north-northeast (one medium to high confidence peak at 023°) and northeast (one medium to low confidence peak at 046°) trends. The dominant orientation of the interpreted brittle lineaments from the final integrated lineaments is similar to the dominant the orientation of interpreted dyke lineaments derived from the geophysical data set (Figure 12). Although their lineament orientation sets display a similar trend, the frequency/length of lineaments within the dominant peaks differ between the interpreted dyke lineaments and the brittle lineaments. In general, the data suggests that brittle lineaments subparallel to the Matachewan and Sudbury dyke swarm tend to be better expressed in the surficial datasets than in the geophysical data, however, it should be noted that due to the abundance of dykes present in the geophysical data, and the way they are represented in the data as strong magnetic highs, this may mask underlying brittle structures in the geophysical data, and thus may hinder their interpretation. Brittle lineaments are also present in the surficial datasets that are subparallel to the Marathon, Biscotasing, Grenville, and North Channel dyke swarms. However, dykes associated with these swarms are not common, and as such no correlation can be inferred.

The abundance, length, and through-going nature of the southeast- to south-southeast brittle and surficial lineaments, suggest that these lineament trends represent the most significant regional orientation of brittle structures. Overall, these trends appear to correlate well with regional fault systems, with mapped brittle faults in the surrounding area generally showing the same southeast- to south-southeast orientations (OGS, 2011). These correlations are described in further detail in Section 5.5.1.

### 5.2.1 Relationship between Lineament Sets and Regional Stress Field

The principal neotectonic compressive stress orientation in central North America is generally oriented approximately east-northeast (63 degrees ± 28 degrees; Zoback ,1992) although anomalous stress orientations have also been reported in the mid-continent that include a 90-degree change in azimuth of the maximum compressive stress axis (Brown et al., 1995) and a north-south maximum horizontal compressive stress (Haimson, 1990). Local variations, and other potential complicating factors involved in characterizing crustal stresses, including the effect of shear stress by mantle flow at the base of the lithosphere (Bokelmann, 2002; Bokelmann and Silver, 2002), the degree of coupling between the North American plate and the underlying mantle (Forte et al., 2010), the effects of crustal depression and Holocene rebound due to glacial loading and unloading, and the influence of the thick lithospheric mantle root under the Canadian Shield, make it premature to correlate the regional neotectonic stress orientation with the orientation of the interpreted lineaments.

However, it is possible to broadly speculate on the potential behavior of the identified lineaments if they were to be reactivated by the regional east-northeast neotectonic stress regime. Two dominant orientations of lineaments were interpreted: southeast to south-southeast, and northeast, and north-northeast, with an additional minor east-west trend. Should the identified lineaments be reactivated under the current stress regime, assuming the faults have a vertical dip, the southeast to south-southeast oriented lineaments would likely reactivate as reverse dip-slip to oblique-slip faults depending on their strike and dip, and the northeast to north-northeast oriented lineaments would likely reactivate as strike-slip to oblique-slip faults.

## 5.3 Lineament Length

Interpreted geophysical, surficial and final integrated lineaments classified by length are presented in Figures 14, 15 and 16. The distributions of lineament lengths are displayed on histograms and

cumulative frequency plots (see inset plots on Figures 14 to 16). On these plots, the x-axis represents the bin lengths for the lineaments (km), and the left y-axis represents the percentage of the total number of interpreted lineaments contained within that length bin. The blue line represents the cumulative frequencies expressed as a fraction between 0 and 1, which can be considered equivalent to probability. The probability is labeled on the right y-axis of the plot. Length statistics are summarized in Appendix A: Figure A5, and Appendix B. Lineament lengths displayed and reported in the figures, statistics tables, and histogram plots only reflect the length of the portion of the lineament that is contained within the individual lineament assessment block. Therefore, the lineament lengths do not necessarily reflect the full length of all lineaments, as lineaments were only traced within the assessment area and could extend beyond its borders.

Overall, lineament lengths for the geophysical, surficial, and final integrated lineaments display a similar distribution, with the distribution of lengths skewed toward shorter lineaments (Figures 14 to 16). For each of the lineament data sets the majority of lineaments tend to have lengths less than 5 km. Approximately 93% of the geophysical lineaments and approximately 96% of the surficial lineaments have lengths that are less than 5 km.

The comparison of median and mean values for all geophysical, integrated surficial, and final integrated lineaments reveals a roughly similar length distribution as described above (Appendix B). The geophysical lineaments exhibit the longest overall mean (1.77 km) and median (0.88 km), whereas the integrated surficial lineaments exhibit the shortest mean (1.38 km) and median (0.79 km). The final integrated lineaments exhibit an intermediate mean (1.63 km) and median (0.87 km), as would be expected as these lineaments are the result of the combination of the slightly longer geophysical and slightly shorter surficial lineaments.

The difference in length between lineaments interpreted from geophysical and surficial data sets can in part be explained by the nature of the lineaments interpreted from each data set. From the geophysical data, lineaments are typically characterized by long continuous magnetic lows or highs (dykes, for example). Conversely, surficial lineaments are typically characterized by a combination of breaks in topography, vegetation and bedrock, and elongated lakes. These surficial features are not as continuous as the lineaments interpreted from geophysical data, often due to their interruption by overburden. This resulted in the interpretation of shorter surficial lineaments relative to the geophysical lineaments.

Analysis of lineament length relative to coincidence values for all final integrated lineaments indicates that lineaments coincident in all three data sets (RA_2=3) are typically longer (mean = 5.17 km, median = 3.52 km) than lineaments reproduced in two (RA_2=2; mean = 2.73 km, median = 1.85 km) or only one (RA_2_1; mean = 1.11 km, median = 0.65 km) data sets (Appendix B). This is to be expected, as lineaments observed in all three data sets may represent significant bedrock structures.

Similarly, an analysis of lineament length relative to certainty values for the final integrated lineaments indicate that lineaments with the highest certainty value (3), are typically longer (mean = 2.39 km, median = 1.23 km) than those with certainty values of 2 (mean = 1.06 km, median = 0.70km) and 1 (mean = 0.91 km, median = 0.73 km) (Appendix B). Again, this is to be expected as lineaments assigned the highest certainty lineaments are most likely to represent significant bedrock structures.

Lineament lengths relative to the dominant lineament orientations suggest that longer lineaments (i.e. lineaments greater than 5 km in length) tend to have a southeast to south-southeast orientation, however sporadic long lineaments were interpreted trending north-south to northeast. As expected, both geophysical and surficial lineaments trending in southeast to south-southeast orientations seem

to contain relatively similar amounts of longer lineaments. Of these long lineaments, most correspond to long and continuous dykes of the Matachewan and Sudbury dyke swarms.

## 5.4 Density

Analyses of lineament and lineament intersection density were conducted for the assessment area as described in Section 3.2.6, and are presented in Figure 17 to Figure 19 (lineament density) and Figure 20 to Figure 22 (lineament intersection density).

### 5.4.1 Lineament Density

An analysis of lineament density for each data set is presented below and in Figure 17 to Figure 19. Locally, lineament density appears to be lower at the margins of the assessment area. This arises because lineaments are only traced to the margins of the assessment area, but the search radius extends beyond the boundary for points less than 1.25 km from the boundary. When generating density plots, this will result in an apparent low lineament density around the border of the area.

#### Geophysical Lineament Density

Throughout the area, lineament density analyses of brittle and dyke lineaments reveal a relatively uniform lineament density, with few discrete zones of elevated and lower lineament density throughout. Rare, small areas of slightly elevated lineament density are located in the north of the area, west of Labitiche Lake, in the northeast of the area, west of Moose Narrows, and in the northwest of the area, west of Red Elk Lake (Figure 17). In general, the majority of the areas of slightly elevated lineament density tend to occur in areas with clusters of southeast-trending dyke lineaments and particularly where these clusters intersect with tight-spaced brittle lineaments and south-southeast-trending dyke lineaments. Areas of slightly lower lineament density are located around the Wakonassin River in the southeast of the area, in the area east of Airport Lake, and in the area south of Russian Lake (Figure 17).

#### Surficial Lineament Density

Lineament density plots for the surficial lineaments reveal a variable lineament density, with discrete zones of elevated and lower lineament density throughout (Figure 18). Areas with elevated lineament density occur in the northeast of the area east Mozhabong Lake, and along the western margin of the area, particularly southwest of Red Elk Lake. These areas appear to be associated with areas of higher topographic elevation. The largest area with the low surficial lineament density is located toward the north of the assessment area, west of Jeanne, Jackson, and Armstrong lakes. The density of surficial lineaments may be in part related to the presence or absence of overburden. In order to properly assess surficial lineament density, it is necessary to take into account the location of surficial features (broad river valleys, large water features, glacial overburden, etc.), as the ability to interpret surficial lineaments may be limited in these areas. A narrow zone of glaciofluvial deposits is present proximal to a north-northwest-trending river valley, in the low lineament density area west of Jeanne, Jackson, and Armstrong lakes. However, the width of the zone of glaciofluvial deposit is substantially narrower than that of the area of low lineament density, and as such it is thought that in this area the overburden has a limited impact on the ability to identify surficial lineaments.

#### Final Integrated Lineament Density

The final integrated lineaments result from the integration of the geophysical and surficial lineaments. Lineament density analyses of the final integrated brittle and dyke lineaments reveal a variable lineament density, with discrete zones of elevated and rare lower lineament density (Figure 19). Similar to the other data sets, zones of slightly higher lineament density correspond to areas with clusters of southeast- and south-southeast-trending dyke lineaments and where these

clusters intersect with tight-spaced brittle lineaments. The zone of highest lineament density is a broad, southeast-trending area of moderately elevated lineament density that occurs from the northwest (west of Red Elk Lake) to the southeast corner of the area that is associated with a tightly-spaced cluster of dykes belonging to the Sudbury dyke swarm, and where these dykes are cross-cut by north-northeast- to northeast-trending brittle lineaments. The lowest lineament density occurs in a small zone the east of Airport Lake.

### 5.4.2 Lineament Intersection Density

An analysis of lineament intersection density for each data set is presented below and in Figure 20 to Figure 22.

#### Geophysical Lineament Intersection Density

Lineament intersection density for geophysical lineaments is variable with multiple well-defined zones of low and high lineament intersection density throughout the area, and lineament intersection density of geophysical lineaments resembles lineament density of the same geophysical lineaments. Elevated lineament intersection density is typically due to the intersection of clusters of southeast- and south-southeast-trending dyke lineaments with sporadic north-northeast- to northeast trending brittle lineaments and sporadic northeast- to east-northeast-trending dyke lineaments (Figure 20). Rare, small zones of elevated geophysical lineament intersection density occur towards the north of the study area in an area, west of Labitiche Lake; in the northwest of the study area around Red Elk Lake; and in the south of the area, north of Alces Lake. Zones with low geophysical lineament intersection density are distributed throughout the area, with the largest area occurring in the southwest of the study area around Russian Lake. This area is coincident with a large cluster of dykes associated with the Sudbury dyke swarm, and sporadic dykes associated with the Matachewan dyke swarm. While southeast- to south-southeast trending dyke lineaments are abundant in this area, there is a general lack of cross-cutting brittle or dyke lineaments, and as such there are a lack of lineament intersections.

#### Surficial Lineament Intersection Density

Lineament intersection density for the integrated surficial lineaments (Figure 21) is relatively uniform throughout the area with sporadic zones of elevated and lower lineament intersection density. Higher density zones are more abundant when compared to the lineament intersection density of geophysical lineaments. The lineament intersection density of the integrated surficial lineaments closely resembles the lineament density of the same integrated surficial lineaments. Zones of elevated lineament intersection density typically occur along or at the intersection of tight-spaced southeast- and south-southeast-trending lineaments, and where they intersect tightly-spaced clusters of north-northeast- and northeast-trending surficial lineaments. Areas with elevated integrated surficial lineament intersection density occur in the northeast of the area, east Mozhabong Lake, and in a corridor along the southwestern margin of the area, particularly southwest of Red Elk Lake. These areas appear to be associated with areas of higher elevation. The largest area with the low surficial lineament density is located toward the north of the assessment area, west of Jeanne, Jackson, and Armstrong lakes. Smaller lower density areas are sporadically distributed throughout the assessment area, including around Mink Lake, and north of Russian Lake. The density of surficial lineaments may in part be related to the presence of overburden. In order to properly assess surficial lineament intersection density, it is necessary to take into account the location of surficial features (river valleys, glacial till cover, etc.), as the ability to interpret surficial lineaments may be limited in these areas. While overburden is not abundant in the study area a zone of glaciofluvial deposits is located around Mink Lake, and as such may contribute to the lack of interpreted surficial lineaments in this area. A narrow zone of glaciofluvial deposits is also present proximal to a north-northwest-trending river valley, in the low lineament density area west of Jeanne, Jackson, and Armstrong lakes. However, the width of the zone of glaciofluvial deposit is substantially narrower

than that of the area of low lineament density, and as such it is thought that in this area the overburden has a limited impact on the ability to identify surficial lineaments.

### Final Integrated Lineament Intersection Density

Lineament intersection density for the final integrated lineaments is variable with multiple well-defined zones of low and high lineament intersection density throughout the area, and lineament intersection density of all final integrated brittle and dyke lineaments closely resembles lineament density of the same final integrated lineaments. Elevated lineament intersection density is typically due to the intersection of corridors of southeast- and south-southeast-trending brittle and dyke lineaments with north-northeast- to northeast trending brittle lineaments and sporadic northeast- to east-northeast-trending dyke lineaments (Figure 22). Similar to the lineament density analysis of all final integrated brittle and dyke lineaments, small zones of slightly elevated lineament intersection density occur near the western margin of the study area and in the northwest of the study area around Red Elk Lake, and around Barn Lake. Zones of low lineament density are sporadically distributed throughout the study area including the area west of Jeanne, Jackson, and Armstrong lakes.

## 5.5 Lineament Truncation and Relative Age Relationships

The structural history of the area, outlined in Section 2.2, provides a framework that may aid in constraining the relative age relationships of the interpreted bedrock lineaments. Previous work in and around the area identified six regionally distinguishable deformation episodes ($D_1 – D_6$) that are inferred to have overprinted the bedrock geological units of the area. The lineament interpretation is roughly consistent with regional observations; however, certain deformation events described in the literature could not be distinguished in the interpreted lineaments. The study area is almost entirely hosted within the Ramsey-Algoma granitoid complex, that was emplaced after cessation of deformation associated with the Kenoran Orogeny, and therefore, no lineaments were interpreted that are characteristic of brittle-ductile deformation associated with the Kenoran Orogeny ($D_1$). Although ductile features are associated with the Penokean Orogeny ($D_5$), these features are restricted to rocks of the Huronian Supergroup, south of the assessment area. A review of literature suggests that all lineaments not interpreted as dykes in the area have brittle characteristics, and therefore, have been interpreted as brittle structures. A review of literature suggests that the interpreted lineaments are consistent in orientation and apparent kinematics with deformation events ranging in age from $D_2$ initial brittle fault development through to the Grenville Orogeny ($D_6$). It should be noted however that the evidence of the Penokean Orogeny ($D_5$) in the area remains controversial (e.g. Davidson et al., 1992; Piercey et al. 2003), and that evidence for deformation associated with the Grenville Orogeny in the area is sparse and its effect on the area is not known. The brittle deformation events could not be separated in the lineament interpretation and were therefore grouped together (i.e., $D_2$ to $D_6$).

The final integrated lineament interpretation for the area shows that brittle lineaments of all orientations truncate or offset each other, and that no one fault set shows consistent offsets, or truncations of other fault sets. This is presumably due to repeated reactivation of older faults ($D_2$ or $D_3$, see Section 2.3), and therefore this prevents accurate delineation or subdivision of the relative ages of individual fault movements. It should be noted, however, that southeast-trending lineaments are typically longer, and more through-going that lineaments in other orientations, and therefore may represent younger faults. In addition, brittle lineaments of all orientations sporadically truncate or offset dyke lineaments attributed to the Matachewan, Marathon, Biscotasing, North Channel, and Sudbury dyke swarms, while dyke lineaments associated with the Grenville dyke swarm are typically short and rarely intersect brittle lineaments. These truncation relationships may be attributed to multiple phases of post-Archean fault reactivation.

Of the 1,887 final integrated lineaments, 1248 were classified as brittle lineaments, and 639 as dyke lineaments (Figure 23). The interpreted brittle lineaments in the final integrated data set are observed with one broad, principal orientation: southeast to south-southeast, with subordinate north-northeast- and northeast-trending lineament sets also identified. The brittle southeast to south-southeast lineament orientations are parallel to subparallel to the Sudbury and Matachewan dyke orientations, respectively, while the north-northeast and northeast lineament orientations are parallel to subparallel to the Marathon and Biscotasing dyke orientations. Despite the geometric relationship between dyke and brittle lineaments, the relative ages of the brittle lineaments do not appear to correlate with the age of emplacement of the dykes (i.e., brittle lineaments subparallel to younger dyke generations do not consistently offset or truncate brittle lineaments subparallel to older dyke generations). Rather, brittle lineaments of all orientations tend to offset and truncate, and are offset and truncated by all other brittle and dyke lineaments. As a result, brittle lineaments could not systematically be differentiated into different generations of brittle deformation, and were therefore classified into the same broad generation of brittle deformation, $D_2$-$D_6$.

Of the 639 final integrated dyke lineaments, six distinct dyke populations can be identified (Figure 23), including 262 dyke lineaments corresponding to the 1.238 Ga southeast-trending Sudbury dyke swarm (Krogh et al., 1987), 253 dyke lineaments corresponding to the 2.473 Ga south-southeast-trending Matachewan dyke swarm (Buchan and Ernst, 2004), 47 dyke lineaments corresponding to the 2.121 Ga. north-trending Marathon dyke swarm (Buchan et al., 1996; Hamilton et al., 2002), 32 dyke lineaments corresponding to the 2.167 Ga northeast-trending Biscotasing dyke swarm (Hamilton et al., 2002), 23 dyke lineaments corresponding to the 1.6 to 2.5 Ga east-southeast-trending North Channel dyke swarm (OGS 2011), and 22 dyke lineaments corresponding to the 590 Ga. east-northeast-trending Grenville dyke swarm (Kamo et al., 1995). As discussed, dyke lineaments may locally truncate and offset, and may be truncated and offset by all possible orientations of brittle lineaments. Considering these possible relationships, one or a combination of several of the following scenarios are possible:

- Dyke emplacement preceded the interpreted brittle faulting, and brittle faults subsequently exploited weaknesses developed in subparallel orientations.
- Dyke swarms exploited and were emplaced along pre-existing faults.
- Dykes and faults were generated coevally in subparallel orientations.
- Brittle faults were reactivated syn- or post-dyke emplacement.

Apart from these relative timing constraints, there are no additional absolute age constraints for aforementioned phases of deformation.

### 5.5.1 Mapped Structure and Lineament Relationships

Relatively few faults and lithological contacts have been mapped in the area (Figure 2), with only one mapped fault and two lithological contacts within the assessment area. However, two brittle faults have been mapped just outside the assessment area, that if projected into the area may be coincident with interpreted lineaments. The relationship of mapped fault and lithological contacts relative to the final integrated lineaments can be seen in Figure 23.

The northeast-trending, Flack Lake Fault is located in the southern half of the area, and transects the Ramsey-Algoma granitoid complex. This fault trace is partially replicated in final integrated lineament interpretation and is located adjacent and parallel to a series of northeast-trending brittle lineaments.

An east-northeast-trending lithological is located in the northwest of the area that is mapped juxtaposing the Ramsey-Algoma granitoid complex to the south with the gneissic tonalite suite to the

north. While a set of three, short, segmented brittle lineaments are adjacent, and subparallel to the mapped lithological contact, overall the lithological contact is not well-represented as a brittle fault in the final integrated lineament interpretation.

A curvi-linear mapped lithological contact crosses the eastern margin of the area and borders a thin sliver of the Benny Lake greenstone belt. This lithological contact was not identified as a brittle fault in the final integrated lineament interpretation.

Two faults have been mapped that terminate just outside the assessment area. North of the assessment area, a mapped fault borders Tasker Lake, and east of the assessment area, a mapped faults borders Wensley Lake. If projected into the assessment area both mapped faults appear to be coincident with a brittle lineament that defines the western margin of Mozhabong Lake and Moose Narrows.

Multiple dykes had been previously interpreted throughout the area from regional-scale resolution geophysical data (Figure 2; Ontario Geological Survey, 2011). These dykes are generally coincident with interpreted south-southeast-trending Matachewan, southeast–trending Sudbury, and northeast-trending Biscotasing dyke lineaments, however certain discrepancies exist due to the higher resolution of the geophysical data set used in this assessment. Dyke lineaments assigned to the Marathon, North Channel, and Grenville dyke swarms were not previously mapped in the assessment area.

# 6 Summary of Results

This report documents the source data, workflow, and results from a lineament interpretation of geophysical (magnetic) and surficial (DEM and FRI digital aerial imagery) data sets acquired as part of the Phase 2 preliminary assessment for the area. The lineament analysis provides an interpretation of the location and orientation of possible individual brittle, and dyke lineaments on the basis of remotely sensed data, and attempts to evaluate their relative timing relationships within the context of the regional geological setting. The workflow involves a three-step process that was designed to address the issues of subjectivity and reproducibility. The distribution of lineaments in the area reflects the bedrock structure, resolution of the data sets used, and surficial cover.

Within the assessment area, a total of 844 geophysical lineaments, 641 DEM lineaments, and 1351 FRI lineaments were interpreted by the two interpreters (RA_1) from their respective data sets. Merging the lineaments derived from the DEM and FRI data resulted in a total of 1427 surficial lineaments (RA_2). Merging the surficial lineaments with those derived from the geophysical data resulted in a total of 1887 final integrated lineaments (RA_2).

The reproducibility assessment (RA_1) revealed a moderate coincidence between interpreters for all three data sets (i.e., 56% for the geophysical lineaments, 42% for the DEM lineaments, and 46% for the FRI lineaments). The variability between interpreters can be attributed to the resolution of the data sets and the judgement of the expert carrying out the interpretation. In general, longer and higher certainty lineaments were identified more often by both interpreters, as well as dyke lineaments (RA_1 = 60%; which are more easily interpreted due to their distinct geophysical signature).

The coincidence assessment (RA_2) revealed a moderate to low coincidence between surficial lineaments interpreted from the DEM and FRI data sets (i.e., 19% of lineaments were coincident in both surficial data sets). Similarly, the final integrated lineaments revealed a low coincidence between lineaments interpreted from the three data sets (i.e., 6% of lineaments were coincident with all three data sets, 16% of lineaments were coincident in at least one other data set, and 78% of lineaments lacked coincidence with other data sets). The variability between lineaments derived from the different data sets can be attributed to multiple factors, including deeper structures identified in the magnetic data that may not have a surface expression, surficial features that may not extend to depth, features identified in the surficial data that may not possess sufficient magnetic susceptibility contrast to be recognized in the magnetic data, the masking of surface expressions of geophysical lineaments by the presence of overburden, and the differing resolution of the various data sets. The low coincidence between surficial and geophysical lineaments does not necessarily imply a low degree of confidence that the lineaments represent a true bedrock structure. The lineaments derived from different datasets should be considered to be complementary because individual lineaments may have a better expression in different datasets. Similar to the reproducibility assessment (RA_1), longer and higher certainty lineaments were more often coincident in the various data sets.

An analysis of lineament orientations revealed an overall consistency between the orientations of lineaments identified in the various data sets, which suggests that lineaments interpreted from all three data sets are identifying the same sets of structures. Lineament orientations within the area reveal two general lineament orientation sets: southeast to south-southeast, and northeast, and north-northeast, with an additional and east-west trend. Of these lineament orientations, the southeast to south-southeast-trending lineaments tend to be broadly distributed but are well-defined in all lineament data sets. The southeast to south-southeast lineament orientations are distributed

throughout the assessment area, and correspond to dyke lineaments of the Sudbury and Matachewan dyke swarms, respectively, and to subparallel brittle lineaments. Brittle and dyke lineaments occur both as clusters of tight-spaced lineaments and in isolation.

Evaluation of lineament length data for the geophysical brittle and dyke, surficial, and final integrated lineaments reveals roughly the same distribution, where the majority of lineaments are less than 5 km in length. In general, the geophysical, and final integrated lineament sets contain more long lineaments relative to the integrated surficial lineaments due to the style in which bedrock structures are manifested within these data sets. Lineaments that were reproduced in all three data sets (RA_2=3), and lineaments with the highest certainty value (3) typically represent the longest lineaments (i.e., greater than 5 km). Long surficial, brittle, and dyke lineaments trend predominantly southeast to south-southeast and correspond to the Sudbury and Matachewan dyke sets, respectively, and to subparallel brittle structures.

The geophysical lineament density of brittle, and dyke lineaments throughout the area is relatively uniform, with few discrete zones of elevated and lower lineament density throughout. Zones of elevated lineament density occur throughout the area and are typically the result of clusters of southeast-trending dyke lineaments and where these clusters intersect with tight-spaced brittle lineaments and south-southeast-trending dyke lineaments.

The integrated surficial lineament density throughout the assessment area also showed a variable lineament density, with few discrete zones of elevated and lower lineament density throughout. Similar to the geophysical data, zones of elevated lineament densities typically occur along or at the intersection of tight-spaced southeast- and northeast-trending surficial lineaments, however, the areas of highest surficial lineament density are correlated with areas of higher topographic elevation. The density of surficial lineaments is in part related to the presence of overburden that may obscure the interpretation of surficial lineaments related to bedrock structures. While overburden is not abundant in the assessment area zones of glaciofluvial deposits are located around Mink Lake, and west of Armstrong Lake, and as such may contribute to the lack of interpreted surficial lineaments in these areas.

The final integrated lineament density throughout the assessment area is similar to geophysical and surficial lineament density analyses. Lineament density analyses of the final integrated brittle and dyke lineaments reveal variable lineament density, with discrete zones of elevated and rare lower lineament density. Similar to the other data sets, zones of slightly higher lineament density correspond to areas with corridors of southeast- and south-southeast-trending dyke lineaments and where these corridors intersect with each other and with tight-spaced north-northeast and northeast-trending brittle lineaments.

Six main regionally distinguishable deformation episodes ($D_1$-$D_6$) have been recognized in the literature in the assessment area, and can be used to constraint the relative age relationships of the interpreted lineaments. The study area is almost entirely hosted within the Ramsey-Algoma granitoid complex, that was emplaced after cessation of deformation associated with the Kenoran Orogeny. Therefore, no lineaments were interpreted that are characteristic of brittle-ductile deformation associated with the Kenoran Orogeny ($D_1$). The 1248 final interpreted brittle lineaments have been classified within the structural history into a single, protracted generation of brittle deformation ($D_2$ to $D_6$). A total of 639 dyke lineaments were also interpreted throughout the assessment area.

$D_2$-$D_6$ brittle lineaments are observed with one broad, principal orientation: southeast to south-southeast, with subordinate north-northeast- and northeast-trending lineament sets also identified. The southeast to south-southeast lineament orientations are parallel to subparallel to the Sudbury and Matachewan dyke orientations, respectively, while the north-northeast and northeast lineament

orientations are parallel to subparallel to the Marathon and Biscotasing dyke orientations. Brittle lineaments in each orientation set are observed to offset and truncate, and be offset and truncated by brittle and dyke lineaments in all the other orientation sets. As a result, brittle lineaments cannot systematically be differentiated into different generations. Therefore, all brittle lineaments were classified into the same broad $D_2$-$D_6$ generation of brittle deformation.

Only one mapped fault and two mapped lithological contacts are present in the area. Interpreted brittle lineaments are at least partially coincident with the Flack Lake fault in the south of the area, as well a lithological contact in the northwest of the study area. No brittle lineaments are coincident with a lithological contact that borders a thin sliver of the Benny Lake greenstone belt at the eastern margin of the area. If projected into the assessment area, two mapped faults that terminate just outside the northern and eastern boundaries of the assessment area, respectively, may be coincident with a brittle lineament that defines the western margin of Mozhabong Lake and Moose Narrows. Multiple dykes had been previously interpreted throughout the areas from regional-scale resolution geophysical data. These dykes are generally coincident with interpreted south-southeast-trending Matachewan, southeast–trending Sudbury, and northeast-trending Biscotasing dyke lineaments. However certain discrepancies exist due to the higher resolution of the geophysical data set used in this assessment.

Of the 639 final integrated dyke lineaments, six distinct dyke populations can be identified, including 262 dyke lineaments corresponding to the 1.238 Ga southeast-trending Sudbury dyke swarm, 253 dyke lineaments corresponding to the 2.473 Ga south-southeast-trending Matachewan dyke swarm, 47 dyke lineaments corresponding to the 2.121 Ga. north-trending Marathon dyke swarm, 32 dyke lineaments corresponding to the 2.167 Ga northeast-trending Biscotasing dyke swarm, 23 dyke lineaments corresponding to the 1.6 to 2.5 Ga east-southeast-trending North Channel dyke swarm, and 22 dyke lineaments corresponding to the 590 Ga. east-northeast-trending Grenville dyke swarm. Dyke lineaments locally truncate and offset, and are truncated and offset by all orientations of brittle lineaments.

# 7 References

Barnett, P.J. 1992. Quaternary Geology of Ontario; in Geology of Ontario, Ontario Geological Survey, Special Volume 4, Part 2, p. 1010–1088.

Barnett, P.J., Henry, A.P., and Babuin, D. 1991. Quaternary geology of Ontario, east-central sheet; Ontario Geological Survey, Map 2555, scale 1:1,000,000.

Bennett, G., Dressler, B.O., and Robertson, J.A. 1991. The Huronian Supergroup and Associated Intrusive Rocks. in Geology of Ontario. Ontario Geological Survey, Special Volume 4, Part 1, p. 549-591.

Berman, R.G., Easton, R.M., and Nadeau, L. 2000. A New Tectonometamorphic Map of the Canadian Shield: Introduction. The Canadian Mineralogist, 38, p. 277-285.

Berman, R.G., Sanborn-Barrie, M., Stern, R.A., and Carson, C.J. 2005. Tectonometamorphism at ca. 2.35 and 1.85 Ga in the Rae Domain, western Churchill Province, Nunavut, Canada: Insights from structural, metamorphic and IN SITU geochronological analysis of the southwestern Committee Bay Belt. The Canadian Mineralogist, 43, p. 409-442.

Bleeker, W., and Hall, B. 2007. The Slave Craton: Geology and metallogenic evolution; in Mineral deposits of Canada: A synthesis of major deposit-types, district metallogeny, the evolution of geological provinces, and exploration methods. Geological Association of Canada, Mineral Deposits Division, Special Publication No. 5, p. 849-879.

Bokelmann, G.H.R. 2002. Which forces drive North America?, Geology, 30, p.1027-1030

Bokelmann, G.H.R., and Silver, P.G. 2002. Shear Stress at the Base of Shield Lithosphere. Geophysical Research Letters, 29, p.61-64

Breaks, F.W., and Bond, W.D. 1993. The English River Subprovince-An Archean Gneiss Belt: Geology, Geochemistry and associated mineralization; Ontario Geological Survey, Open File Report 5846, 1, p. 1-483.

Brown, A., Everitt, R.A., Martin, C.D., and Davison, C.C. 1995. Past and future fracturing In AECL research areas in the Superior Province of the Canadian Precambrian Shield, with emphasis on the Lac Du Bonnet Batholith; Whiteshell Laboratories, Pinawa, Manitoba

Buchan, K.L., and Ernst, R.E. 2004. Diabase dyke swarms and related units in Canada and adjacent regions. Geological Survey of Canada, Map 2022A, scale 1:5,000,000.

Buchan, K.L., Halls, H.C., and Mortensen, J.K. 1996. Paleomagnetism, U-Pb geochronology, and geochemistry of Marathon dykes, Superior Province, and comparison with the Fort Frances swarm. Canadian Journal of Earth Sciences, 33, pp. 1583-1595.

Buchan, K.L., Mortensen, J.K., and Card, K.D. 1993. Northeast-trending Early Proterozoic dykes of southern Superior Province: multiple episodes of emplacement recognized from integrated paleomagnetism and U - Pb geochronology Canadian Journal Earth Science, 30, p. 1286-1296.

Card, K.D. 1978. Geology of the Sudbury-Manitoulin area, districts of Sudbury and Manitoulin. Ontario Geological Survey, Report 166, 238 p.

Card, K.D. 1979. Regional geological synthesis, Central Superior Province. Geological Survey of Canada, Paper 79-1A, p. 87-90.

Card, K.D., and Innes, D.G. 1981. Geology of the Benny Area, District of Sudbury. Ontario Geological Survey Report 206, 117 p.

Card, K. D., Church, W.R., Franklin, J.M., Frarey, M.J., Robertson, J.A., West, G.F., and Young, G.M. 1972. The Southern Province; in Variations in Tectonic Styles in Canada., Geological Association of Canada, Special Paper No. 11. p. 335-380

Corfu, F., and Grunsky, E.C. 1987. Igneous and tectonic evolution of the Batchawana greenstone belt, Superior Province: a U-Pb zircon and titanite study. Journal of Geology, 95, p. 87-105.

Corfu, F., Stott, G.M., and Breaks, F.W. 1995. U-Pb Geochronology and evolution of the English River Subprovince, an Archean low P-highT metasedimentary belt in the Superior Province. Tectonics, 14, p. 1220-1233.

Corrigan, D., Galley, A.G., and Pehrsson, S. 2007. Tectonic evolution and metallogeny of the southwestern Trans-Hudson Orogen; in ; Mineral deposits of Canada: A synthesis of major deposit-types, district metallogeny, the evolution of geological provinces, and exploration methods. Geological Association of Canada, Mineral Deposits Division, Special Publication No. 5, p. 881-902.

Cowan, W.R. 1976. Quaternary Geology of the Sault Ste. Marie Area, District of Algoma; in Summary of Fieldwork, 1976. Geological Branch, Ontario Division of Mines, Miscellaneous Paper 67, p. 134- 136.

Cowan, W.R. 1985. Deglacial Great Lakes Shorelines at Sault Ste. Marie, Ontario; in Quaternary Evolution of the Great Lakes. Geological Association of Canada Special Paper 30, p. 33-37.

Cowan, W.R., and Bennett, G. 1998. Urban Geology: City of Sault Ste. Marie, Ontario; in Urban Geology of Canadian Cities. Geological Association of Canada Special Paper 42, p. 197-205.

Cruden, A.R. 2006. Emplacement and growth of plutons: implications for rates of melting and mass transfer in continental crust; in Evolution and Differentiation of the Continental Crust. Cambridge University Press, Cambridge, UK, p. 455-519.

Davidson, A., van Breeman, O., and Sullivan, R.W. 1992. Circa 1.75 Ga ages for plutonic rocks of the Southern Province and adjacent Grenville Province: what is the expression of the Penokean orogeny? in Radiogenic Age and Isotopic Studies: Report 6, Geological Survey of Canada, Paper 92-2, p.107- 118.

Easton, R.M. 2000a. Metamorphism of the Canadian Shield, Ontario, Canada. I. The Superior Province. The Canadian Mineralogist, 38, p. 287-317.

Easton, R.M. 2000b. Metamorphism of the Canadian Shield, Ontario, Canada. II. Proterozoic metamorphic history. The Canadian Mineralogist, 38, p. 319-344.

Easton, R. M. 2005, Geology of Porter and Vernon townships, Southern Province; in Summary of Field Work and Other Activities, 2005. Ontario Geological Survey, Open File Report 6172, p. 13–1 to 13–20.

Easton, R.M. 2009. Compilation Mapping, Pecors–Whiskey Lake Area, Southern and Superior Provinces; in Summary of Field Work and Other Activities 2010. Ontario Geological Survey, Open File Report 6240, 254 p.

Easton, R.M. 2010. Compilation Mapping, Pecors–Whiskey Lake Area, Southern and Superior Provinces; in Summary of Field Work and Other Activities 2010. Ontario Geological Survey, Open File Report 6260, p. 8-1 to 8-12.

Easton, R.M., John-Bevans L.S., and James, R.S. 2004. Geological Guidebook to the Paleoproterozoic East Bull Lake Intrusive Suite Plutons at East Bull Lake, Agnew Lake and River Valley, Ontario. Ontario Geological Survey, Open File Report 6315, 84 p.

Eschman, D.F., and Karrow, P.F. 1985. Huron Basin Glacial Lakes: A Review; in Quaternary Evolution of the Great Lakes. Geological Association of Canada Special Paper 30, p. 79-93.

Fedo, C.M., Young, G.M., Nesbitt, H.W., and Hanchar, J.M. 1997. Potassic and sodic metasomatism in the Southern Province of the Canadian Shield: evidence from the Paleoproterozoic Serpent Formation, Huronian Supergroup, Canada; Precambrian Research, 84, p. 17-36.

Ford, M.J. 1993. Quaternary geology of the Rawhide Lake Area, District of Algoma. Ontario Geological Survey, Open File Report 5867.

Forte, A., Moucha, R., Simmons, N., Grand, S., and Mitrovica, J. 2010. Deep-mantle contributions to the surface dynamics of the North American continent. Tectonophysics, 481, p. 3–15.

Fraser, J.A., and Heywood, W.W. (editors). 1978. Metamorphism in the Canadian Shield. Geological Survey of Canada, Paper 78-10, 367 p.

Gartner, J.F. 1978a. Northern Ontario Engineering Geology Terrain Study, data base map, Cartier, NTS 41I/NW. Ontario Geological Survey, Map M5000, scale 1:100,000.

Gartner, J.F. 1978b. Northern Ontario Engineering Geology Terrain Study, data base map, Espanola, NTS 41I/SW. Ontario Geological Survey, Map M5002, scale 1:100,000.

Gartner, J.F. 1978c. Northern Ontario Engineering Geology Terrain Study, general construction capability map, Cartier, NTS 41I/NW. Ontario Geological Survey, Map M5004, scale 1:100,000.

Gartner, J.F. 1980a. Cartier Area (NTS 41I/NW), Districts of Algoma and Sudbury. Ontario Geological Survey, Northern Ontario Engineering Geology Terrain Study 94, 18 p.

Gartner, J.F. 1980b. Espanola Area (NTS 41I/SW), Districts of Manitoulin and Sudbury. Ontario Geological Survey, Northern Ontario Engineering Geology Terrain Study 99, 14 p.

Gartner, J.F., Mollard, J.D., and Roed, M.A. 1981. Ontario Engineering Geology Terrain Study User's Manual. Ontario Geological Survey, Northern Ontario Engineering Geology Terrain Study 1.

Giblin, P.E. 1976. Report of the Northeastern Regional Geologist and Sault Ste. Marie Resident Geologist; p. 91-99 in Annual Report of the Regional and Resident Geologist, 1975, edited by C.R. Kustra, Ontario Division of Mines, MP64, 146p.Giblin, P.E. and E.J. Leahy, 1979. Sault Ste. Marie-Elliot Lake, Geological Compilation Series, Algoma, Manitoulin and Sudbury Districts. Ontario Geological Survey, Map 2419, scale 1:253,440.

Giblin, P.E., Leahy E.J., and Robertson, J.A. 1977. Geological Compilation of the Blind River-Elliot Lake Sheet, Districts of Algoma and Sudbury. Ontario Geological Survey Preliminary Map P.304, scale 126,720.

Golder. 2014. Phase 1 Desktop Geoscientific Preliminary Assessment of Potential Suitability for Siting a Deep Geological Repository for Canada's Used Nuclear Fuel, City of Elliot Lake, Town of Blind River, Township of The North Shore, and Town of Spanish, Ontario. Report for the Nuclear Waste Management Organization (NWMO). NWMO report number: APM-REP-06144-009

Gordon, C.A. 2012 Preliminary Results from the Otter–Morin Townships Bedrock Mapping Project, Southern and Superior Provinces; in Summary of Field Work and Other Activities 2012. Ontario Geological Survey, Open File Report 6280, p. 17-1 to 17-10.

Haimson, B.C. 1990. Scale effects in rock stress measurements. In Proceedings international workshop on scale effects in rock masses, Loen, AA Balkema, Rotterdam, p.89-101.

Halls, H.C., Davis, D.W., Stott, G.M., Ernst, R.E., and Hamilton, M.A. 2008. The Paleoproterozoic Marathon Large Igneous Province: New evidence for a 2.1 Ga long-lived mantle plume event along the southern margin of the North American Superior Province. Precambrian Research, 162, p. 327- 353.

Hamilton, M.A., David, D.W., Buchan, K.L., and Halls, H.C. 2002. Precise U-Pb dating of reversely magnetized Marathon diabase dykes and implications for emplacement of giant dyke swarms along the southern margin of the Superior Province, Ontario. Geological Survey of Canada, Current Research 2002-F6, 10p.

Heather, K.B., Shore, G.T., and van Breeman, O. 1995. The convoluted "layer cake", an old recipe with new ingredients for the Swayze greenstone belt, southern Superior Province, Ontario; in Current Research 1995-C, p. 1-10.

Holm, D.K., Schneider, D.A., O'Boyle, C., Hamilton, M.A., Jercinovic, M.J., and Williams, M.L. 2001. Direct timing constraints on Paleoproterozoic metamorphism, southern Lake Superior region: results from SHRIMP and EMP U-Pb dating of metamorphic monazites; Geological Society of America, Abstracts with Program, v.33, no.6, p.A-401.Jackson, S.L., 2001. On the structural geology of the Southern Province between Sault Ste. Marie and Espanola, Ontario. Ontario Geological Survey, Open File Report 5995, 55 p.

Jackson, S.L. 2001. On the structural geology of the Southern Province between Sault Ste. Marie and Espanola, Ontario. Ontario Geological Survey, Open File Report 5995, 55p.

Jackson, S.L., and Fyon, J.A. 1991. The Western Abitibi Subprovince in Ontario; in Geology of Ontario. Ontario Geological Survey, Special Volume 4, Part 1, p. 405-482.

[JDMA] J.D. Mollard and Associates Limited. 2014a. Phase 1 Geoscientific Desktop Preliminary Assessment Lineament Interpretation. City of Elliot Lake, Town of Blind River, Township of the North Shore and Town of Spanish, Ontario. Report prepared for Golder Associates Ltd. and NWMO, October 2014. APM-REP-06144-0094. Report available at www.nwmo.ca

[JDMA] J.D. Mollard and Associates Limited. 2014b. Phase 1 Geoscientific Desktop Preliminary Assessment, Terrain and Remote Sensing Study, City of Elliot Lake, Town of Blind River, Township of The North Shore, Town of Spanish, Ontario. Prepared for Nuclear Waste Management Organization (NWMO). NWMO Report Number: APM-REP-06144-0092.

Jensen, L.S. 1994. Geology of the Whiskey Lake Greenstone Belt (West Half), Districts of Sault Ste. Marie and Sudbury. Ontario Geological Survey, Open File Report 5883, 101 p.

Jolly, W.T. 1978. Metamorphic history of the Archean Abitibi Belt; in Metamorphism in the Canadian Shield. Geological Survey of Canada, Paper 78-10, p. 63-78.

Kamo, S.L., Krogh, T.E., and Kumarapeli, P.S. 1995. Age of the Grenville dyke swarm, Ontario – Quebec: implications for the timing of lapetan rifting; Canadian Journal of Earth Science, 32, p. 273-280.

Karrow, P.F. 1987. Glacial and glaciolacustrine events in northwestern Lake Huron, Michigan and Ontario, Geological Society of America Bulletin, 98, p. 113-120.

Kraus, J., and Menard, T. 1997. A thermal gradient at constant pressure: Implications for low- to mediumpressure metamorphism in a compressional tectonic setting, Flin Flon and Kisseynew domains, Trans-Hudson Orogen, Central Canada. The Canadian Mineralogist, 35, p. 1117-1136.

Krogh, T.E., Corfu, F., Davis, D.W., Dunning, G.R., Heaman, L.M., Kamo, S.L., Mashado, N., Greenhough, J.D., and Nakamura, E. 1987. Precise U-Pb isotopic ages of diabase dykes and mafic to ultramafic rocks using trace amounts of baddeleyite and zircon; In: Mafic Dyke Swarms, Geological Association of Canada, Special Paper 34, p.147-152.

McCrank, G.F.D., Kamineni, D.C., Ejeckam R.B., and Sikorsky, R. 1989. Geology of the East Bull Lake gabbro-anorthosite pluton, Algoma District, Ontario, Canadian Journal of Earth Sciences, 26, p. 357-375.

Menard, T., and Gordon, T.M. 1997. Metamorphic P-T paths from the Eastern Flin Flon Belt and Kisseynew Domain, Snow Lake, Manitoba; The Canadian Mineralogist, 35, p. 1093-1115.

Nur, A. 1982. The origin of tensile fractures. Journal of Structural Geology, 4, p. 31-40.

[NWMO] Nuclear Waste Management Organization. 2014a. Preliminary Assessment for Siting a Deep Geological Repository for Canada's Used Nuclear Fuel, City of Elliot Lake, Ontario – Findings from Step 3, Phase One Studies. NWMO Report Number: APM-REP-06144-0097.

[NWMO] Nuclear Waste Management Organization. 2014b. Preliminary Assessment for Siting a Deep Geological Repository for Canada's Used Nuclear Fuel, Town of Blind River, Ontario – Findings from Step 3, Phase One Studies. NWMO Report Number: APM-REP-06144-0089.

[OGS] Ontario Geological Survey. 1997. Bedrock geology of Ontario, explanatory notes and legend, Ontario Geological Survey, Map 2545

[OGS] Ontario Geological Survey. 2011. 1:250 000 Scale Bedrock Geology of Ontario, Miscellaneous Release – Data 126 – Revision 1. ISBN 978-1-4435-5704-7 (CD) ISBN 978-1-4435-5705-4 [zip file]

[OMNR] Ontario Ministry of Natural Resources. 2009. Forest Information Manual – Forest Resources Inventory Technical Specifications.

Osmani, I.A. 1991. Proterozoic mafic dyke swarms in the Superior Province of Ontario. in Geology of Ontario, Ontario Geological Survey, Special Volume 4, Part 1, pp. 661-681

Pease, V., Percival, J., Smithies, H., Stevens, G., and Van Kranendonk, M. 2008. When did plate tectonics begin? Evidence from the orogenic record; In: Condie, K.C. and Pease, V., eds., When Did Plate Tectonics Begin on Earth?; Geological Society of America Special Paper 440, p.199-228.

Percival, J.A., Sanborn-Barrie, M., Skulski, T., Stott, G.M., Helmstaedt, H., and White, D.J. 2006. Tectonic evolution of the western Superior Province from NATMAP and Lithoprobe studies; Canadian Journal of Earth Sciences, 43, p.1085-1117.

[PGW] Paterson, Grant and Watson Limited. 2014. Phase 1 Geoscientific Desktop Preliminary Assessment, Processing and Interpretation of Geophysical Data, Communities of Elliot Lake, Blind River, The North Shore and Spanish and Surrounding Area, Ontario. Prepared for Nuclear Waste Management Organization (NWMO). NWMO Report Number: APM-REP-06144-0093.

Piercey, P. 2006. Proterozoic Metamorphic Geochronology of The Deformed Southern Province, Northern Lake Huron Region, Canada: unpublished M.Sc. Thesis, Ohio University, 67 p.

Piercey, P., Schneider, D.A., and Holm, D.K. 2003. Petrotectonic evolution of Paleoproterozoic rocks across the 1.8 Ga Central Penokean orogen, northern MI & WI. Geological Society of America, Abstracts, 35, 554 p.

Powell, W.G., Carmichael, D.M., and Hodgson, C.J. 1993. Thermobarometry in a subgreenschist to greenschist transition in metabasites of the Abitibi greenstone belt, Superior Province, Canada. Journal of Metamorphic Geology, 11, p. 165-178.

Raharimahefa, T., Tinkham, D.K., and Lafrance, B. 2011. New U-Pb Geochronological Constraints on the Structural Evolution of the Southern Province, Sudbury, Canada. Paper No. 101-10. 2011 GSA Annual Meeting in Minneapolis. 9-12 October 2011.

Riller, U., Schwerdtner, W.M., Halls, H.C., and Card, K.D. 1999. Transpressive tectonism in the eastern Penokean orogen, Canada: Consequences for Proterozoic crustal kinematics and continental fragmentation. Precambrian Research, 93, p. 51–70.

Robertson, J.A. 1962. Geology of Townships 137 and 138, District of Algoma. Ontario Department of Mines Geological Report 10, 94p.

Robertson, J.A. 1965a. Ontario Department of Mines Preliminary Geology Map No P318, Shedden Township Part IR No 7.

Robertson, J.A. 1965b. Ontario Department of Mines Preliminary Geology Map No P319, IR No 7 East and Offshore, District of Algoma.

Robertson, J.A. 1965c. Ontario Department of Mines Preliminary Geology Map No P320, IR No 5 West and Offshore Islands, District of Algoma.

Robertson, J.A. 1968. Geology of Township 149 and Township 150, District of Algoma. Ontario Department of Mines, Geological Report 57, 162 p.

Robertson, J.A. 1970. Geology of the Spragge area, District of Algoma. Ontario Department of Mines, Geological Report Number 76, 109 p.

Robertson, J.A., and Johnson, J.M. 1965. Ontario Department of Mines Preliminary Geology Map No P317, Deagle Township, District of Algoma.

Roed, M.A., and Hallett, D.R. 1979a. Northern Ontario Engineering Geology Terrain Study, data base map, Biscotasing, NTS 41O/SE. Ontario Geological Survey, Map M5017, scale 1:100,000.

Roed, M.A., and Hallett, D.R. 1979b. Northern Ontario Engineering Geology Terrain Study, data base map, Wenebegon Lake, NTS 41O/SW. Ontario Geological Survey, Map M5016, scale 1:100,000.

Roed, M.A., and Hallett, D.R. 1979c. Northern Ontario Engineering Geology Terrain Study, data base map, Westree, NTS 41P/SW. Ontario Geological Survey, Map M5022, scale 1:100,000.

Roed, M.A., and Hallett, D.R. 1979d. Westree Area (NTS 41P/SW), Districts of Sudbury and Timiskaming. Ontario Geological Survey, Northern Ontario Engineering Geology Terrain Study 88, 12 p.

Roed, M.A., and Hallett, D.R. 1980a. Biscotasing Area (NTS 41O/SE), Districts of Algoma and Sudbury. Ontario Geological Survey, Northern Ontario Engineering Geology Terrain Study 87, 15 p.

Roed, M.A., and Hallett, D.R. 1980b. Wenebegon Lake Area (NTS 41P/SW), Districts of Algoma and Sudbury. Ontario Geological Survey, Northern Ontario Engineering Geology Terrain Study 86, 12 p.

Rogers, M.C. 1992. Geology of the Whiskey Lake Area, East Half. Ontario Geological Survey, Open File Report 5834, 109 p.

Sage, R.P. 1988. Geology of Carbonatite Alkalic Rock Complexes in Ontario: Seabrook Lake Carbonatite Complex, District of Algoma. Ontario Geological Survey, Study 31, 45 p.

Siemiatkowska, K.M. 1977. Geology of the Wakomata Lake area. Ontario Division of Mines, Geological Report 151, 57p. Accompanied by map 2350, scale 1 inch to 1/2 mile (1:31,680).

SGL (Sander Geophysics Limited) 2017. Phase 2 Geoscientific Preliminary Assessment, Acquisition, Processing and Interpretation of High-Resolution Airborne Geophysical Data, Blind River, Elliot Lake and Area, Ontario. NWMO Report Number: APM-REP-01332-0217.

SRK. 2013a. Phase 1 Geoscientific Desktop Preliminary Assessment, Lineament Interpretation, Township of Schreiber, Ontario. NWMO Report Number: APM-REP-06144-0038.

SRK. 2013b. Phase 1 Geoscientific Desktop Preliminary Assessment, Lineament Interpretation, Township of Ear Falls. NWMO Report Number: APM-REP-06144-0022.

SRK. 2014a. Phase 1 Geoscientific Desktop Preliminary Assessment, Lineament Interpretation, Township of Manitouwadge. NWMO Report Number: APM-REP-06144-0078.

SRK. 2014b. Phase 1 Geoscientific Desktop Preliminary Assessment, Lineament Interpretation, Township of White River. NWMO Report Number: APM-REP-06144-0086.

SRK. 2015a. Phase 2 Geoscientific Desktop Preliminary Assessment, Lineament Interpretation, Township of Creighton. NWMO Report Number: APM-REP-06145-0011.

SRK. 2015b. Phase 2 Geoscientific Desktop Preliminary Assessment, Lineament Interpretation, Township of Schreiber. NWMO Report Number: APM-REP-06145-0007.

SRK. 2015c. Phase 2 Geoscientific Desktop Preliminary Assessment, Lineament Interpretation, Township of Ignace. NWMO Report Number: APM-REP-06145-0003

Spray, J.G., Butler, H.R., and Thompson, L.M. 2004. Tectonic influences on the morphometry of the Sudbury impact structure: Implications for terrestrial cratering and modeling. Meteoritics and Planetary Science, 39, 2, p. 287-301.

Thurston, P.C. 1991. Geology of Ontario: Introduction; in Geology of Ontario, Special Volume No. 4, Part 1, p. 3-26.

van Breemen, O., Heather, K.B., and Ayer, J.A. 2006. U-Pb geochronology of the Neoarchean Swayze sector of the southern Abitibi greenstone belt. Current Research 2006 F1, Geological Survey of Canada

VanDine, D.F. 1979a. Northern Ontario Engineering Geology Terrain Study, database map, Bark Lake, NTS 41J/NE. Ontario Geological Survey, Map 5006, scale 1:100,000.

VanDine, D.F. 1979b. Northern Ontario Engineering Geology Terrain Study, database map, Blind River, NTS 41J/SE. Ontario Geological Survey, Map 5008, scale 1:100,000.

VanDine, D.F. 1979c. Northern Ontario Engineering Geology Terrain Study, database map, Thessalon, NTS 41J/SW. Ontario Geological Survey, Map 5007, scale 1:100,000.

VanDine, D.F. 1979d. Northern Ontario Engineering Geology Terrain Study, database map, Wakomata Lake, NTS 41J/NW. Ontario Geological Survey, Map 5005, scale 1:100,000.

VanDine, D.F. 1980a. Bark Lake Area (NTS 41J/NE), Districts of Algoma and Sudbury. Ontario Geological Survey, Northern Ontario Engineering Geology Terrain Study 93, 12 p.

VanDine, D.F. 1980b. Blind River Area (NTS 41J/SE), Districts of Algoma, Manitoulin, and Sudbury. Ontario Geological Survey, Northern Ontario Terrain Study 98, 14 p.

VanDine, D.F. 1980c. Thessalon Area (NTS 41J/SW), District of Algoma. Ontario Geological Survey, Northern Ontario Engineering Geology Terrain Study 97, 16 p.

VanDine, D.F. 1980d. Wakomata Lake Area (NTS 41J/NW), District of Algoma. Ontario Geological Survey, Northern Ontario Engineering Geology Terrain Study 92, 13 p.Vogel D.C., R.S. James and R.R. Keays, 1998. The early tectono-magmatic evolution of the Southern Province: implications from the Agnew Intrusion, central Ontario, Canada. Canadian Journal of Earth Sciences, 35, p. 854-870.

Vogel D.C., James, R.S., and Keays, R.R. 1998. The early tectono-magmatic evolution of the Southern Province: implications from the Agnew Intrusion, central Ontario, Canada. Canadian Journal of Earth Sciences, 35, 854-870.

Williams, H., Hoffman, P.F., Lewry, J.F., Monger, J.W.H., and Rivers, T. 1991. Anatomy of North America: thematic portrayals of the continent. Tectonophysics, 187, p. 117–134.

Young, G.M. 1983. Tectono-sedimentary history of early Proterozoic rocks of the northern Great Lakes region; in Early Proterozoic Geology of the Great Lakes Region. Geological Society America Memoir 160, p.15–32.

Zoback, M.L. 1992. First- and second-order patterns of stress in the lithosphere: the world stress map project; Journal of Geophysical. Research, 97, p.11,703-11,728.

Zolnai, A.l., Price, R.A., and Helmstaedt, H. 1984. Regional cross section of the Southern Province adjacent to Lake Huron, Ontario: implications for the tectonic significance of the Murray Fault Zone. Canadian Journal of Earth Sciences, 21, 447-456.

# APPENDIX A:
# Additional Supporting Figures

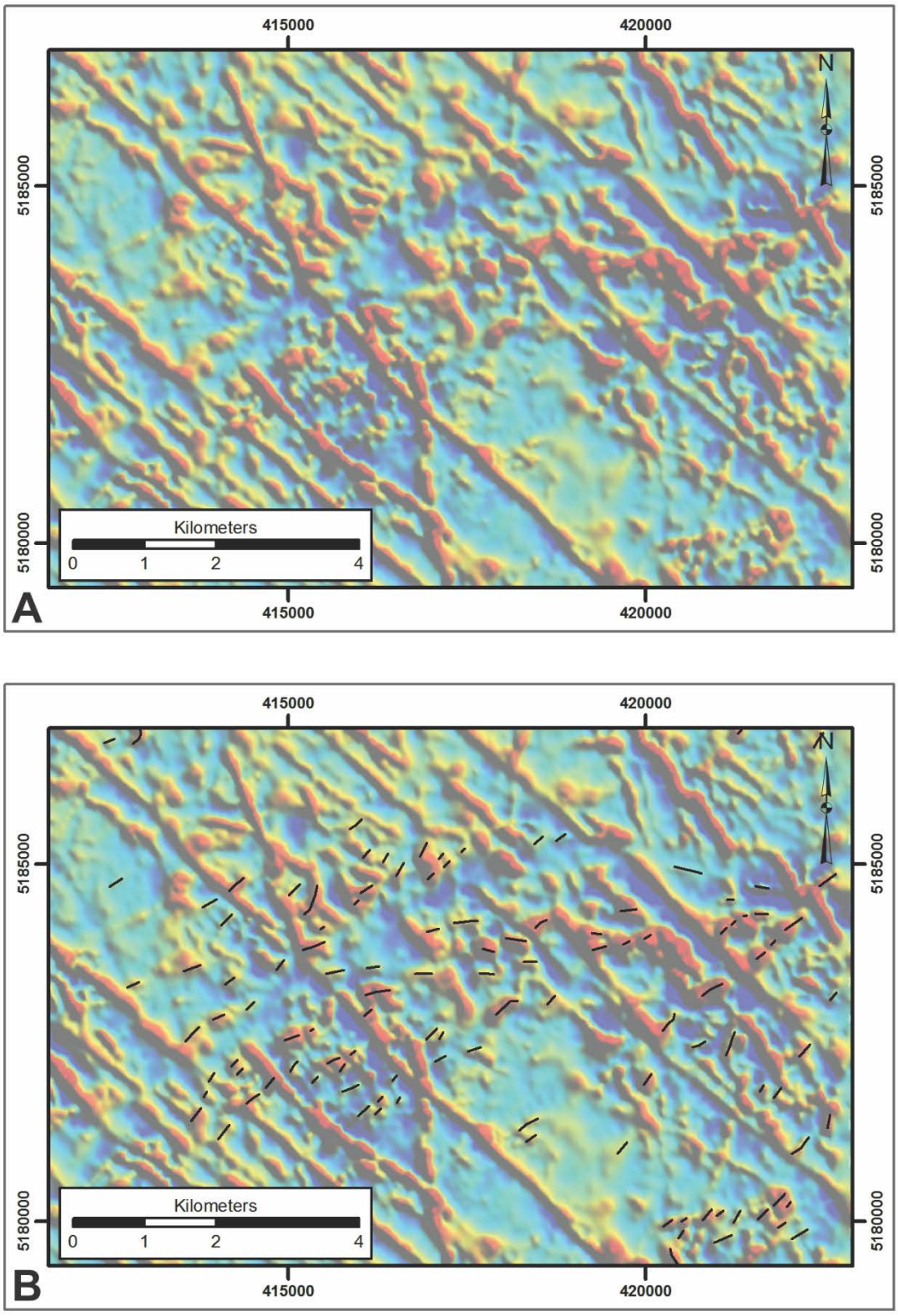



**Figure A1: Example of Form Lines from the Area North of Elliot Lake and Blind River**

A: Pole Reduced Magnetic Data

B: Form Line Interpretation of Pole Reduced Magnetic Data

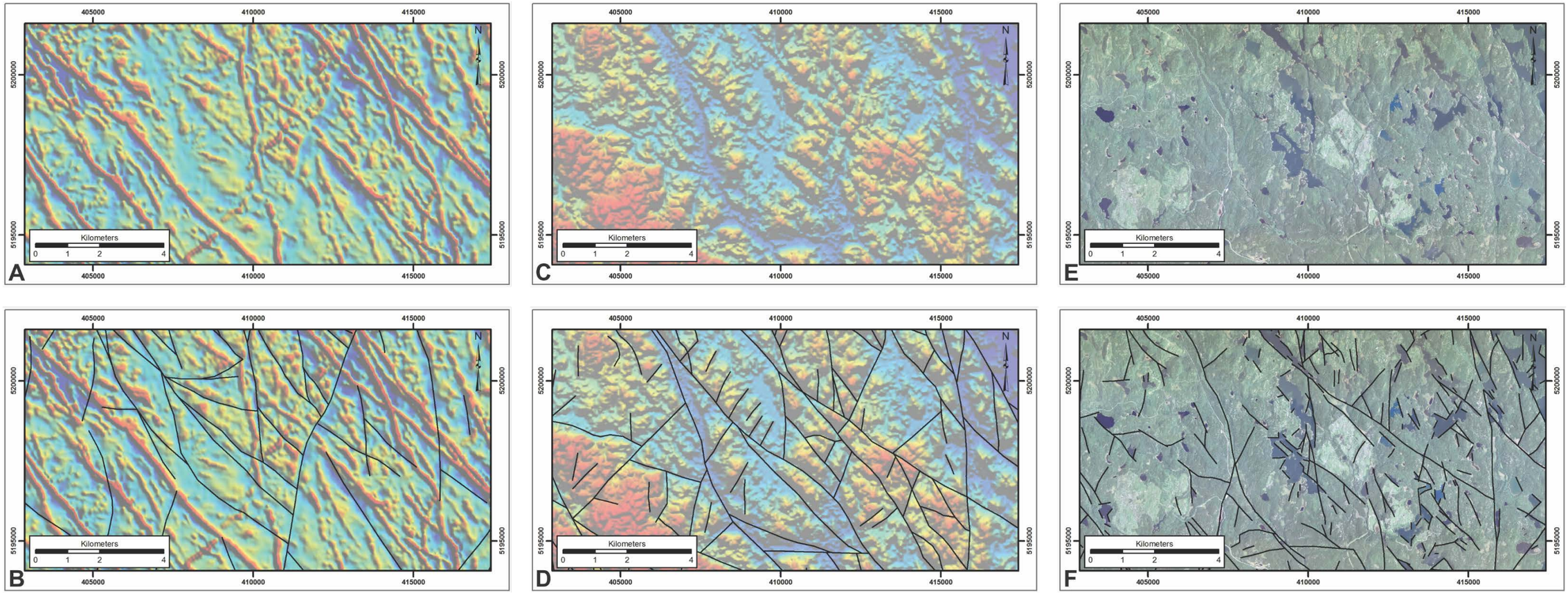



**Figure A2: Example of Brittle Lineaments from the Same Location in the Area North of Elliot Lake and Blind River manifested in magnetic, DEM and FRI data sets, respectively**

A: Pole Reduced Magnetic Data

B: Brittle Lineament Interpretation of Pole Reduced Magnetic Data

C: Digital Elevation Data

D: Brittle Lineament Interpretation of Digital Elevation Data

E: Forest Resource Inventory (FRI) Data

F: Brittle Lineament Interpretation of Forest Resource Inventory (FRI) Data

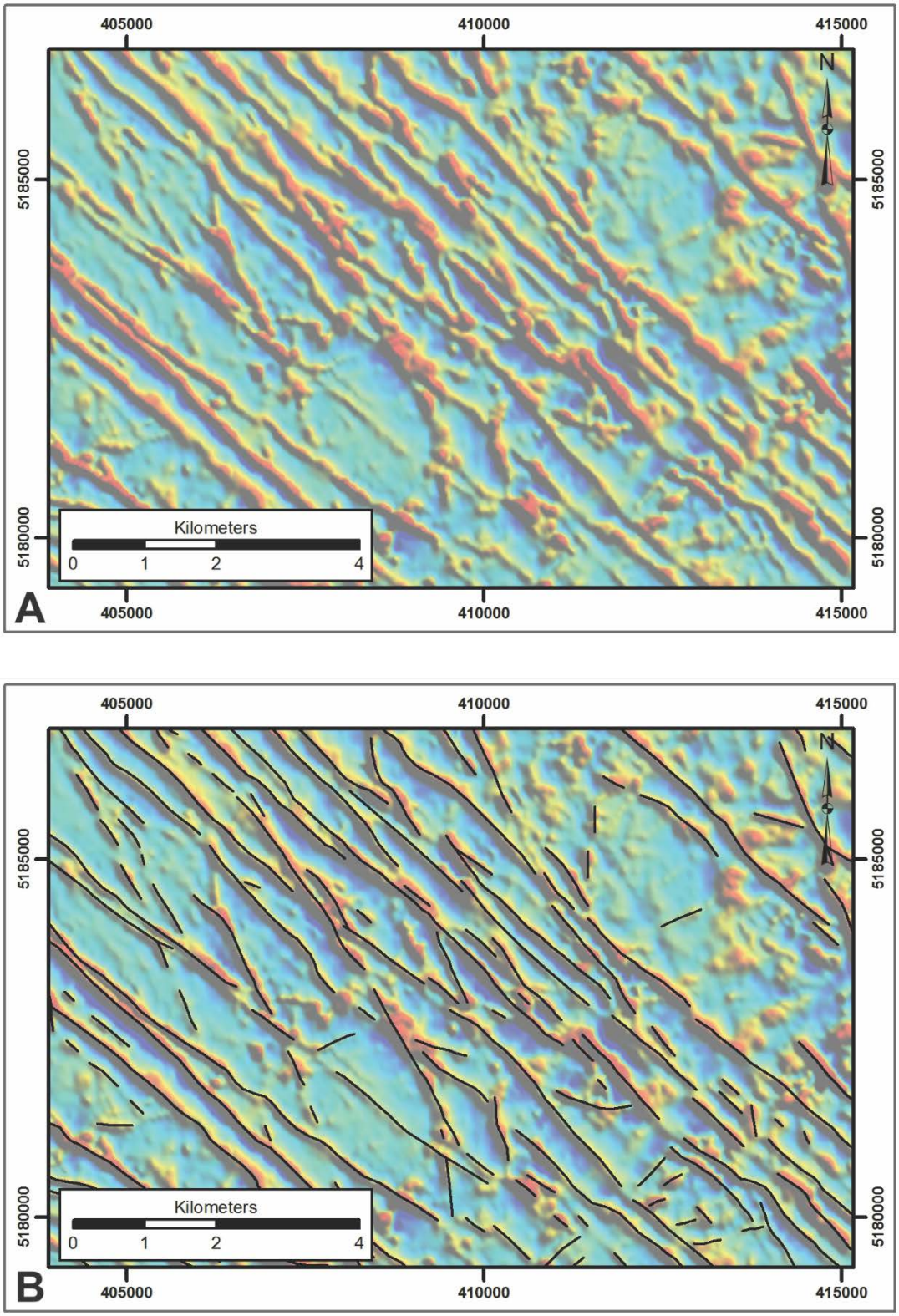



**Figure A3: Example of Dyke Lineaments from the Area North of Elliot Lake and Blind River**

A: Pole Reduced Magnetic Data

B: Dyke Lineament Interpretation of Pole Reduced Magnetic Data

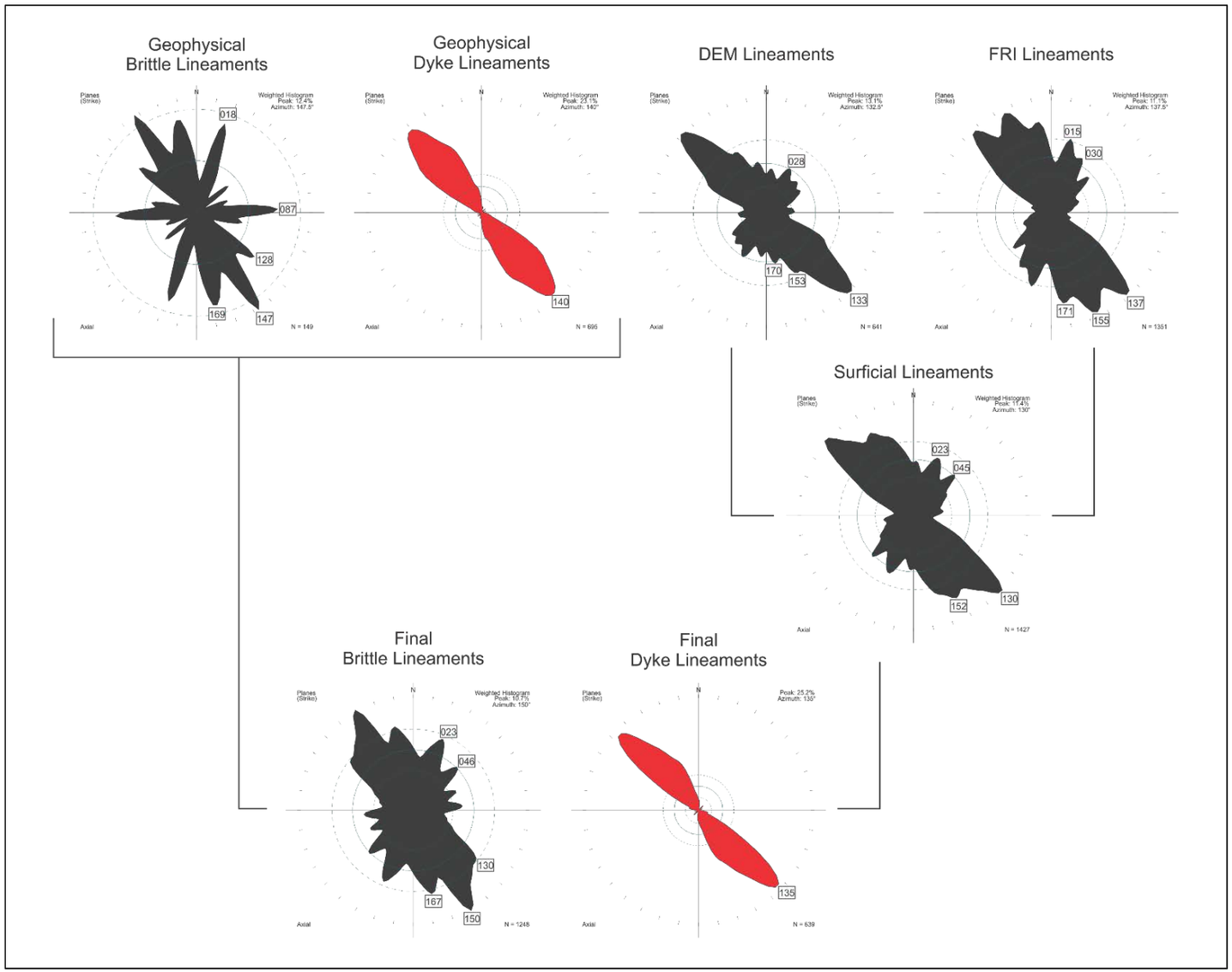



**Figure A4: Summary of Lineament Orientations for the North of Elliot Lake and Blind River**

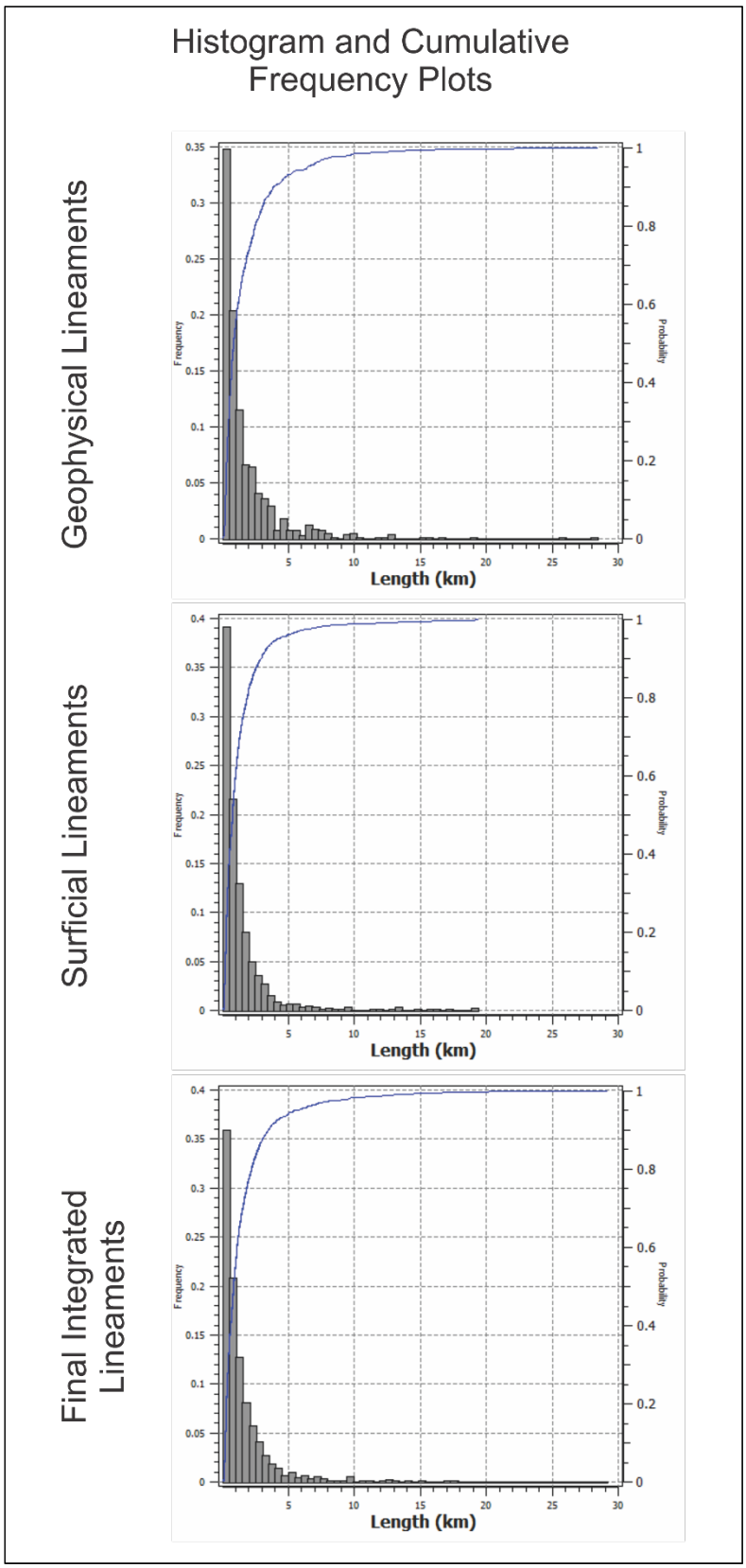



**Figure A5: Summary of Length Statistics for the North of Elliot Lake and Blind River**

# APPENDIX B:
# Summary of Lineament Statistics

**Table B1: Summary of Geophysical Lineament Statistics**

| | All Lineaments | Brittle | Dyke |
|---|---|---|---|
| Total Number of Lineaments | 844 | 149 | 695 |
| Max Length (kilometres) | 28.36 | 15.48 | 28.36 |
| Minimum Length (kilometres) | 0.1 | 0.54 | 0.1 |
| Median Length (kilometres) | 0.88 | 2.54 | 0.7 |
| Mean Length (kilometres) | 1.77 | 3.41 | 1.41 |
| Certainty 1 (number) | 52 | 25 | 27 |
| Certainty 1 (percent) | 6 | 17 | 4 |
| Certainty 2 (number) | 172 | 51 | 121 |
| Certainty 2 (percent) | 20 | 34 | 17 |
| Certainty 3 (number) | 620 | 73 | 547 |
| Certainty 3 (percent) | 74 | 49 | 79 |
| RA1 = 2 (number) | 470 | 55 | 415 |
| RA1 = 2 (percent) | 56 | 37 | 60 |
| RA1 = 1 (number) | 374 | 94 | 280 |
| RA1 = 1 (percent) | 44 | 63 | 40 |

**Table B2: Summary of DEM Lineament Statistics**

| | All Lineaments |
|---|---|
| Total Number of Lineaments | 641 |
| Max Length (kilometres) | 31.12 |
| Minimum Length (kilometres) | 0.35 |
| Median Length (kilometres) | 1.56 |
| Mean Length (kilometres) | 2.35 |
| Certainty 1 (number) | 187 |
| Certainty 1 (percent) | 29 |
| Certainty 2 (number) | 317 |
| Certainty 2 (percent) | 50 |
| Certainty 3 (number) | 137 |
| Certainty 3 (percent) | 21 |
| RA1 = 2 (number) | 268 |
| RA1 = 2 (percent) | 42 |
| RA1 = 1 (number) | 373 |
| RA1 = 1 (percent) | 58 |

**Table B3: Summary of FRI Lineament Statistics**

| | All Lineaments |
|---|---|
| Total Number of Lineaments | 1351 |
| Max Length (kilometres) | 10.77 |
| Minimum Length (kilometres) | 0.07 |
| Median Length (kilometres) | 0.49 |
| Mean Length (kilometres) | 0.82 |
| Certainty 1 (number) | 394 |
| Certainty 1 (percent) | 29 |
| Certainty 2 (number) | 639 |
| Certainty 2 (percent) | 47 |
| Certainty 3 (number) | 318 |
| Certainty 3 (percent) | 24 |
| RA1 = 2 (number) | 620 |
| RA1 = 2 (percent) | 46 |
| RA1 = 1 (number) | 731 |
| RA1 = 1 (percent) | 54 |

**Table B4: Summary of Integrated Surficial Lineament Statistics**

| | All Lineaments |
|---|---|
| Total Number of Lineaments | 1427 |
| Max Length (kilometres) | 19.38 |
| Minimum Length (kilometres) | 0.07 |
| Median Length (kilometres) | 0.79 |
| Mean Length (kilometres) | 1.38 |
| Certainty 1 (number) | 406 |
| Certainty 1 (percent) | 28 |
| Certainty 2 (number) | 698 |
| Certainty 2 (percent) | 49 |
| Certainty 3 (number) | 323 |
| Certainty 3 (percent) | 23 |
| RA2 = 2 (number) | 270 |
| RA2 = 2 (percent) | 19 |
| RA2 = 1 (number) | 1157 |
| RA2 = 1 (percent) | 81 |

**Table B5: Summary of Final Integrated Lineament Statistics**

| | All Lineaments | Brittle | Dyke |
|---|---|---|---|
| Total Number of Lineaments | 1887 | 1248 | 639 |
| Max Length (kilometres) | 29.13 | 19.38 | 29.13 |
| Minimum Length (kilometres) | 0.07 | 0.07 | 0.11 |
| Median Length (kilometres) | 0.87 | 0.9 | 0.81 |
| Mean Length (kilometres) | 1.63 | 1.6 | 1.69 |
| Certainty 1 (number) | 351 | 332 | 19 |
| Certainty 1 (percent) | 19 | 27 | 3 |
| Certainty 2 (number) | 689 | 587 | 102 |
| Certainty 2 (percent) | 36 | 47 | 16 |
| Certainty 3 (number) | 847 | 329 | 518 |
| Certainty 3 (percent) | 45 | 26 | 81 |
| RA2 = 3 (number) | 124 | 67 | 57 |
| RA2 = 3 (percent) | 6 | 5 | 9 |
| RA2 = 2 (number) | 296 | 225 | 71 |
| RA2 = 2 (percent) | 16 | 18 | 11 |
| RA2 = 1 (number) | 1467 | 956 | 511 |
| RA2 = 1 (percent) | 78 | 77 | 80 |

**Table B6: Summary of Final Integrated Brittle and Dyke Lineament Length Statistics**

| | Mean length (kilometres) | Median length (kilometres) |
|---|---|---|
| Certainty 1 | 0.91 | 0.73 |
| Certainty 2 | 1.06 | 0.70 |
| Certainty 3 | 2.39 | 1.23 |
| RA2 = 3 | 5.17 | 3.52 |
| RA2 = 2 | 2.73 | 1.85 |
| RA2 = 1 | 1.11 | 0.65 |

# Figures

**Figure 1: Location and Overview of the Area North of Elliot Lake and Blind River**

**Figure 2: Bedrock Geology of the Area North of Elliot Lake and Blind River**

**Figure 3: Terrain Features of the Area North of Elliot Lake and Blind River**

**Figure 4: Pole Reduced Magnetic Data (First Vertical Derivative) of the Area North of Elliot Lake and Blind River**

**Figure 5: Digital Elevation Data of the Area North of Elliot Lake and Blind River**

**Figure 6: Forest Resource Inventory Digital Aerial Imagery of the Area North of Elliot Lake and Blind River**

**Figure 7: Form Lines from Pole Reduced Magnetic Data of the Area North of Elliot Lake and Blind River**

**Figure 8: Interpreted Lineaments from Pole Reduced Magnetic Data of the Area North of Elliot Lake and Blind River**

**Figure 9: Interpreted Lineaments from Digital Elevation Data of the Area North of Elliot Lake and Blind River**

**Figure 10: Interpreted Lineaments from Forest Resource Inventory (FRI) Imagery of the Area North of Elliot Lake and Blind River**

**Figure 11: Interpreted Lineaments from Surficial Data of the Area North of Elliot Lake and Blind River**

**Figure 12: Interpreted Lineaments from Pole Reduced Magnetic Data of the Area North of Elliot Lake and Blind River**

**Figure 13: Select Final Integrated Lineaments of the Area North of Elliot Lake and Blind River**

**Figure 14: Interpreted Lineaments from Pole Reduced Magnetic Data (by Length) of the Area North of Elliot Lake and Blind River**

**Figure 15: Interpreted Lineaments (by Length) from Surficial Data of the Area North of Elliot Lake and Blind River**

**Figure 16: Final Integrated Lineaments (by Length) of the Area North of Elliot Lake and Blind River**

**Figure 17: Lineament Density for All Interpreted Lineaments from Pole Reduced Magnetic Data of the Area North of Elliot Lake and Blind River**

**Figure 18: Lineament Density for Interpreted Lineaments from Surficial Data of the Area North of Elliot Lake and Blind River**

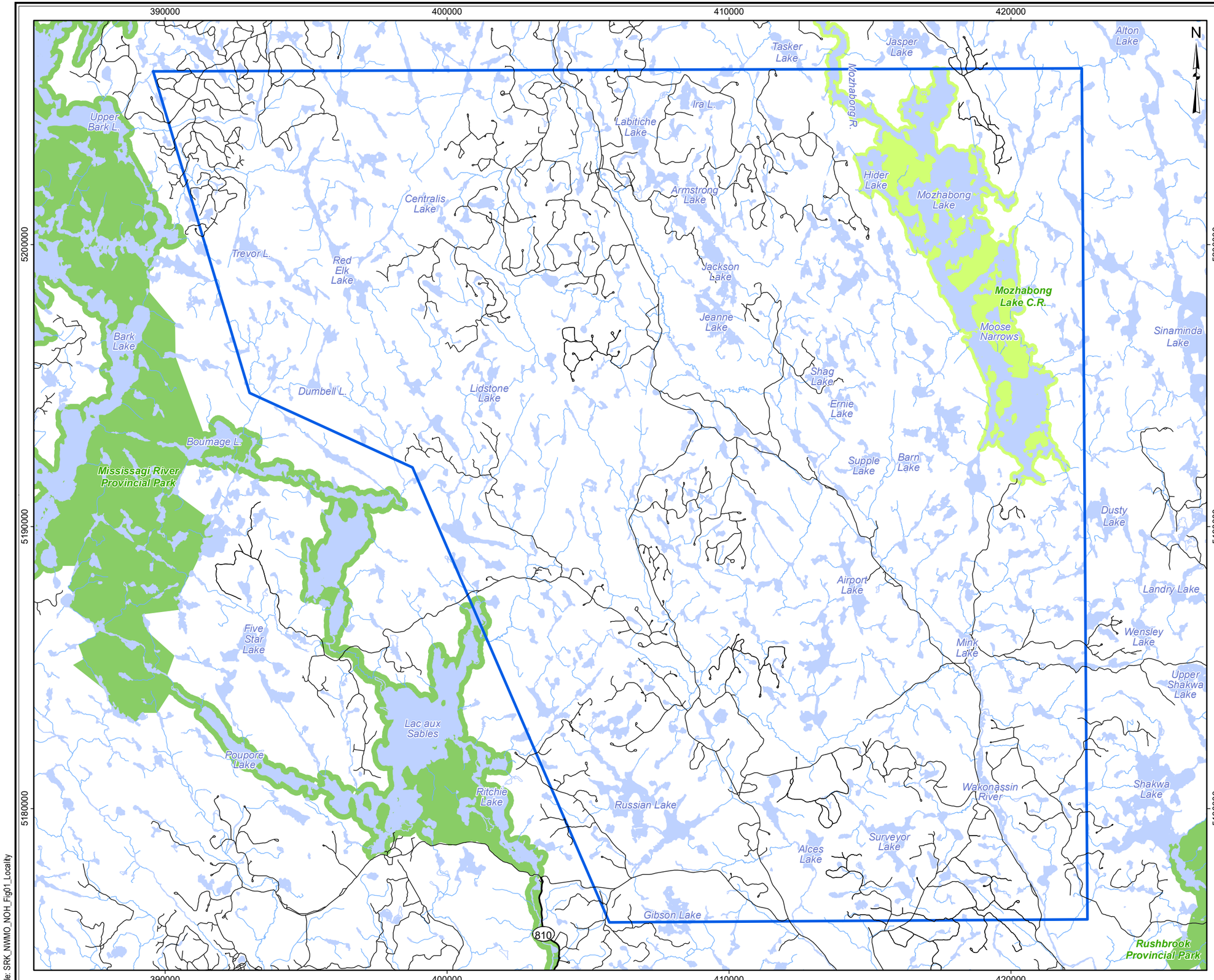
**Figure 19: Lineament Density for All Final Integrated Lineaments of the Area North of Elliot Lake and Blind River**

**Figure 20: Lineament Intersection Density for All Interpreted Lineaments from Pole Reduced Magnetic Data of the Area North of Elliot Lake and Blind River**

**Figure 21: Lineament Intersection Density for Interpreted Surficial Lineaments of the Area North of Elliot Lake and Blind River**

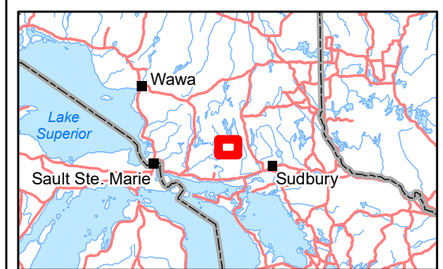
**Figure 22: Lineament Intersection Density for All Final Integrated Lineaments of the Area North of Elliot Lake and Blind River**

**Figure 23: Lineament Relative Age Relationships of the Area North of Elliot Lake and Blind River**




**LEGEND**

- Assessment Area
- Major Road
- Minor Road
- Watercourse
- Waterbody
- Provincial Park
- Conservation Reserve




**REFERENCE**

Base Data: Land Information Ontario (obtained 2015); CanVec Topography (obtained 2015)

0 5 km

srk consulting

PROJECT

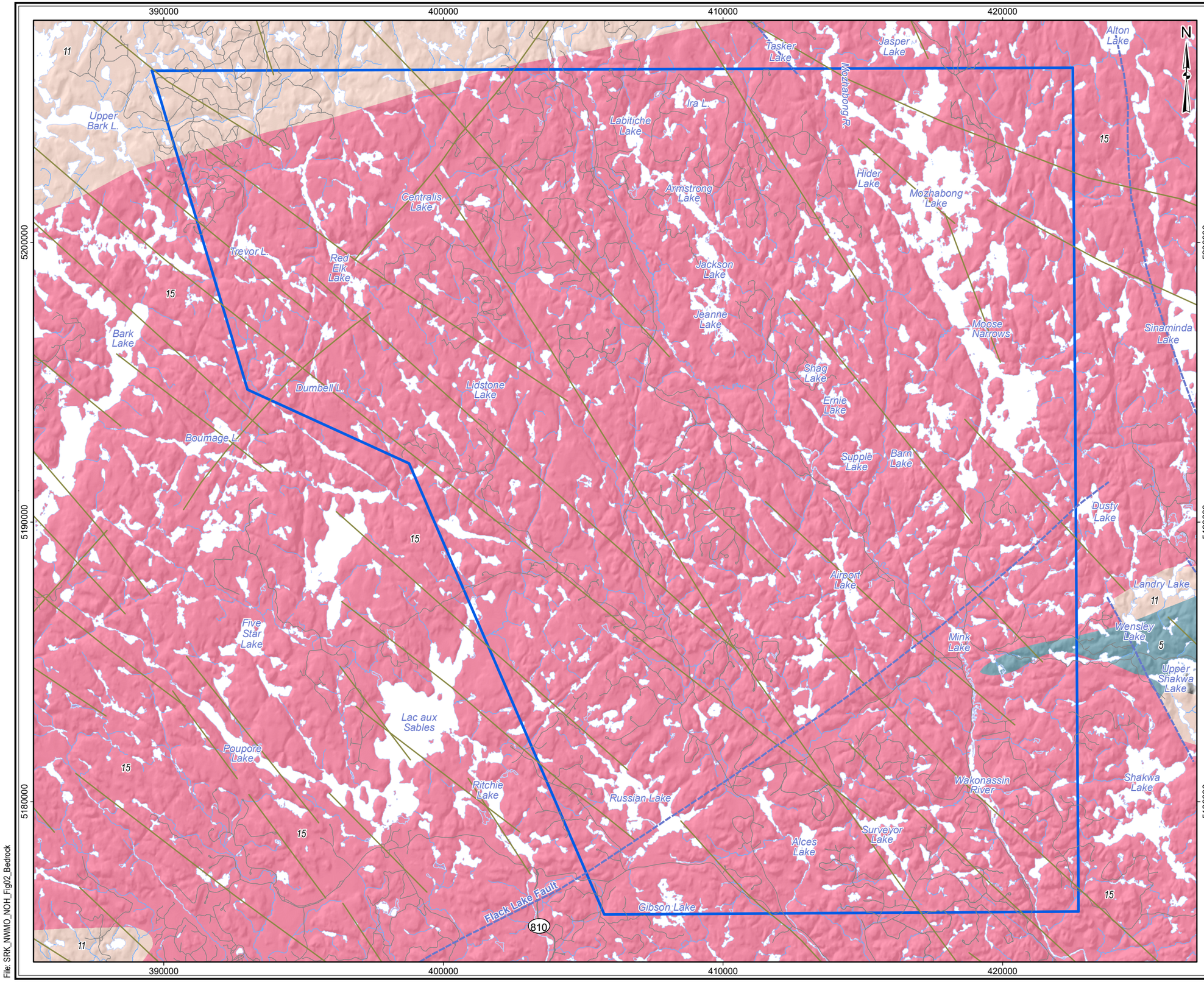
Lineament Interpretation
Area North of Elliot Lake and Blind River, Ontario

TITLE

**Location and Overview of the Area North of Elliot Lake and Blind River**

| | | | | |
|---|---|---|---|---|
| DESIGN | KR | 02 SEP 2014 | **Figure 1** | REVISION 2 |
| GIS | JA | 20 NOV 2017 | | UTM ZONE 17N |
| CHECK | SC | 20 NOV 2017 | | NAD 1983 |
| REVIEW | JPS | 20 NOV 2017 | | 1:130,000 |

File: SRK_NWMO_NOH_Fig01_Locality

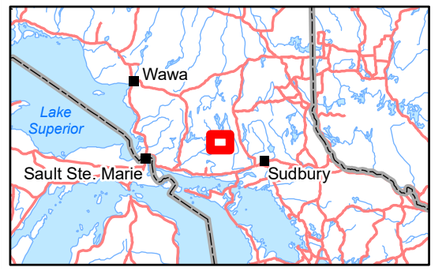



**LEGEND**

- Assessment Area
- Major Road
- Minor Road
- Watercourse
- Waterbody

**Bedrock Geology**

- Mapped Fault
- Mapped Dyke
- Massive granodiorite to granite (15)
- Gneissic tonalite suite (11)
- Benny Lake Greenstone Belt (5)




**REFERENCE**

Base Data: Land Information Ontario (obtained 2015);
CanVec Topography (obtained 2015)
Geology: MRD 126-REV1 (Ontario Geological Survey, 2011)

0 5 km

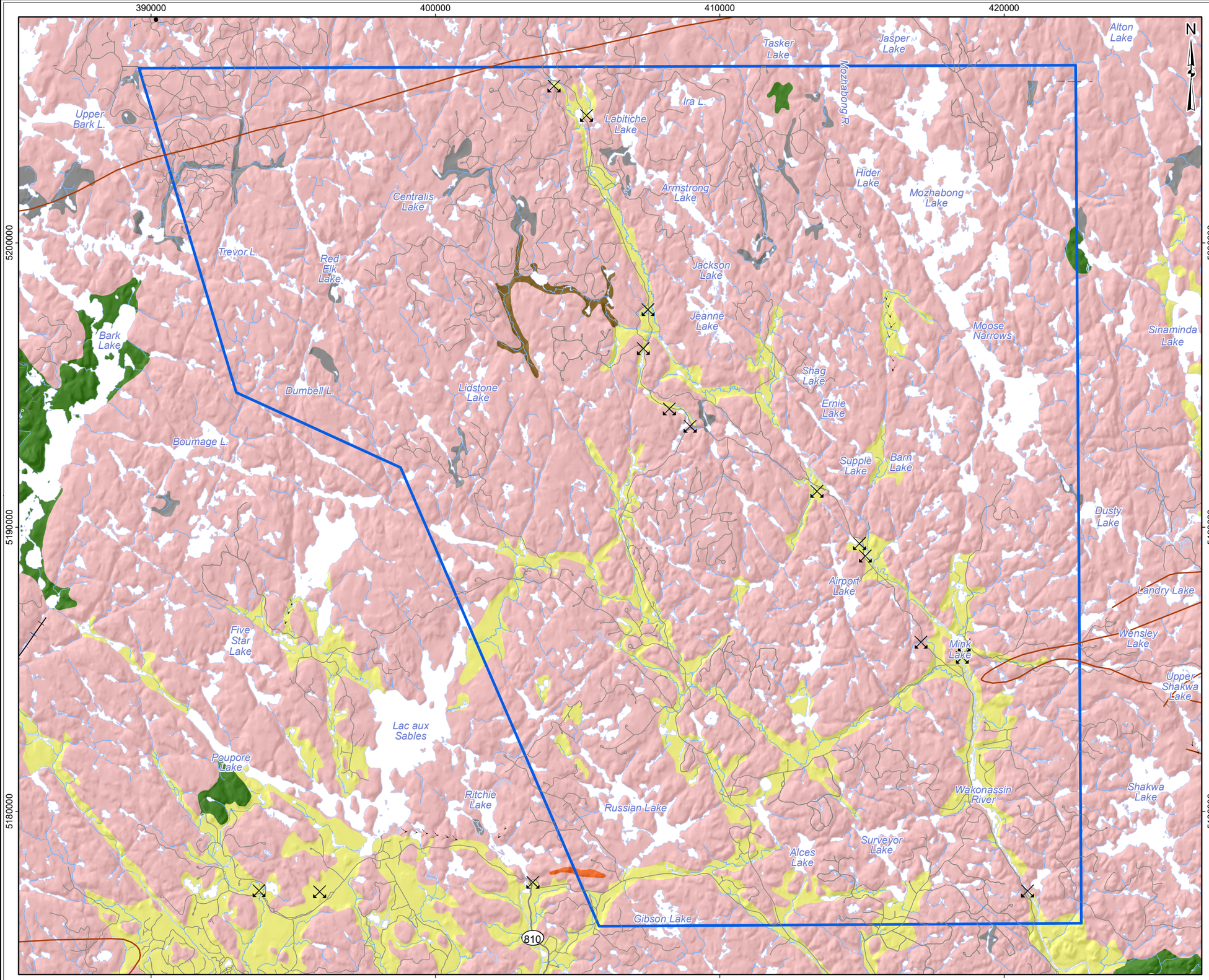
srk consulting

PROJECT
Lineament Interpretation
Area North of Elliot Lake and Blind River, Ontario

TITLE
**Bedrock Geology of the Area North of Elliot Lake and Blind River**

| | | | | |
|---|---|---|---|---|
| DESIGN | KR | 02 SEP 2014 | **Figure 2** | REVISION 2 |
| GIS | JA | 20 NOV 2017 | | UTM ZONE 17N |
| CHECK | SC | 20 NOV 2017 | | NAD 1983 |
| REVIEW | JPS | 20 NOV 2017 | | 1:130,000 |

File: SRK_NWMO_NOH_Fig02_Bedrock

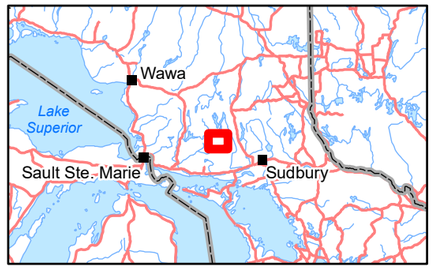



**LEGEND**

- Assessment Area
- Major Road
- Minor Road
- Watercourse
- Waterbody
- Geological contact

**Surficial Geology**

- Sand/Gravel pit
- Esker
- End Moraine
- Steep-walled Valley
- Man Made
- Ground Moraine
- Glaciofluvial Esker
- Glaciofluvial Outwash
- Alluvial
- Organics
- Bedrock




**REFERENCE**

Base Data: Land Information Ontario (obtained 2015); CanVec Topography (obtained 2015)
Surficial Geology: MRD-160 (Digital Northern Ontario Engineering Geology Terrain Study, 2005)

0 5 km

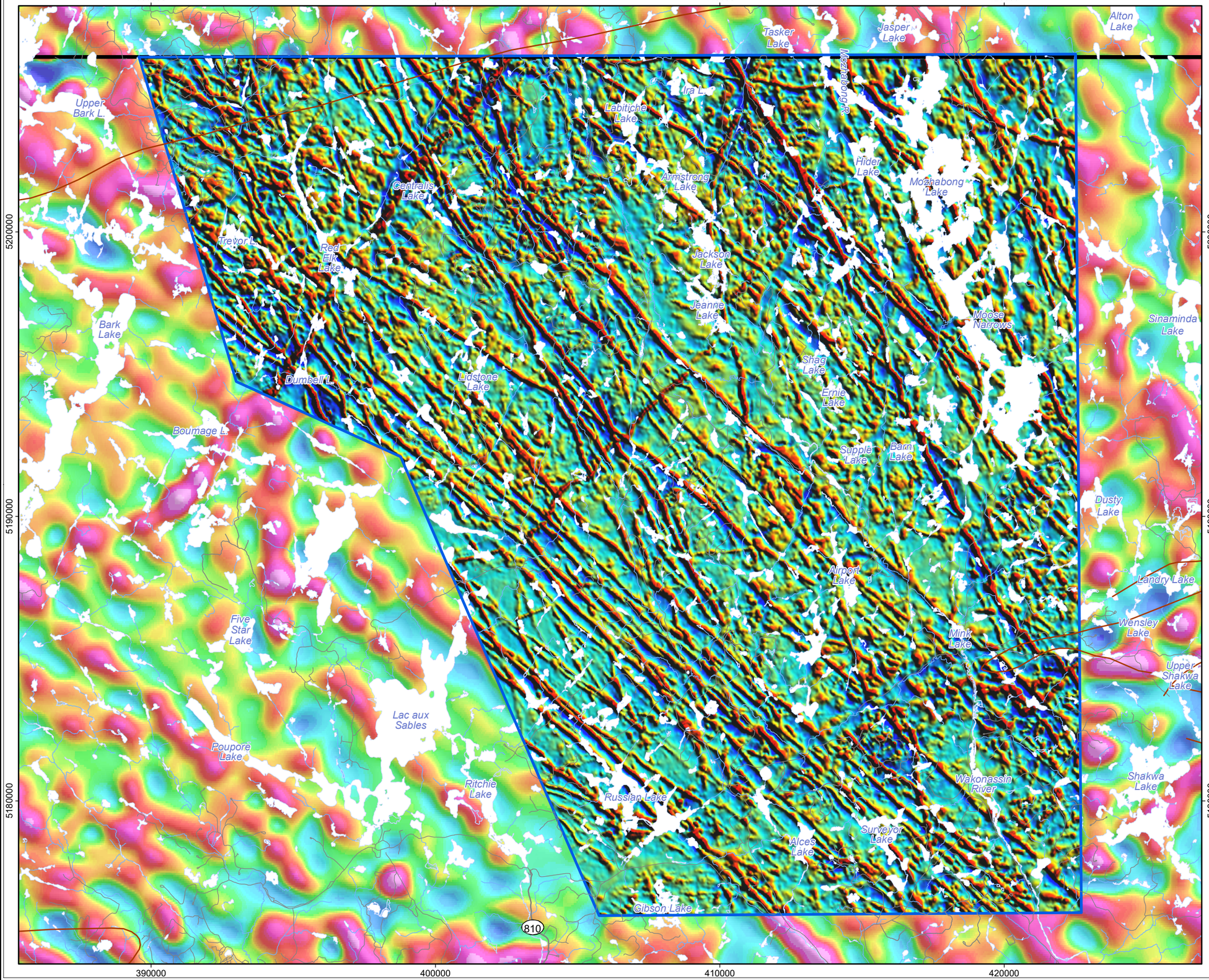
srk consulting

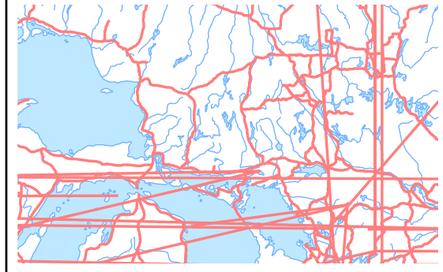
PROJECT
Lineament Interpretation
Area North of Elliot Lake and Blind River, Ontario

TITLE
**Terrain Features of the Area North of Elliot Lake and Blind River**

| | | | | |
|---|---|---|---|---|
| DESIGN | KR | 02 SEP 2014 | **Figure 3** | REVISION 2 |
| GIS | JA | 20 NOV 2017 | | UTM ZONE 17N |
| CHECK | SC | 20 NOV 2017 | | NAD 1983 |
| REVIEW | JPS | 20 NOV 2017 | | 1:130,000 |

File: SRK_NWMO_NOH_Fig03_Terrain



## REFERENCE

Base Data: Land Information Ontario (obtained 2017);
CanVec Topography (obtained 2017)
Background Regional Geophysics: Single Master Gravity and Aeromagnetic Data for Ontario (Ontario Geological Survey, 1999)
Detailed Geophysics: Pole Reduced Magnetic Data (First Vertical Derivative) (SGL, 2017)

srk consulting

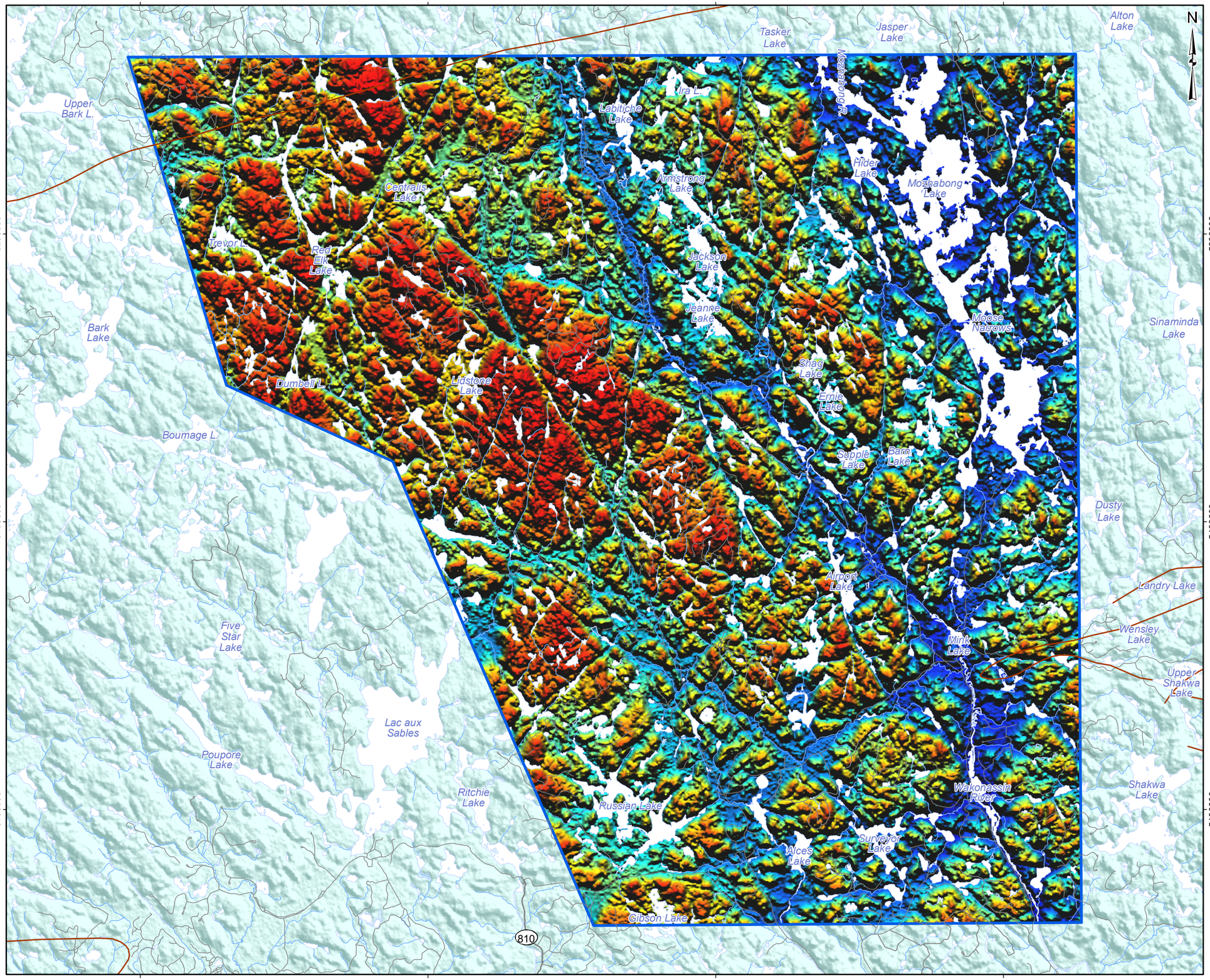
PROJECT

Lineament Interpretation
Area North of Elliot Lake and Blind River, Ontario

TITLE

**Pole Reduced Magnetic Data (First Vertical Derivative) of the Area North of Elliot Lake and Blind River**

| | | | | |
|---|---|---|---|---|
| DESIGN | KR | 02 SEP 2014 | **Figure 4** | REVISION 2 |
| GIS | JA | 20 NOV 2017 | | UTM ZONE 17N |
| CHECK | SC | 20 NOV 2017 | | NAD 1983 |
| REVIEW | JPS | 20 NOV 2017 | | 1:130,000 |



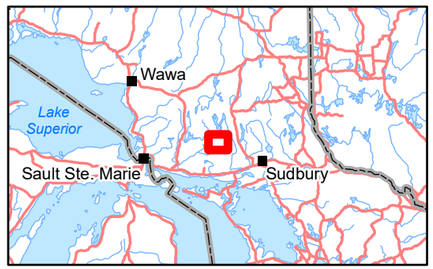

**LEGEND**

- Assessment Area
- Major Road
- Minor Road
- Watercourse
- Waterbody
- Geological contact

**Elevation (masl)**

567m

260m




**REFERENCE**

Base Data: Land Information Ontario (obtained 2017);
CanVec Topography (obtained 2017)
Background Relief: 1 Arc-Second Digital Elevation Model (SRTM, 2000)
Detailed Relief: Digital Elevation Model (SGL, 2017)

0 5 km

srk consulting

PROJECT
Lineament Interpretation
Area North of Elliot Lake and Blind River, Ontario

TITLE
**Digital Elevation Data of the Area North of Elliot Lake and Blind River**

| | | | | |
|---|---|---|---|---|
| DESIGN | KR | 02 SEP 2014 | **Figure 5** | REVISION 2 |
| GIS | JA | 20 NOV 2017 | | UTM ZONE 17N |
| CHECK | SC | 20 NOV 2017 | | NAD 1983 |
| REVIEW | JPS | 20 NOV 2017 | | 1:130,000 |

File: SRK_NWMO_NOH_Fig05_DEM

390000 400000 410000 420000

5200000 5190000 5180000

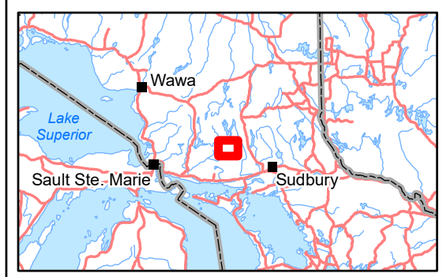
N

Upper Bark L.
Tasker Lake
Jasper Lake
Alton Lake
Ira L.
Labiche Lake
Nozabong R.
Hider Lake
Mozhabong Lake
Armstrong Lake
Centralls Lake
Trevor L.
Red Elk Lake
Jackson Lake
Jeanne Lake
Moose Narrows
Sinaminda Lake
Bark Lake
Dumbell L.
Lidstone Lake
Shag Lake
Ernie Lake
Boumage L.
Supple Lake
Barni Lake
Dusty Lake
Airport Lake
Landry Lake
Wensley Lake
Mink Lake
Upper Shakwa Lake
Five Star Lake
Lac aux Sables
Poupore Lake
Ritchie Lake
Wakonassin River
Shakwa Lake
Russian Lake
Surveyor Lake
Alces Lake
Gibson Lake
810

390000 400000 410000 420000

## LEGEND

- Assessment Area
- Major Road
- Minor Road
- Watercourse
- Waterbody
- Geological contact




## REFERENCE

Base Data: Land Information Ontario (obtained 2017);
CanVec Topography (obtained 2017)
Background Imagery: Pan-sharpened LandSAT-8 (LP DAAC, 2017)
Detailed Imagery: Forest Resource Inventory Digital Aerial Imagery
(Land Information Ontario, 2007-2011)

0 5 km

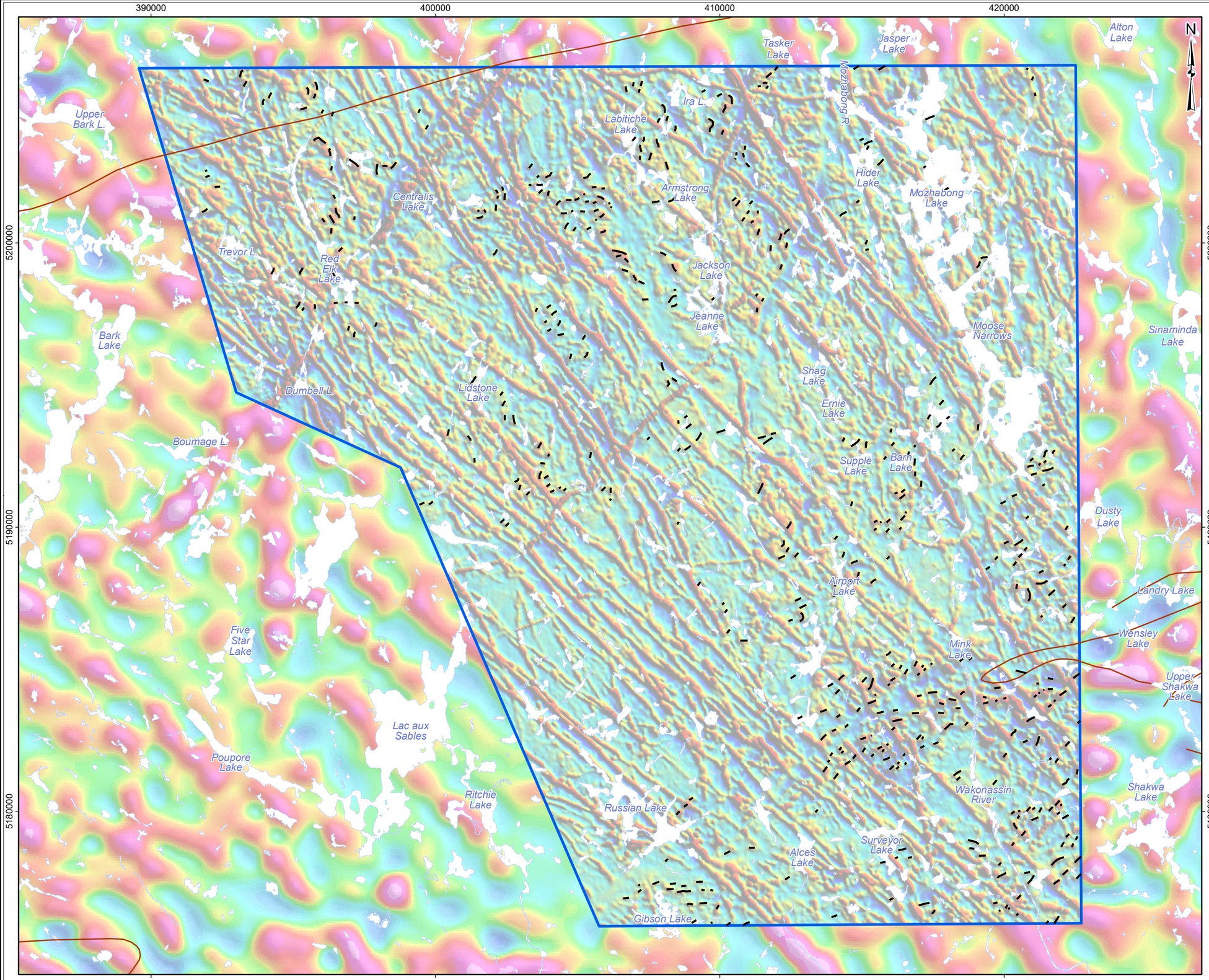
srk consulting

PROJECT
Lineament Interpretation
Area North of Elliot Lake and Blind River, Ontario

TITLE
**Forest Resource Inventory**
**Digital Aerial Imagery**
**of the Area North of Elliot Lake and Blind River**

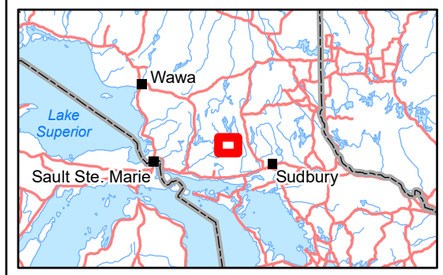
| | | | | |
|---|---|---|---|---|
| DESIGN | KR | 02 SEP 2014 | **Figure 6** | REVISION 2 |
| GIS | JA | 20 NOV 2017 | | UTM ZONE 17N |
| CHECK | SC | 20 NOV 2017 | | NAD 1983 |
| REVIEW | JPS | 20 NOV 2017 | | 1:130,000 |

File: SRK_NWMO_NOH_Fig06_SAT




**LEGEND**

- Assessment Area
- Waterbody
- Geological contact
- Form Line




**REFERENCE**

Base Data: Land Information Ontario (obtained 2017); CanVec Topography (obtained 2017)
Background Regional Geophysics: Single Master Gravity and Aeromagnetic Data for Ontario (Ontario Geological Survey, 1999)
Detailed Geophysics: Pole Reduced Magnetic Data (First Vertical Derivative) (SGL, 2017)

0 5 km

srk consulting

PROJECT
Lineament Interpretation
Area North of Elliot Lake and Blind River, Ontario

TITLE
**Form Lines from Pole Reduced Magnetic Data of the Area North of Elliot Lake and Blind River**

| | | | | |
|---|---|---|---|---|
| DESIGN | KR | 02 SEP 2014 | **Figure 7** | REVISION 2 |
| GIS | JA | 20 NOV 2017 | | UTM ZONE 17N |
| CHECK | SC | 20 NOV 2017 | | NAD 1983 |
| REVIEW | JPS | 20 NOV 2017 | | 1:130,000 |

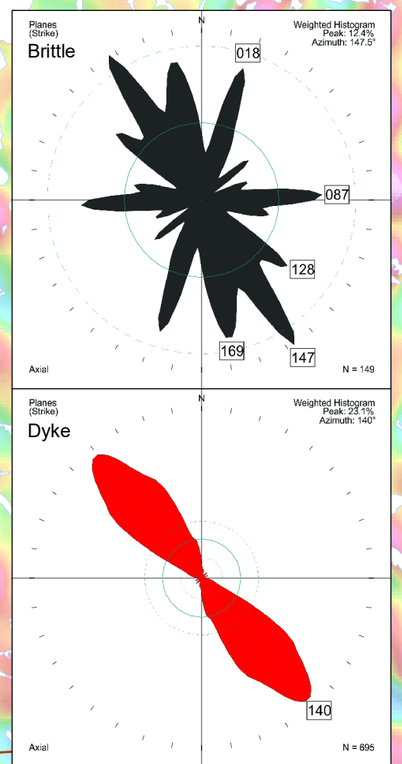
File: SRK_NWMO_NOH_Fig07_Formlines

390000 400000 410000 420000

5200000 5190000 5180000

N

Upper Bark L.
Bark Lake
Trevor L.
Red Elk Lake
Centralis Lake
Labitiche Lake
Ira L.
Tasker Lake
Jasper Lake
Alton Lake
Mozhabong R.
Armstrong Lake
Hider Lake
Mozhabong Lake
Jackson Lake
Jeanne Lake
Moose Narrows
Sinaminda Lake
Dumbell L.
Lidstone Lake
Shag Lake
Ennie Lake
Boumage L.
Supple Lake
Barn Lake
Dusty Lake
Airport Lake
Landry Lake
Wensley Lake
Mink Lake
Upper Shakwa Lake
Lac aux Sables
Ritchie Lake
Russian Lake
Wakonassin River
Shakwa Lake
Alces Lake
Surveyor Lake
Gibson Lake




## LEGEND

- Assessment Area
- Waterbody
- Geological contact

**Brittle Lineament (RA1)**

- Brittle, 1
- Brittle, 2

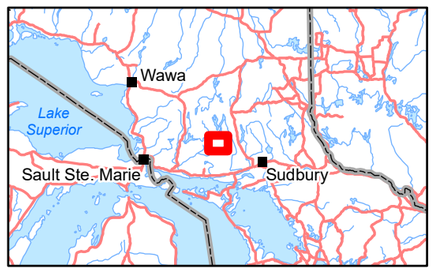
**Dyke Lineament (RA1)**

- Dyke, 1
- Dyke, 2

**Magnetic Intensity (nT/km)**

8800

-6570




## REFERENCE

Base Data: Land Information Ontario (obtained 2017); CanVec Topography (obtained 2017)
Background Regional Geophysics: Single Master Gravity and Aeromagnetic Data for Ontario (Ontario Geological Survey, 1999)
Detailed Geophysics: Pole Reduced Magnetic Data (First Vertical Derivative) (SGL, 2017)

0 5 km

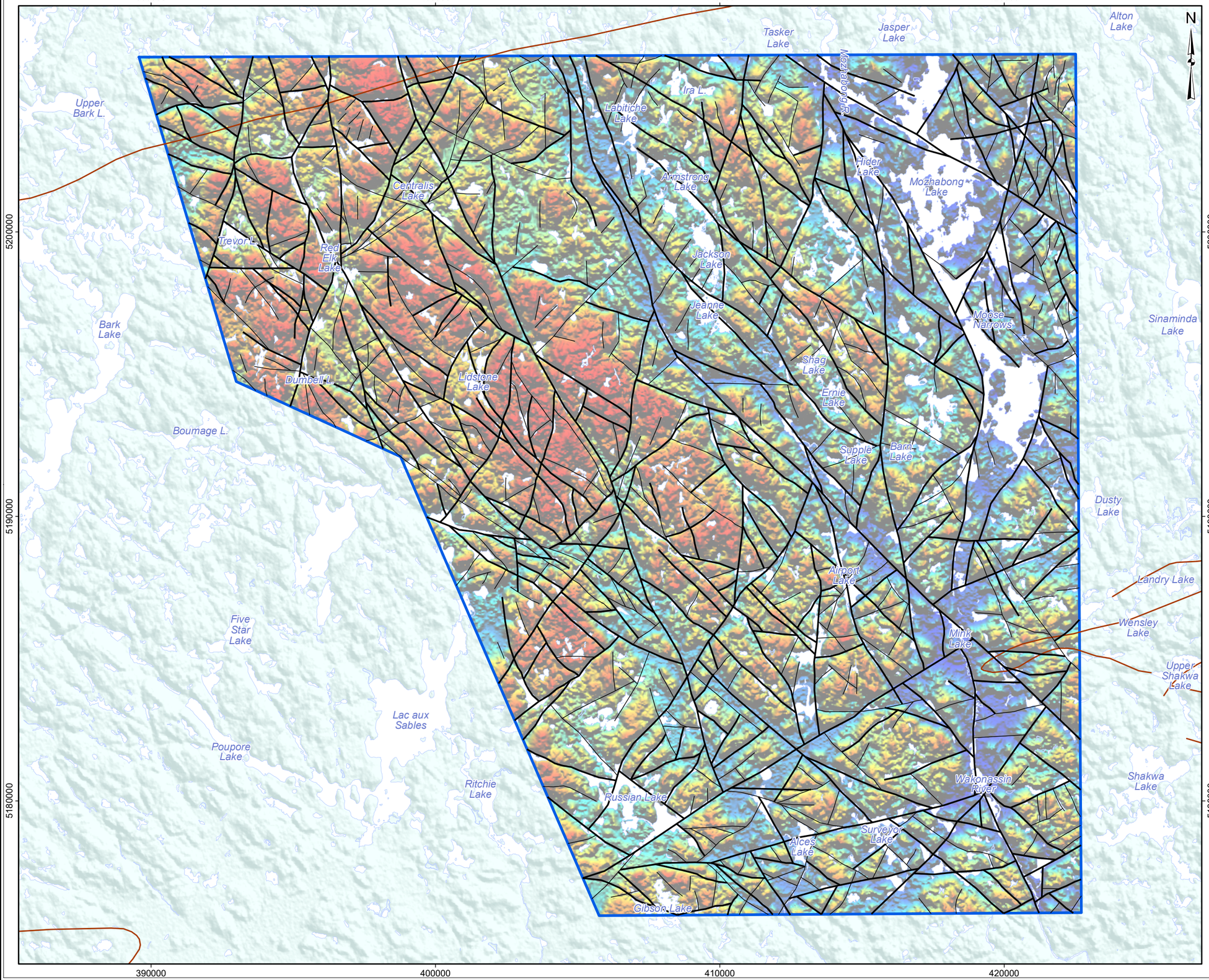
srk consulting

PROJECT
Lineament Interpretation
Area North of Elliot Lake and Blind River, Ontario

TITLE
**Interpreted Lineaments from Pole Reduced Magnetic Data of the Area North of Elliot Lake and Blind River**

| | | | | |
|---|---|---|---|---|
| DESIGN | KR | 02 SEP 2014 | **Figure 8** | REVISION 2 |
| GIS | JA | 20 NOV 2017 | | UTM ZONE 17N |
| CHECK | SC | 20 NOV 2017 | | NAD 1983 |
| REVIEW | JPS | 20 NOV 2017 | | 1:130,000 |

File: SRK_NWMO_NOH_Fig08_MagRA1




**LEGEND**

- Assessment Area
- Waterbody
- Geological contact

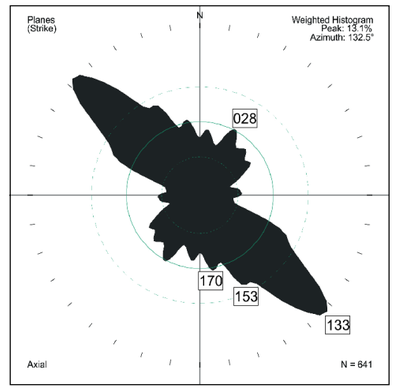
**DEM Lineament (RA1)**

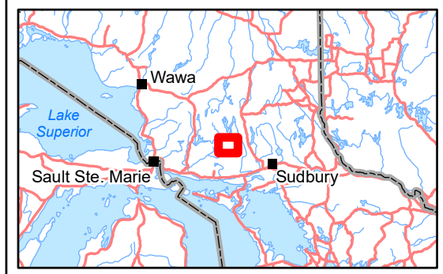
- 1
- 2

**Elevation (masl)**

567m

260m




**REFERENCE**

Base Data: Land Information Ontario (obtained 2017);
CanVec Topography (obtained 2017)
Background Relief: 1 Arc-Second Digital Elevation Model (SRTM, 2000)
Detailed Relief: Digital Elevation Model (SGL, 2017)

0 5 km

srk consulting

PROJECT
Lineament Interpretation
Area North of Elliot Lake and Blind River, Ontario

TITLE
**Interpreted Lineaments from Digital Elevation Data of the Area North of Elliot Lake and Blind River**

| | | | | |
|---|---|---|---|---|
| DESIGN | KR | 02 SEP 2014 | **Figure 9** | REVISION 2 |
| GIS | JA | 20 NOV 2017 | | UTM ZONE 17N |
| CHECK | SC | 20 NOV 2017 | | NAD 1983 |
| REVIEW | JPS | 20 NOV 2017 | | 1:130,000 |

File: SRK_NWMO_NOH_Fig09_DEMra1

390000 400000 410000 420000

5200000 5190000 5180000

N

Alton Lake
Tasker Lake
Jasper Lake
Mozhabong R.
Ira L.
Labitiche Lake
Upper Bark L.
Centralis Lake
Armstrong Lake
Hider Lake
Mozhabong Lake
Trevor L.
Red Elk Lake
Jackson Lake
Jeanne Lake
Bark Lake
Moose Narrows
Sinaminda Lake
Shag Lake
Dumbell L.
Lidstone Lake
Ernie Lake
Boumage L.
Supple Lake
Barn Lake
Dusty Lake
Airport Lake
Landry Lake
Wensley Lake
Mink Lake
Five Star Lake
Upper Shakwa Lake
Lac aux Sables
Poupore Lake
Ritchie Lake
Wakonassin River
Shakwa Lake
Russian Lake
Surveyor Lake
Alces Lake
Gibson Lake

390000 400000 410000 420000

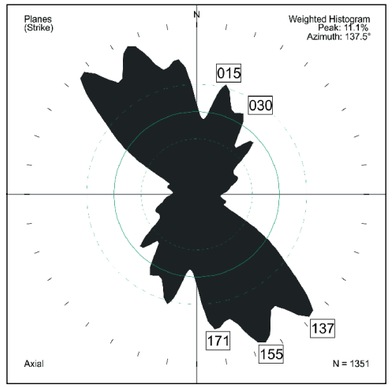
File: SRK_NWMO_NOH_Fig10_SATra1

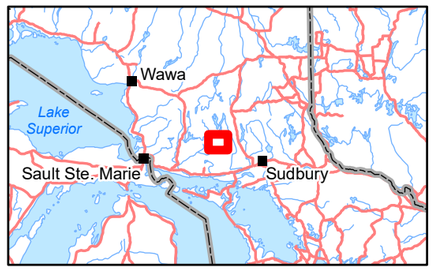
**LEGEND**

- Assessment Area
- Waterbody
- Geological contact

**FRI Lineament (RA1)**

- 1
- 2




**REFERENCE**

Base Data: Land Information Ontario (obtained 2017);
CanVec Topography (obtained 2017)
Background Imagery: Pan-sharpened LandSAT-8 (LP DAAC, 2017)
Detailed Imagery: Forest Resource Inventory Digital Aerial Imagery (Land Information Ontario, 2007-2011)

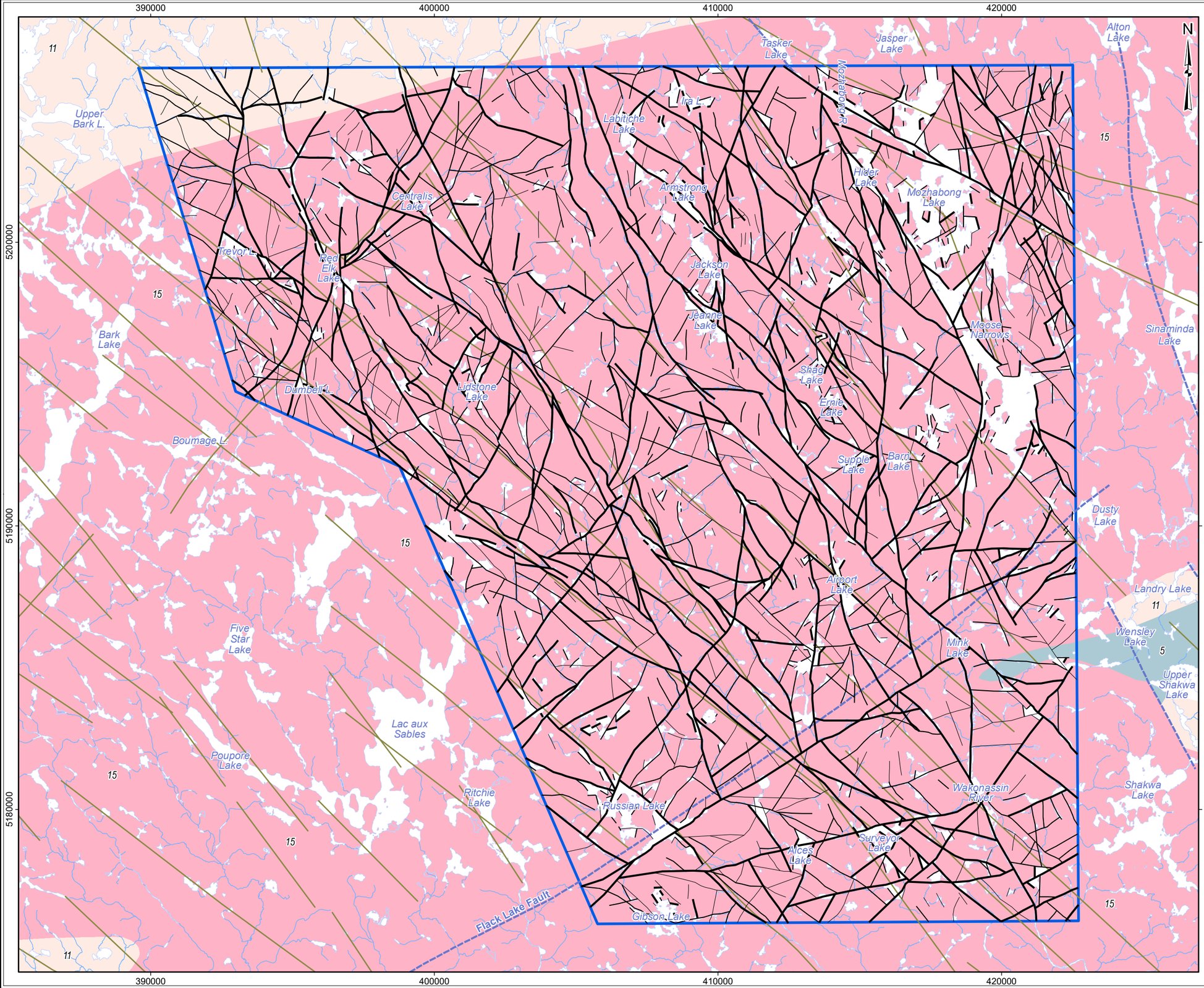
0 5 km

srk consulting

PROJECT
Lineament Interpretation
Area North of Elliot Lake and Blind River, Ontario

TITLE
**Interpreted Lineaments from Forest Resource Inventory (FRI) Imagery of the Area North of Elliot Lake and Blind River**

| | | | | |
|---|---|---|---|---|
| DESIGN | KR | 02 SEP 2014 | **Figure 10** | REVISION 2 |
| GIS | JA | 20 NOV 2017 | | UTM ZONE 17N |
| CHECK | SC | 20 NOV 2017 | | NAD 1983 |
| REVIEW | JPS | 20 NOV 2017 | | 1:130,000 |




**LEGEND**

- Assessment Area
- Watercourse
- Waterbody

**Bedrock Geology**

- Mapped Fault
- Mapped Dyke
- Massive granodiorite to granite (15)
- Gneissic tonalite suite (11)
- Benny Lake Greenstone Belt (5)

**Surficial Lineament**

- Certainty 1
- Certainty 2
- Certainty 3

**REFERENCE**

Base Data: Land Information Ontario (obtained 2015);
CanVec Topography (obtained 2015)
Geology: MRD 126-REV1 (Ontario Geological Survey, 2011)

srk consulting

PROJECT
Lineament Interpretation
Area North of Elliot Lake and Blind River, Ontario

TITLE
**Interpreted Lineaments from Surficial Data of the Area North of Elliot Lake and Blind River**

| | | | | |
|---|---|---|---|---|
| DESIGN | KR | 02 SEP 2014 | **Figure 11** | REVISION 2 |
| GIS | JA | 20 NOV 2017 | | UTM ZONE 17N |
| CHECK | SC | 20 NOV 2017 | | NAD 1983 |
| REVIEW | JPS | 20 NOV 2017 | | 1:130,000 |

File: SRK_NWMO_NOH_Fig11_SurfCert

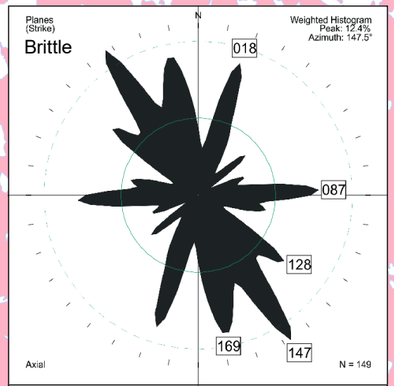
390000 400000 410000 420000

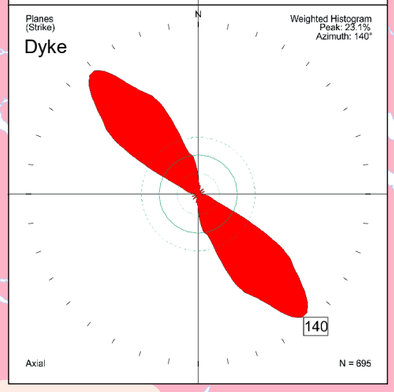
5200000 5190000 5180000

N

11 15 5

Upper Bark L. Tasker Lake Jasper Lake Alton Lake Ira L. Nozhabong L. Labitiche Lake Hider Lake Mozhabong Lake Armstrong Lake Centralls Lake Trevor L. Red Elk Lake Jackson Lake Jeanne Lake Moose Narrows Sinaminda Lake Bark Lake Dumbell L. Lidstone Lake Shag Lake Ennie Lake Boumage L. Supple Lake Barn Lake Dusty Lake Landry Lake Wensley Lake Mink Lake Upper Shakwa Lake Airport Lake Lac aux Sables Ritchie Lake Russian Lake Wakonassin River Shakwa Lake Surveyor Lake Alces Lake Gibson Lake




**LEGEND**

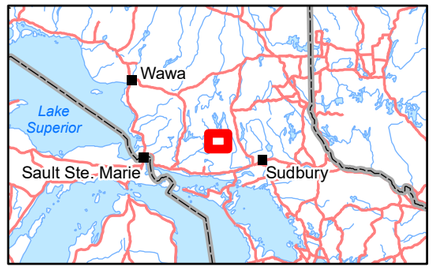
- Assessment Area
- Waterbody
- Massive granodiorite to granite (15)
- Gneissic tonalite suite (11)
- Benny Lake Greenstone Belt (5)

**Brittle Lineament**

- Certainty 1
- Certainty 2
- Certainty 3

**Dyke Lineament**

- Certainty 1
- Certainty 2
- Certainty 3




**REFERENCE**

Base Data: Land Information Ontario (obtained 2015); CanVec Topography (obtained 2015)
Geology: MRD 126-REV1 (Ontario Geological Survey, 2011)

0 5 km

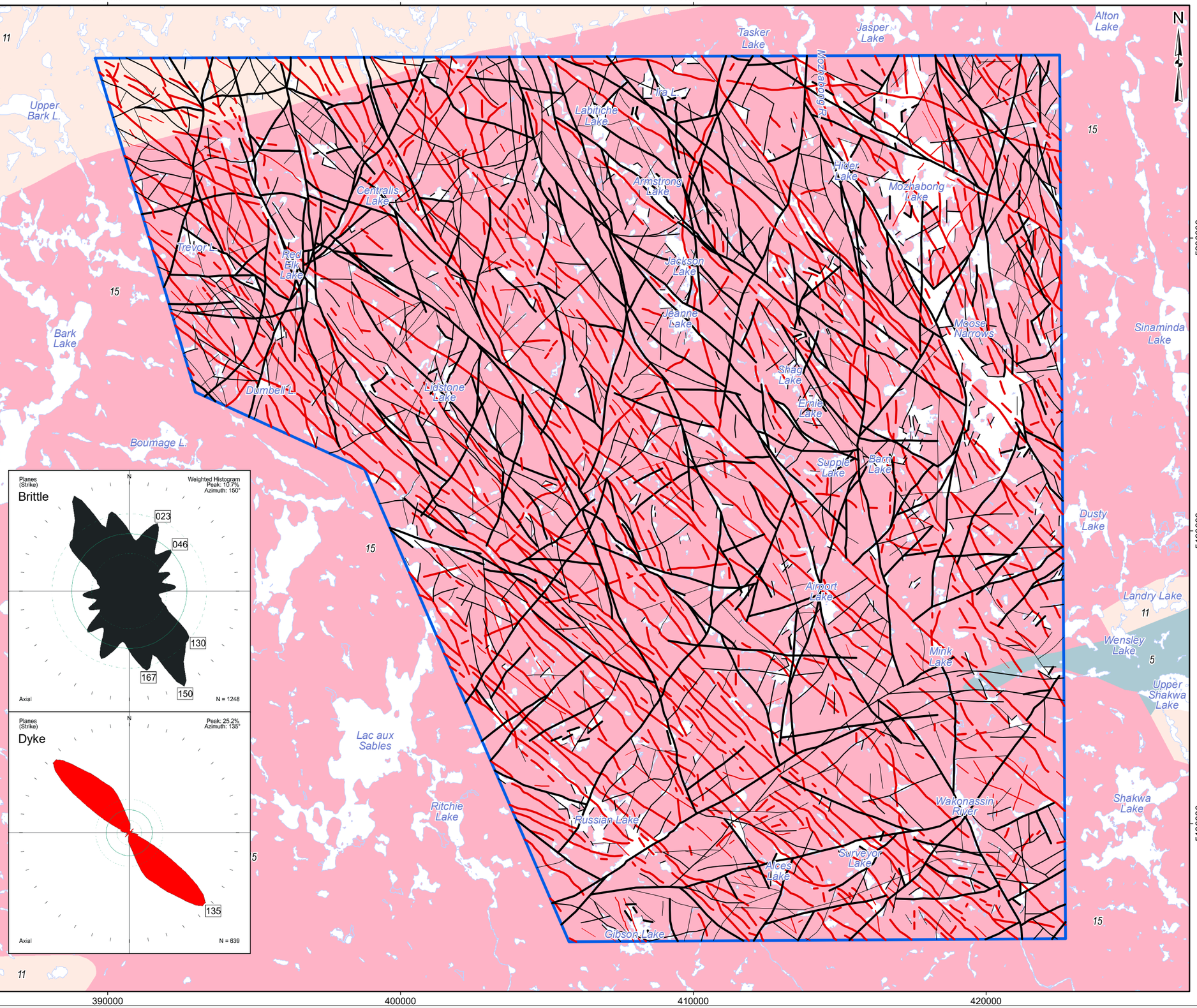
srk consulting

PROJECT
Lineament Interpretation
Area North of Elliot Lake and Blind River, Ontario

TITLE
**Interpreted Lineaments from Pole Reduced Magnetic Data of the Area North of Elliot Lake and Blind River**

| | | | | |
|---|---|---|---|---|
| DESIGN | KR | 02 SEP 2014 | **Figure 12** | REVISION 2 |
| GIS | JA | 20 NOV 2017 | | UTM ZONE 17N |
| CHECK | SC | 20 NOV 2017 | | NAD 1983 |
| REVIEW | JPS | 20 NOV 2017 | | 1:130,000 |

File: SRK_NWMO_NOH_Fig12_MagCert




**LEGEND**

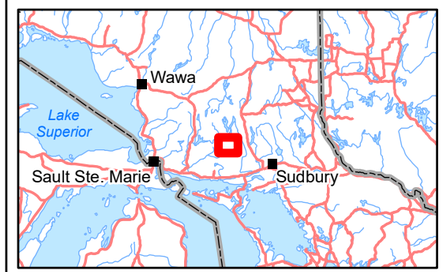
- Assessment Area
- Waterbody
- Massive granodiorite to granite (15)
- Gneissic tonalite suite (11)
- Benny Lake Greenstone Belt (5)

**Brittle Lineament**

- Certainty 1
- Certainty 2
- Certainty 3

**Dyke Lineament**

- Certainty 1
- Certainty 2
- Certainty 3




**REFERENCE**

Base Data: Land Information Ontario (obtained 2015);
CanVec Topography (obtained 2015)
Geology: MRD 126-REV1 (Ontario Geological Survey, 2011)

0 5 km

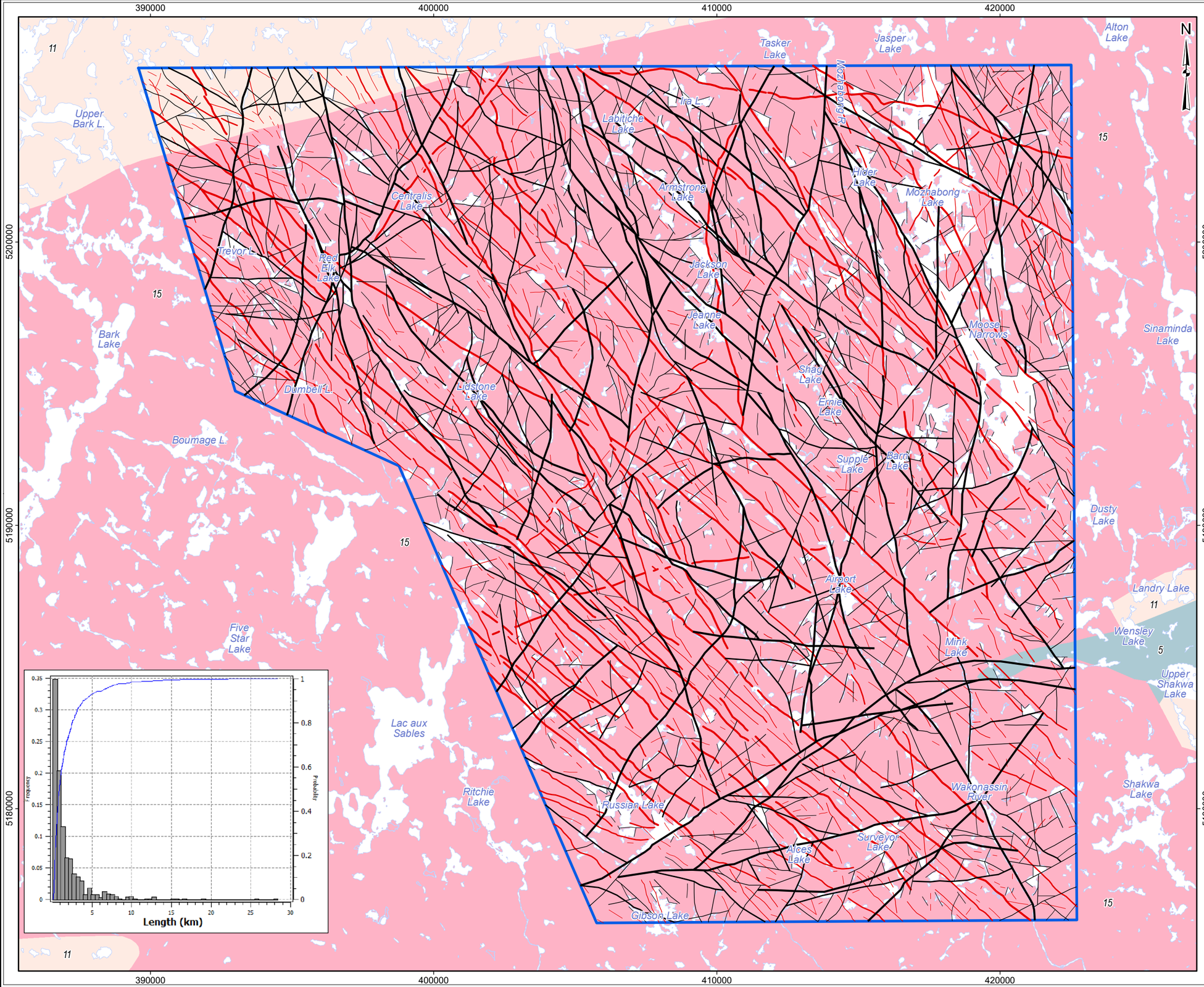
srk consulting

PROJECT
Lineament Interpretation
Area North of Elliot Lake and Blind River, Ontario

TITLE
**Select Final Integrated Lineaments of the Area North of Elliot Lake and Blind River**

| | | | | |
|---|---|---|---|---|
| DESIGN | KR | 02 SEP 2014 | **Figure 13** | REVISION 2 |
| GIS | JA | 20 NOV 2017 | | UTM ZONE 17N |
| CHECK | SC | 20 NOV 2017 | | NAD 1983 |
| REVIEW | JPS | 20 NOV 2017 | | 1:130,000 |

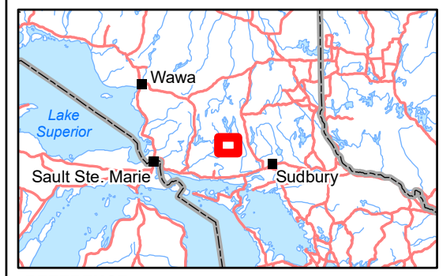
File: SRK_NWMO_NOH_Fig13_FinCert




**LEGEND**

- Assessment Area
- Waterbody
- Massive granodiorite to granite (15)
- Gneissic tonalite suite (11)
- Benny Lake Greenstone Belt (5)

| Brittle Lineament | Dyke Lineament |
|---|---|
| < 1 km | < 1 km |
| 1 - 2.5 | 1 - 2.5 |
| 2.5 - 5 | 2.5 - 5 |
| > 5 km | > 5 km |




**REFERENCE**

Base Data: Land Information Ontario (obtained 2015);
CanVec Topography (obtained 2015)
Geology: MRD 126-REV1 (Ontario Geological Survey, 2011)

0 5 km

srk consulting

PROJECT
Lineament Interpretation
Area North of Elliot Lake and Blind River, Ontario

TITLE
**Interpreted Lineaments from Pole Reduced Magnetic Data (by Length) of the Area North of Elliot Lake and Blind River**

| | | | | |
|---|---|---|---|---|
| DESIGN | KR | 02 SEP 2014 | **Figure 14** | REVISION 2 |
| GIS | JA | 20 NOV 2017 | | UTM ZONE 17N |
| CHECK | SC | 20 NOV 2017 | | NAD 1983 |
| REVIEW | JPS | 20 NOV 2017 | | 1:130,000 |

File: SRK_NWMO_NOH_Fig14_MagLen

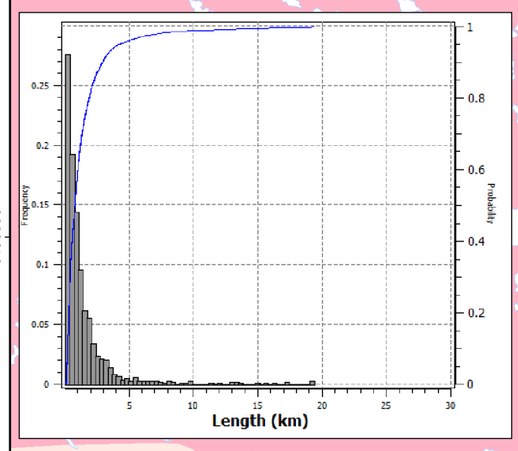
390000 400000 410000 420000

5200000 5190000 5180000

N

11 15 5

Upper Bark L. Bark Lake Boumage L. Five Star Lake Lac aux Sables Ritchie Lake Gibson Lake Russian Lake Alces Lake Surveyor Lake Wakonassin River Shakwa Lake Upper Shakwa Lake Wensley Lake Landry Lake Dusty Lake Sinaminda Lake Alton Lake Jasper Lake Tasker Lake Mozhabong Lake Hider Lake Ira L. Labitiche Lake Armstrong Lake Centralis Lake Trevor L. Red Elk Lake Jackson Lake Jeanne Lake Moose Narrows Shag Lake Ernie Lake Supple Lake Barrill Lake Dumbell L. Lidstone Lake Airport Lake Mink Lake

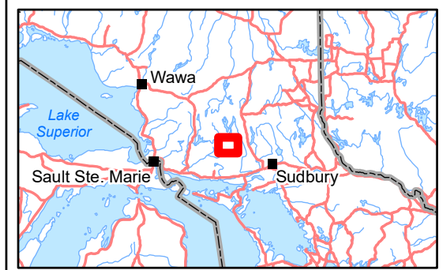



**LEGEND**

- Assessment Area
- Waterbody
- Massive granodiorite to granite (15)
- Gneissic tonalite suite (11)
- Benny Lake Greenstone Belt (5)

**Surficial Lineament**

- < 1 km
- 1 - 2.5
- 2.5 - 5
- > 5 km




**REFERENCE**

Base Data: Land Information Ontario (obtained 2015);
CanVec Topography (obtained 2015)
Geology: MRD 126-REV1 (Ontario Geological Survey, 2011)

0 5 km

srk consulting

PROJECT
Lineament Interpretation
Area North of Elliot Lake and Blind River, Ontario

TITLE
**Interpreted Lineaments (by Length) from Surficial Data of the Area North of Elliot Lake and Blind River**

| | | | | |
|---|---|---|---|---|
| DESIGN | KR | 02 SEP 2014 | **Figure 15** | REVISION 2 |
| GIS | JA | 20 NOV 2017 | | UTM ZONE 17N |
| CHECK | SC | 20 NOV 2017 | | NAD 1983 |
| REVIEW | JPS | 20 NOV 2017 | | 1:130,000 |

File: SRK_NWMO_NOH_Fig15_SurfLen

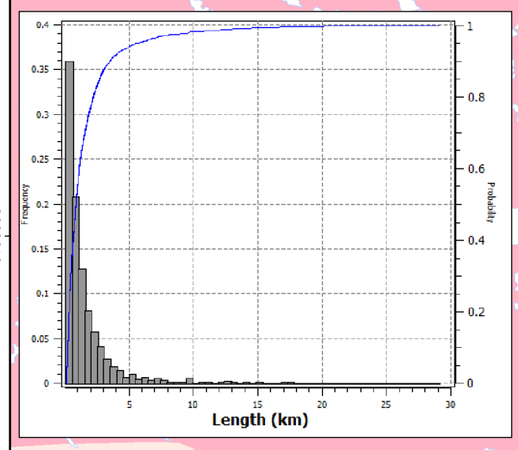
390000 400000 410000 420000

5200000 5190000 5180000

N

Upper Bark L.
Tasker Lake
Jasper Lake
Alton Lake
Ira L.
Labitiche Lake
Mozhabong L.
Centralis Lake
Armstrong Lake
Hider Lake
Mozhabong Lake
Trevor L.
Red Elk Lake
Jackson Lake
Jeanne Lake
Moose Narrows
Sinaminda Lake
Bark Lake
Dumbell L.
Lidstone Lake
Shag Lake
Ennie Lake
Boumage L.
Supple Lake
Barrie Lake
Dusty Lake
Airport Lake
Landry Lake
Wensley Lake
Mink Lake
Upper Shakwa Lake
Five Star Lake
Lac aux Sables
Ritchie Lake
Wakonassin River
Shakwa Lake
Russian Lake
Surveyor Lake
Alces Lake
Gibson Lake

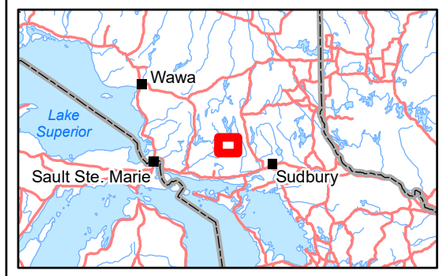
11 15 15 11 15 5 11




## LEGEND

- Assessment Area
- Waterbody
- Massive granodiorite to granite (15)
- Gneissic tonalite suite (11)
- Benny Lake Greenstone Belt (5)

| Brittle Lineament | Dyke Lineament |
|---|---|
| < 1 km | < 1 km |
| 1 - 2.5 | 1 - 2.5 |
| 2.5 - 5 | 2.5 - 5 |
| > 5 km | > 5 km |




## REFERENCE

Base Data: Land Information Ontario (obtained 2015);
CanVec Topography (obtained 2015)
Geology: MRD 126-REV1 (Ontario Geological Survey, 2011)

0 5 km

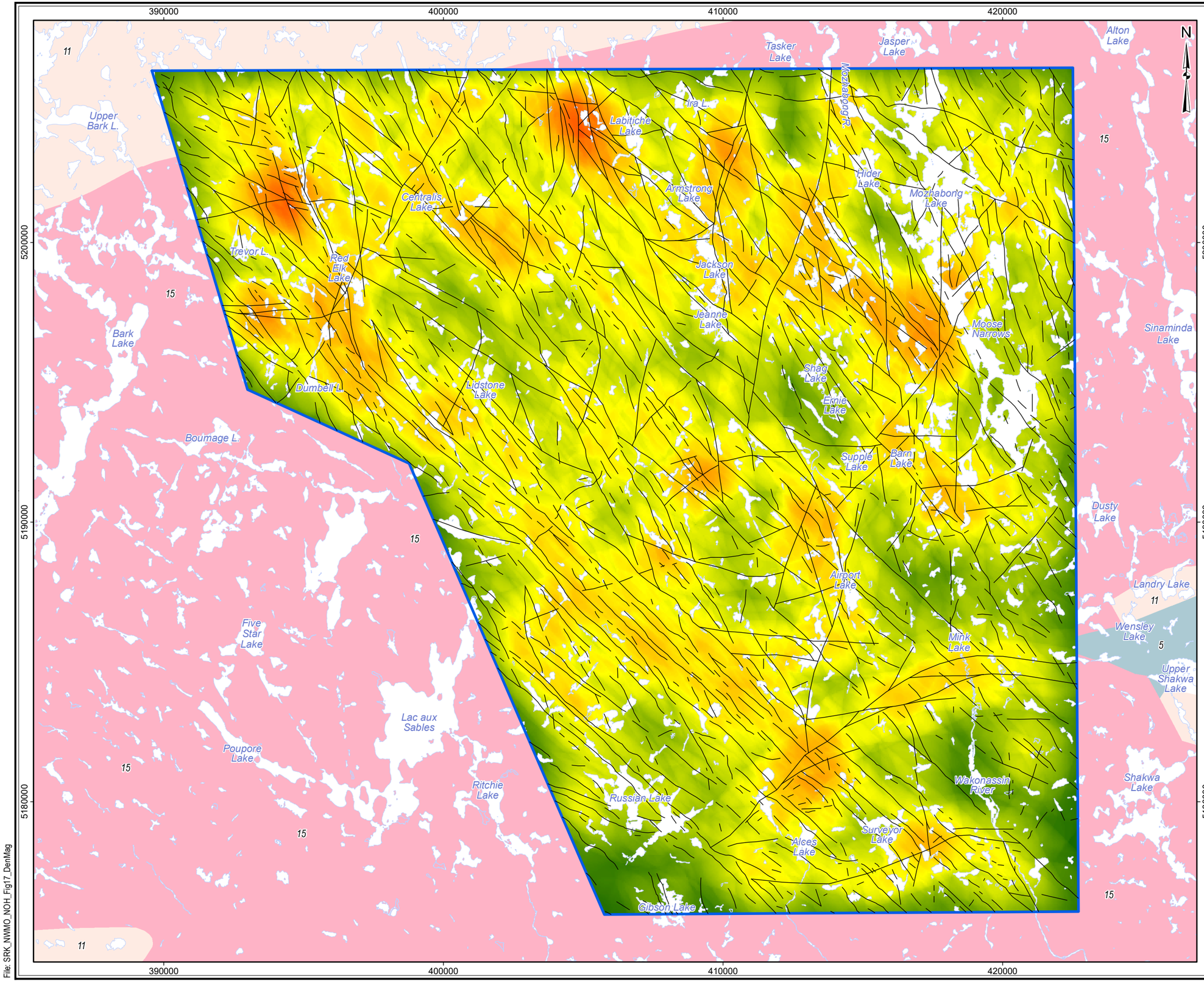
srk consulting

PROJECT
Lineament Interpretation
Area North of Elliot Lake and Blind River, Ontario

TITLE
**Final Integrated Lineaments (by Length) of the Area North of Elliot Lake and Blind River**

| | | | | |
|---|---|---|---|---|
| DESIGN | KR | 02 SEP 2014 | **Figure 16** | REVISION 2 |
| GIS | JA | 20 NOV 2017 | | UTM ZONE 17N |
| CHECK | SC | 20 NOV 2017 | | NAD 1983 |
| REVIEW | JPS | 20 NOV 2017 | | 1:130,000 |

File: SRK_NWMO_NOH_Fig16_FinLen



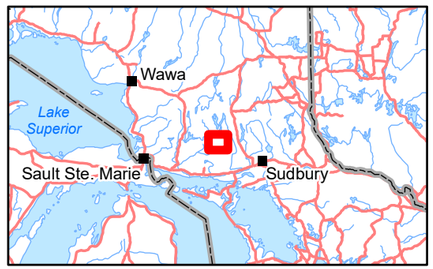

**LEGEND**

- Assessment Area
- Waterbody
- Massive granodiorite to granite (15)
- Gneissic tonalite suite (11)
- Benny Lake Greenstone Belt (5)
- Magnetic Lineament

**Lineament Density (/km²)**

High : 4.5

Low : 0




**REFERENCE**

Base Data: Land Information Ontario (obtained 2015);
CanVec Topography (obtained 2015)
Geology: MRD 126-REV1 (Ontario Geological Survey, 2011)

0 5 km

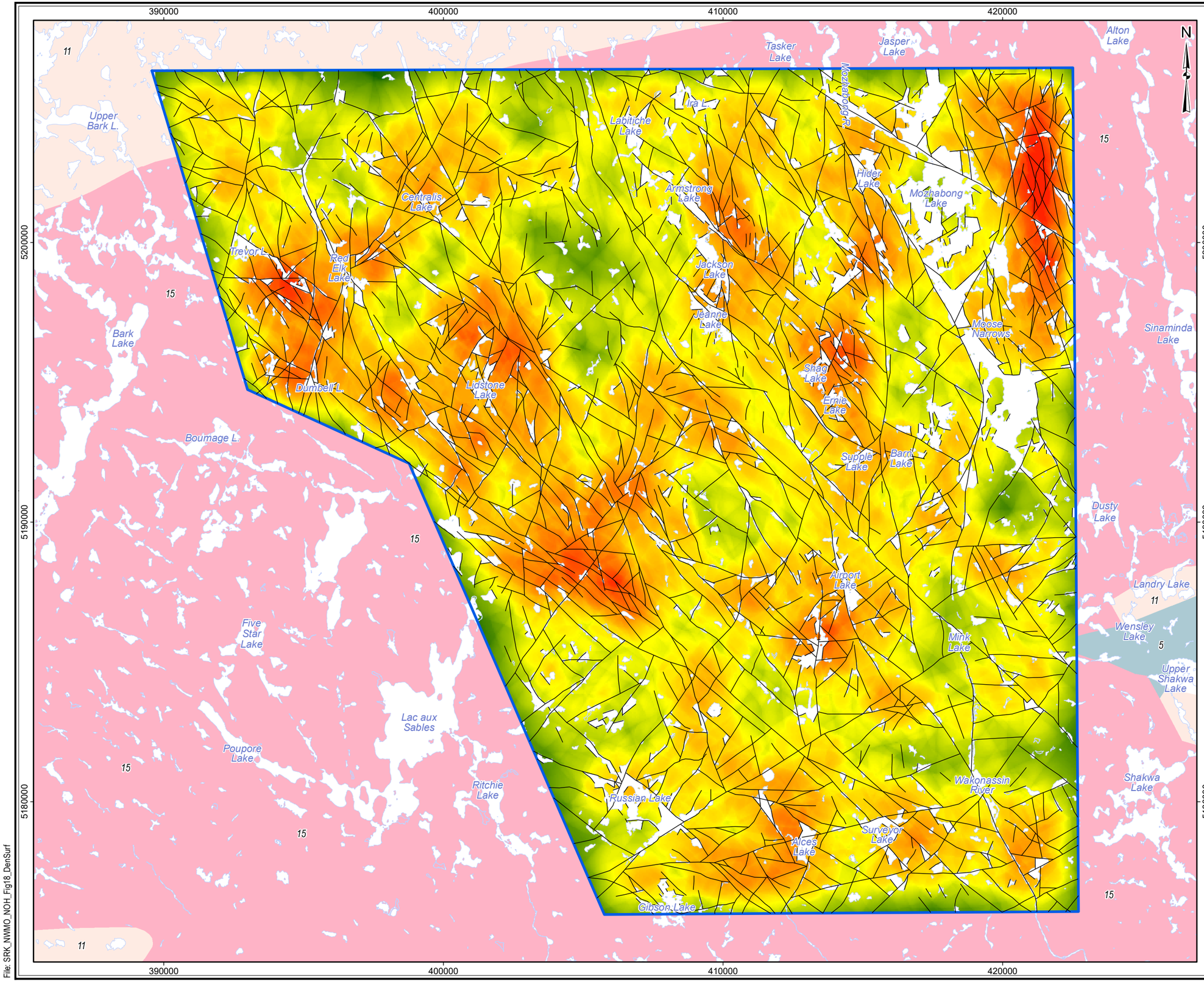
srk consulting

PROJECT
Lineament Interpretation
Area North of Elliot Lake and Blind River, Ontario

TITLE
**Lineament Density for All Interpreted Lineaments Pole Reduced Magnetic Data of the Area North of Elliot Lake and Blind River**

| | | | | |
|---|---|---|---|---|
| DESIGN | KR | 02 SEP 2014 | **Figure 17** | REVISION 2 |
| GIS | JA | 20 NOV 2017 | | UTM ZONE 17N |
| CHECK | SC | 20 NOV 2017 | | NAD 1983 |
| REVIEW | JPS | 20 NOV 2017 | | 1:130,000 |

File: SRK_NWMO_NOH_Fig17_DenMag



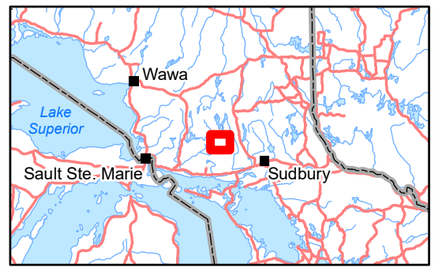

**LEGEND**

- Assessment Area
- Waterbody
- Massive granodiorite to granite (15)
- Gneissic tonalite suite (11)
- Benny Lake Greenstone Belt (5)
- Surficial Lineament

**Lineament Density (/km²)**

High : 4.5

Low : 0




**REFERENCE**

Base Data: Land Information Ontario (obtained 2015);
CanVec Topography (obtained 2015)
Geology: MRD 126-REV1 (Ontario Geological Survey, 2011)

0 5 km

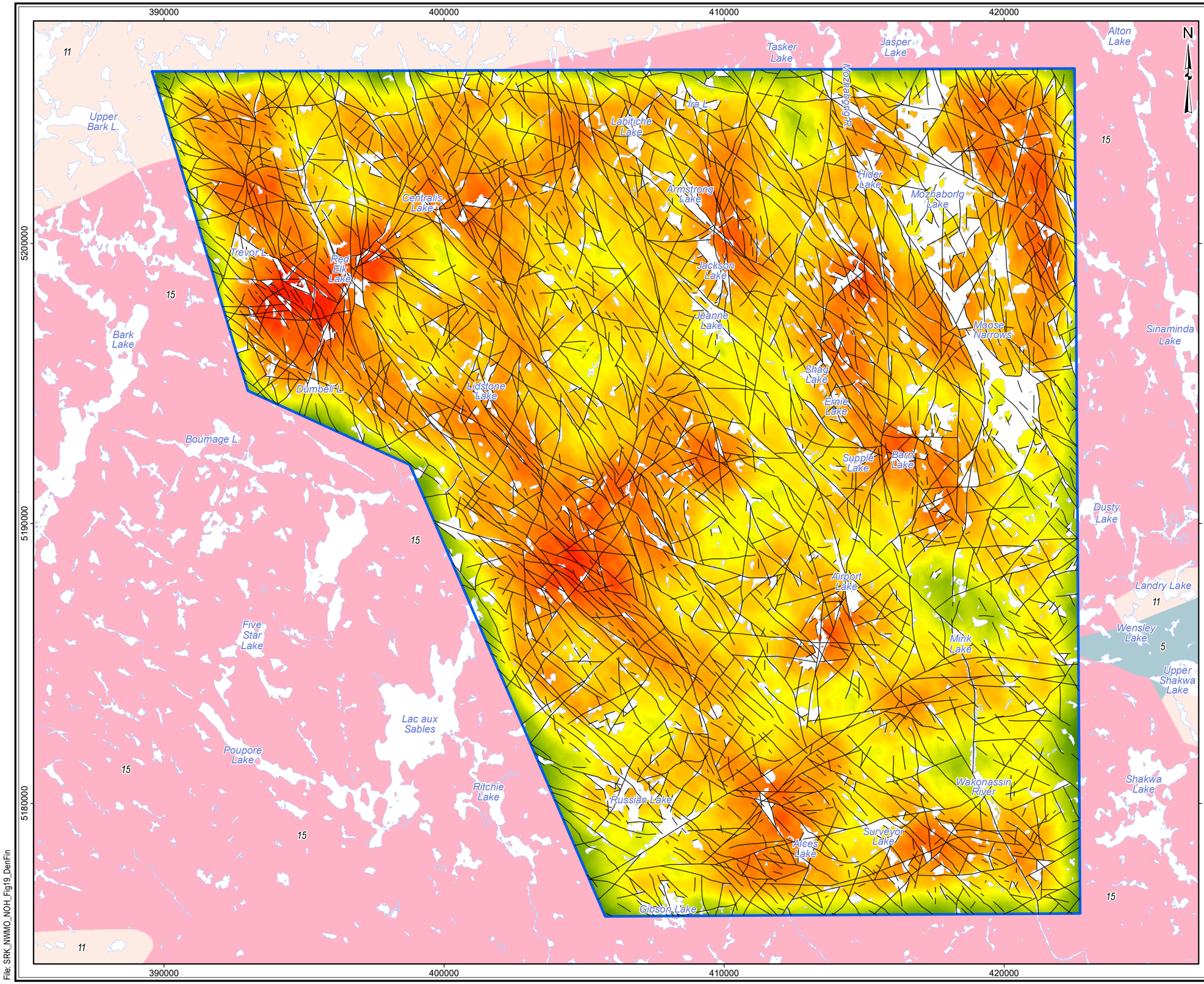
srk consulting

PROJECT
Lineament Interpretation
Area North of Elliot Lake and Blind River, Ontario

TITLE
**Lineament Density for Interpreted Lineaments from Surficial Data of the Area North of Elliot Lake and Blind River**

| | | | | |
|---|---|---|---|---|
| DESIGN | KR | 02 SEP 2014 | **Figure 18** | REVISION 2 |
| GIS | JA | 20 NOV 2017 | | UTM ZONE 17N |
| CHECK | SC | 20 NOV 2017 | | NAD 1983 |
| REVIEW | JPS | 20 NOV 2017 | | 1:130,000 |

File: SRK_NWMO_NOH_Fig18_DenSurf



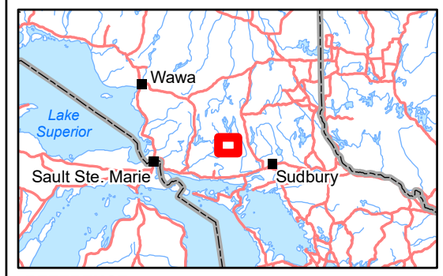

**LEGEND**

- Assessment Area
- Waterbody
- Massive granodiorite to granite (15)
- Gneissic tonalite suite (11)
- Benny Lake Greenstone Belt (5)
- Integrated Lineament

**Lineament Density (/km²)**

High : 6

Low : 0




**REFERENCE**

Base Data: Land Information Ontario (obtained 2015);
CanVec Topography (obtained 2015)
Geology: MRD 126-REV1 (Ontario Geological Survey, 2011)

0 5 km

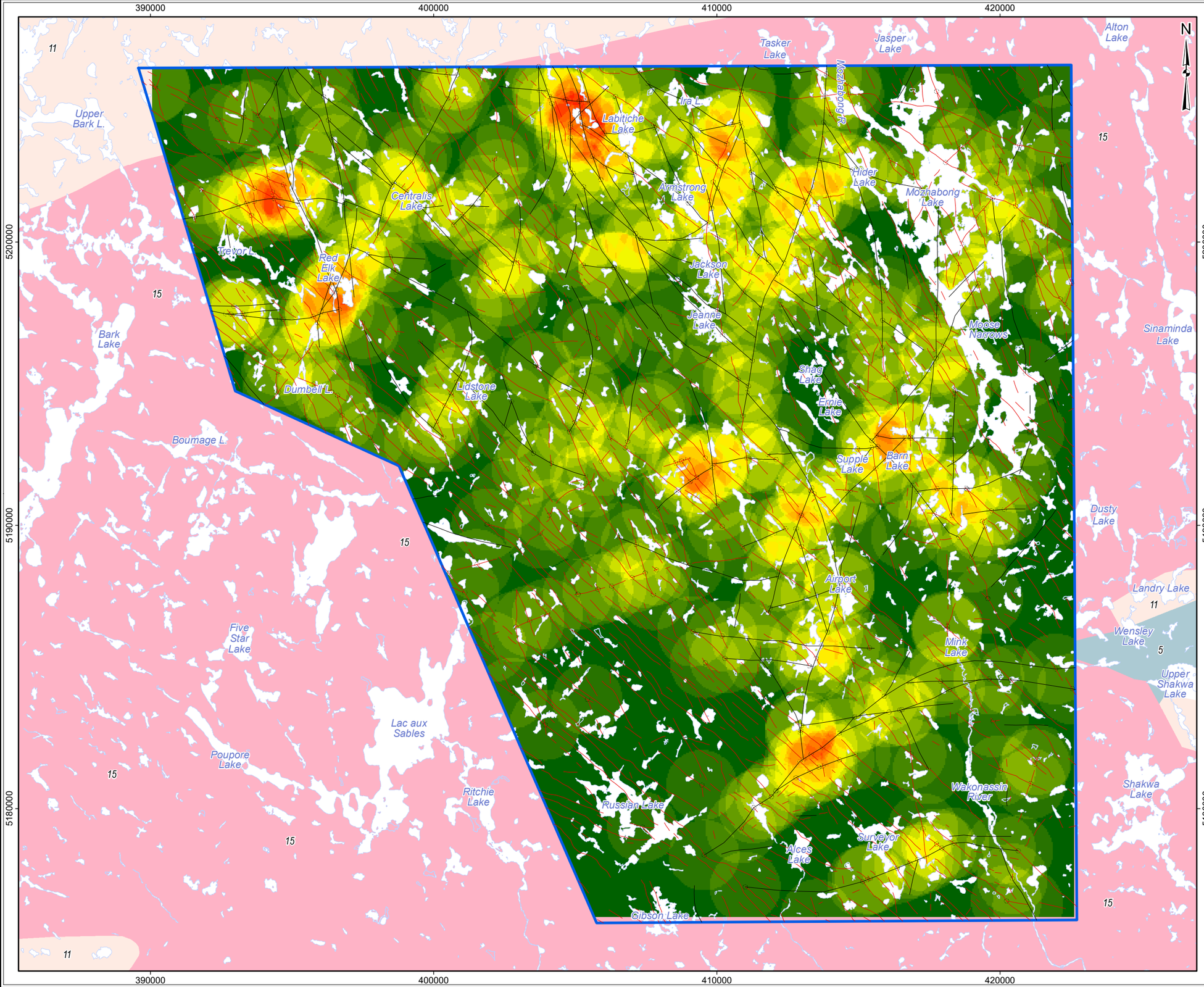
srk consulting

PROJECT
Lineament Interpretation
Area North of Elliot Lake and Blind River, Ontario

TITLE
**Lineament Density for All Final Integrated Lineaments of the Area North of Elliot Lake and Blind River**

| | | | | |
|---|---|---|---|---|
| DESIGN | KR | 02 SEP 2014 | **Figure 19** | REVISION 2 |
| GIS | JA | 20 NOV 2017 | | UTM ZONE 17N |
| CHECK | SC | 20 NOV 2017 | | NAD 1983 |
| REVIEW | JPS | 20 NOV 2017 | | 1:130,000 |

File: SRK_NWMO_NOH_Fig19_DenFin




**LEGEND**

- Assessment Area
- Waterbody
- Massive granodiorite to granite (15)
- Gneissic tonalite suite (11)
- Benny Lake Greenstone Belt (5)

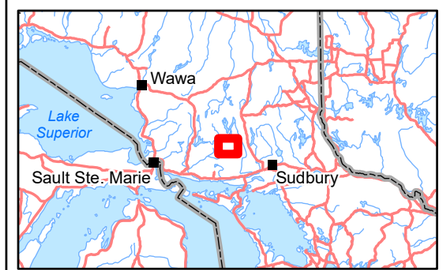
**Lineament**

- Brittle
- Dyke
- Magnetic Lineament Intersection

**Lineament Density (/km²)**

High : 3

Low : 0




**REFERENCE**

Base Data: Land Information Ontario (obtained 2015);
CanVec Topography (obtained 2015)
Geology: MRD 126-REV1 (Ontario Geological Survey, 2011)

0 5 km

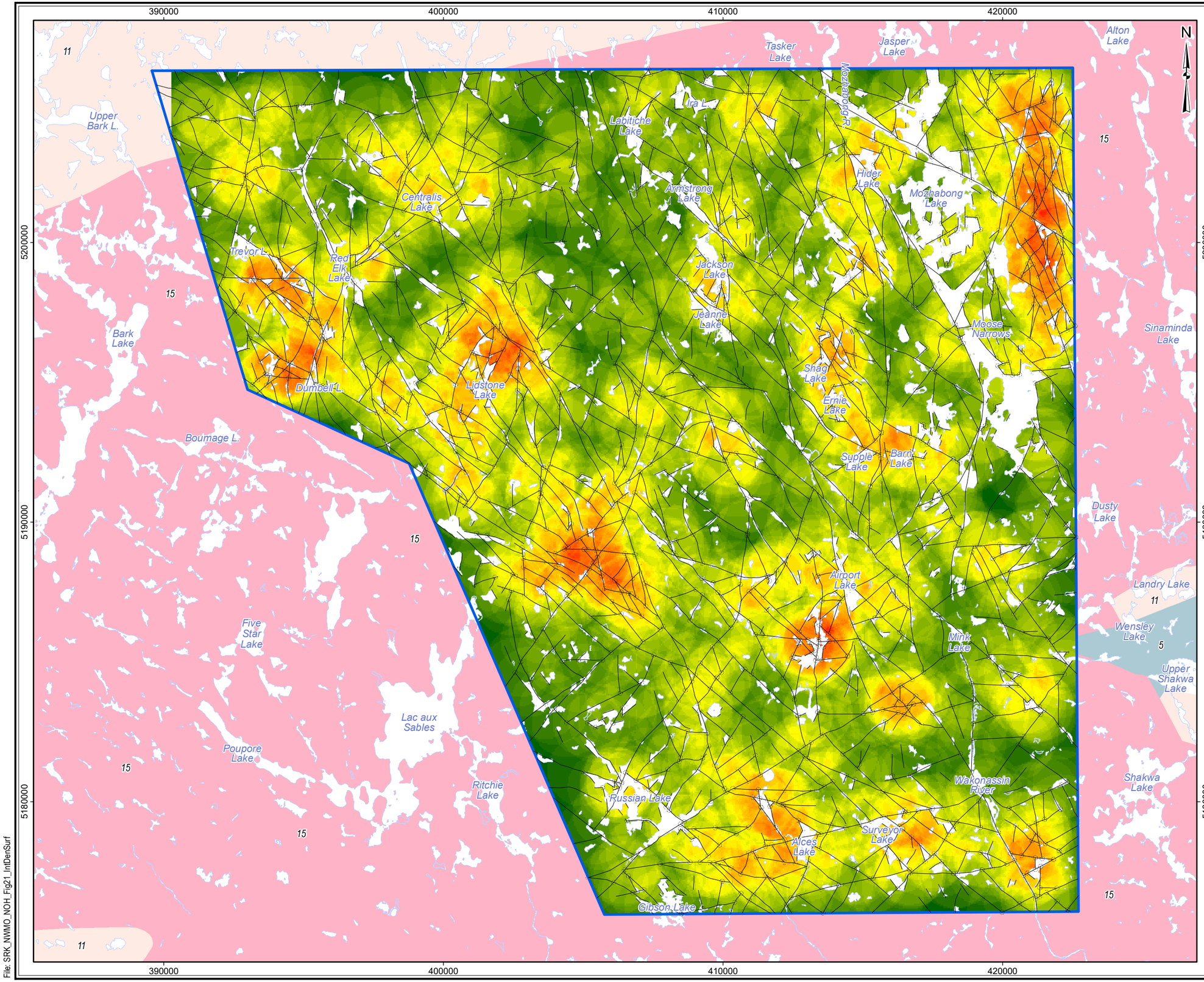
srk consulting

PROJECT
Lineament Interpretation
Area North of Elliot Lake and Blind River, Ontario

TITLE
**Lineament Intersection Density for All Interpreted Lineaments from Pole Reduced Magnetic Data of the Area North of Elliot Lake and Blind River**

| | | | | |
|---|---|---|---|---|
| DESIGN | KR | 02 SEP 2014 | **Figure 20** | REVISION 2 |
| GIS | JA | 20 NOV 2017 | | UTM ZONE 17N |
| CHECK | SC | 20 NOV 2017 | | NAD 1983 |
| REVIEW | JPS | 20 NOV 2017 | | 1:130,000 |

File: SRK_NWMO_NOH_Fig20_IntDenMag



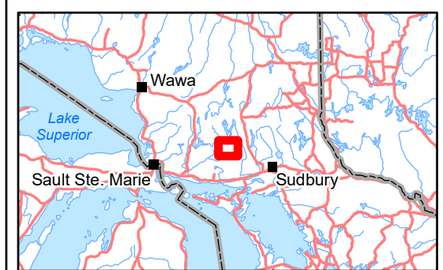

**LEGEND**

- Assessment Area
- Waterbody
- Massive granodiorite to granite (15)
- Gneissic tonalite suite (11)
- Benny Lake Greenstone Belt (5)
- Surficial Lineament Intersection
- Surficial Lineament

**Lineament Density (/km²)**

High : 6

Low : 0




**REFERENCE**

Base Data: Land Information Ontario (obtained 2015);
CanVec Topography (obtained 2015)
Geology: MRD 126-REV1 (Ontario Geological Survey, 2011)

0 5 km

srk consulting

PROJECT
Lineament Interpretation
Area North of Elliot Lake and Blind River, Ontario

TITLE
**Lineament Intersection Density for Interpreted Lineaments from Surficial Data of the Area North of Elliot Lake and Blind River**

| | | | | |
|---|---|---|---|---|
| DESIGN | KR | 02 SEP 2014 | **Figure 21** | REVISION 2 |
| GIS | JA | 20 NOV 2017 | | UTM ZONE 17N |
| CHECK | SC | 20 NOV 2017 | | NAD 1983 |
| REVIEW | JPS | 20 NOV 2017 | | 1:130,000 |

File: SRK_NWMO_NOH_Fig21_IntDenSurf



**REFERENCE**

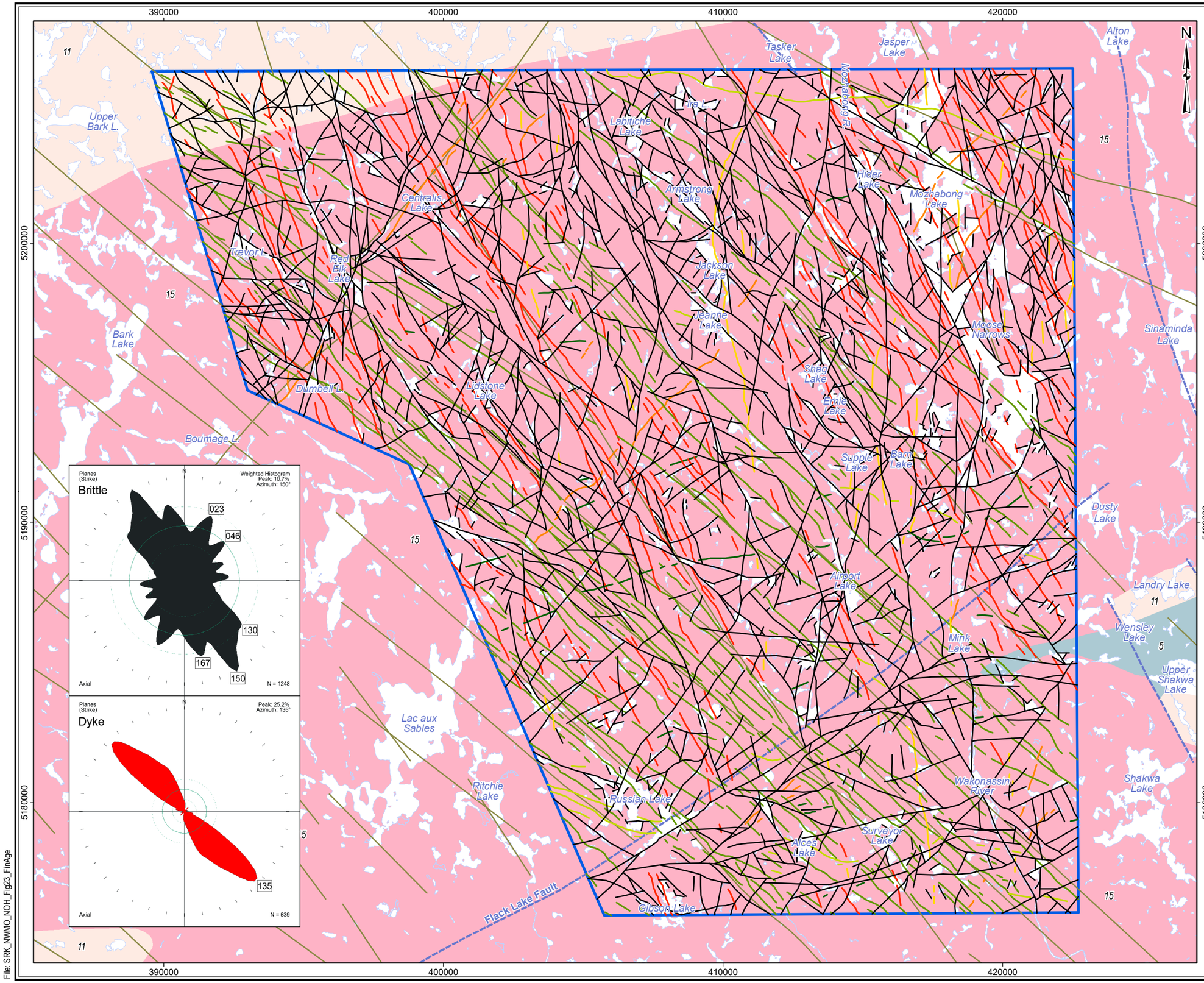
Base Data: Land Information Ontario (obtained 2015);
CanVec Topography (obtained 2015)
Geology: MRD 126-REV1 (Ontario Geological Survey, 2011)

srk consulting

Lineament Interpretation
Area North of Elliot Lake and Blind River, Ontario

**Lineament Intersection Density for All Final Integrated Lineaments of the Area North of Elliot Lake and Blind River**

| | | | | |
|---|---|---|---|---|
| DESIGN | KR | 02 SEP 2014 | **Figure 22** | REVISION 2 |
| GIS | JA | 20 NOV 2017 | | UTM ZONE 17N |
| CHECK | SC | 20 NOV 2017 | | NAD 1983 |
| REVIEW | JPS | 20 NOV 2017 | | 1:130,000 |




**LEGEND**

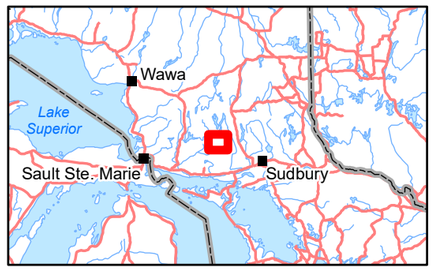
- Assessment Area
- Waterbody

**Bedrock Geology**

- Mapped Fault
- Mapped Dyke
- Massive granodiorite to granite (15)
- Gneissic tonalite suite (11)
- Benny Lake Greenstone Belt (5)

**Lineament**

- Brittle, D2-D6
- Grenville Dyke
- Sudbury Dyke
- North Channel Dyke
- Marathon Dyke
- Biscotasing Dyke
- Matachewan Dyke




**REFERENCE**

Base Data: Land Information Ontario (obtained 2015);
CanVec Topography (obtained 2015)
Geology: MRD 126-REV1 (Ontario Geological Survey, 2011)

0 5 km

srk consulting

PROJECT
Lineament Interpretation
Area North of Elliot Lake and Blind River, Ontario

TITLE
**Lineament Relative Age Relationships of the Area North of Elliot Lake and Blind River**

| | | | | |
|---|---|---|---|---|
| DESIGN | KR | 02 SEP 2014 | **Figure 23** | REVISION 2 |
| GIS | JA | 20 NOV 2017 | | UTM ZONE 17N |
| CHECK | SC | 20 NOV 2017 | | NAD 1983 |
| REVIEW | JPS | 20 NOV 2017 | | 1:130,000 |

File: SRK_NWMO_NOH_Fig23_FinAge